Uncertainties in the nuclear transition matrix elements of neutrinoless double beta decay

Thesis submitted for the award of the degree

of

Doctor of Philosophy

in

Applied Physics

by

Ratindra Gautam

Enrolment No.: 685/12

Under the Supervision of

Dr. Ramesh Chandra

Department of Applied Physics

School for Physical Sciences

Babasaheb Bhimrao Ambedkar University, Lucknow

U.P., (India) – 226025

2020

DEDICATED

TO

MY

LOVING

PARENTS

DECLARATION

I declare that the thesis titled "**Uncertainties in the nuclear transition matrix elements of neutrinoless double beta decay**" has been prepared by me under the supervision of **Dr. Ramesh Chandra**, Assistant Professor, Department of Applied Physics, School for Physical Sciences, Babasaheb Bhimrao Ambedkar University, Lucknow. No part of this thesis has formed the basis for the award of any degree, diploma or fellowship previously. Further, I declare that the material embodied in the present work is based on original research work and the indebtedness to others has been duly acknowledged at relevant places. This is also declared that the thesis is essentially free from all kinds of plagiarism.

Ratindra
07/02/2020

(Ratindra Gautam)

Department of Applied Physics

School for Physical Sciences

Babasaheb Bhimrao Ambedkar University

Vidya Vihar, Raebareli Road

Lucknow, (U.P.), India- 226025

Date: 07/02/2020

Place: Lucknow

CERTIFICATE

This is to certify that the thesis titled **"Uncertainties in the nuclear transition matrix elements of neutrinoless double beta decay"** submitted by **Mr. Ratindra Gautam** is an original research work and has not been previously submitted in part or full for the award of any other degree or diploma to this or any other University.

This thesis submitted to Babasaheb Bhimrao Ambedkar University Lucknow satisfies all the requirements as stipulated in the Doctor of Philosophy (Ph.D.) regulations-1999 as amended in 2008/2010/2013 and it is fit for submission and evaluation for the award of degree of Doctor of Philosophy of the University.

Date: 07-02-2020

Supervisor

Head of the Department

ACKNOWLEDGEMENT

I am truly blessed to be surrounded by many wonderful people in my life. From some I have learnt Science, from some I have learnt life and from some I have learnt both. I believe that I am an accumulation of their good character, their positive thoughts and their skillful nature. Each and every one of them is a share holder in all of my successes. Here, I would like to acknowledge and dedicate this thesis work to all of them who have played influential roles in my life and have left a never lasting impression on me.

First and foremost I sincerely thanks my Ph. D supervisor Dr. Ramesh Chandra (Assistant Professor, B. B. A. U.) for his invaluable guidance, vision, sincerity and motivation that kept me deeply inspired during whole course of research work. All of my hard work during research was only a reciprocation of his conscientious nature and our daily interactions that also made these 5 years really constructive and memorable for me. I respect and thank him for his great companionship throughout my Ph. D journey. I feel obliged to take this opportunity to express my heartfelt reverences towards him.

I would also pay my deep gratitude towards Prof. P. K. Rath (Professor, Lucknow University) who continuously provided valuable suggestions and concise comments on given state of research work without which it would have been an impossible task.

I would express my gratitude towards Prof. Bal Chand Yadav (Head of the Department, Professor, B. B. A. U.), Prof. Devesh Kumar (Professor, B. B. A. U.), Dr. A. K. Yadav (Assistant Professor, B. B. A. U.) and Dr. K. B. Thapa (Assistant Professor, B. B. A. U.) for his patient guidance and assistance at critical times. I would specially mention Dr. Devendra Singh (Assistant Professor, B. B. A. U.) for his enthusiastic encouragement that kept me progressing and raising the bar to satisfactory level.

I would mention the help provided by my lab members Dr. Yash Kaur Singh, Dr. Ruchi Mishra, Mr. Vivek Kumar Nautiyal who were ever willing to lend helping hand

even during odd hours, their help provided during course of Ph.D. research and manuscript preparation is highly acknowledged. Paucity of space does not allow me to mention the names of other researchers of the department, their support is also highly acknowledged. I am extremely thankful to Mrs. A. Moses (Head of the department, Associate Professor, I. T. College) and Dr. H. O. Dwivedi (Associate Professor, I. T. College) for all possible help that they could do at the very need of hour. At last I thank from the bottom of my heart to one and all who have directly or indirectly helped me or inspired me to achievement of my goal.

Next I would like to express my deep sense of gratitude towards my family. My father Mr. Govind Gautam and Mother Mrs. Meera Gautam have been constant torch bearers for me constantly encouraging and providing all necessary guidance, support and inspiration towards acquiring new skills. Support of my elder sister Ms. Sangeeta Gautam, Mrs. Ratika Gautam and my brother in law Mr. Akash Bharti needs no mention, without them it would have not been such a smooth task. I am highly indebted to my brother Er. Ravindra Gautam, Mr. Utkarsh Gautam, especially my cute nephews and nieces Kavyansh, Sheetanshu, Ilesha Gautam and Darshana Depankar for proving out to be stress buster for me in all those hectic routine, I would also thank all other family members, they helped me glide smoothly during times of despair.

I would like to thank Lord Buddha for His continuous showers of blessings throughout my research work without which it would not have been possible to begin this task. Thank you God for this day on which the research work stands successfully compiled in this thesis. I would appreciate support and facilities extended by staff at Library and Computer Center of the Department as well as the University for aiding in literature survey and other requirements. I gratefully acknowledge to University Grant Commission, Govt. of India for financial support in the form of Junior and Senior Reserach Fellowship

(JRF and SRF) grant.

Finally, I am also very thankful to my close friends Dr. Utkarsh Kumar, Mr. Anurag Sonker, Mr. Ravi Singh, Mr. Toton Haldhar, Dr. Umesh Verma, Mr. Yogesh Bhargawa, Mr. Tariq Azim, Mr. Gaurav Tripathi, Mr. Saty Prakash Bharti, Mohd. Asif, Ms. Shivani Chaudhary, Ms. Laxmi Kumari, Ms. Isha Singh, Ms. Sandhya Yadav, Ms. Priyanka Singh, Mr. Vimal Raj, Er. Narendra Kumar and Mr. Shasi Sekhar Sonu Sharma for not just being a part of this journey but also for providing mental strength at different part of the journey. A special mention for "Malkoti Ashram" and all its member as most of our time is spend in the ashram discussing physics and the world. I am very thankful to all those helping hands that directly and indirectly encouraged me and helped me to complete my research work.

My final words of thanks will be for Bharat Ratna Dr. Bhimrao Ambedkar and almighty God, for theircountless blessings, mercy and companionship through all turmoil of my life.

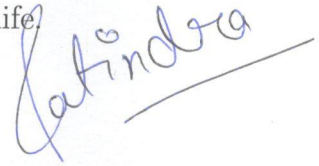

(Ratindra Gautam)

ABSTRACT

The discovery of neutrino mass is one of the most important event in particle physics, the evidences for which comes from the neutrino oscillation experiments. The access to neutrino mass from oscillation experiments is not an easy task as these experiments give only mass-squared differences. Therefore, the next step should be the determination of the mass and nature of the neutrinos. The only proof for the Majorana nature of the neutrinos would be the discovery of neutrinoless double beta ($0\nu\beta^-\beta^-$) decay.

The $0\nu\beta^-\beta^-$ decay has not been experimentally observed till date. The experiments devoted to observe this particular decay mode provide only limits on half-lives $T^{0\nu}_{1/2}$ of $0\nu\beta^-\beta^-$ decay. Various effective lepton number violating parameters can be extracted using these half-life limits and appropriate nuclear transition matrix elements (NTMEs) of $0\nu\beta^-\beta^-$ decay. The common practice is to first calculate NTMEs $M_{2\nu}$ for $2\nu\beta^-\beta^-$ decay as both the decay modes involve same set of initial and final nuclear wave functions. The $2\nu\beta^-\beta^-$ decay has been observed in eleven nuclei and experimental value of $M_{2\nu}$ is available. The validity of a nuclear model can be tested by its ability to reproduce experimental $M_{2\nu}$. It is observed in all cases of $2\nu\beta^-\beta^-$ decay that the NTMEs $M_{2\nu}$ are sufficiently quenched. The realization of this quenching mechanism is the main motive of all the theoretical calculations. In the present work, the $2\nu\beta^-\beta^-$ decay for the $0^+ \rightarrow J^+$ transition and $0\nu\beta^-\beta^-$ decay for the $0^+ \rightarrow 0^+$ transition have been studied.

PREFACE

The aim of present work is to study the $\beta^-\beta^-$ decay of ^{94,96}Zr, ^{100}Mo, ^{104}Ru, ^{110}Pd, ^{128,130}Te and ^{150}Nd isotopes. The present thesis is organized in following five chapters.

In Chapter 1, we give the introduction of present work and literature survey on the work done so far to study the $2\nu\beta^-\beta^-$ as well as $0\nu\beta^-\beta^-$ decay.

In Chapter 2, we test the reliability of PHFB wave functions by comparing the calculated yrast spectra, reduced $B(E2 : 0^+ \rightarrow 2^+)$ transition probabilities and deformation parameters β_2 of ^{94,96}Zr, ^{94,96,100}Mo, ^{100,104}Ru, ^{104,110}Pd, ^{110}Cd, ^{128,130}Te, ^{128,130}Xe, ^{150}Nd and ^{150}Sm participating in the $\beta^-\beta^-$ decay, with the available experimental data.

In Chapter 3, the PHFB wave functions are employed to study the $2\nu\beta^-\beta^-$ decay for the $0^+ \rightarrow J^+$ transition. The structure of ^{94,96}Zr, ^{94,96,100}Mo, ^{100,104}Ru, ^{104,110}Pd and ^{110}Cd nuclei are studied in a model space spanned by $(1p_{1/2}, 2s_{1/2,} 1d_{3/2}, 1d_{5/2}, 0g_{7/2}, 0g_{9/2}$ and $0h_{11/2})^{\pi,\nu}$ orbits taking even-even ^{76}Sr (N=Z=38) as a core. In case of ^{128,130}Te, ^{128,130}Xe, ^{150}Nd and ^{150}Sm nuclei, we have treated the doubly even nucleus ^{100}Sn (N=Z=50) as an inert core with the valence space spanned by $2s_{1/2,}$ $1d_{3/2}$, $1d_{5/2}$, $1f_{7/2}$, $0g_{7/2}$, $0h_{9/2}$ and $0h_{11/2}$ orbits for protons and neutrons. We use a pairing plus multipole (PQQHH) interaction in the two-body part of the Hamiltonian.

In Chapter 4, we study the $0\nu\beta^-\beta^-$ decay of ^{94,96}Zr, ^{100}Mo, ^{110}Pd, ^{128,130}Te and ^{150}Nd nuclei for the $0^+ \rightarrow 0^+$ transitions in m_ν, λ and η mechanisms. We calculate the NTMEs M_α in the PHFB model and study the role of finite size effect, short-range correlations. We extract limits on gauge theoretical parameters namely, effective electron-neutrino mass $\langle m_\nu \rangle$ and effective weak coupling constants $\langle \lambda \rangle$ and $\langle \eta \rangle$ for the coupling of right-handed leptonic current with right-handed and left-handed hadronic currents, respectively, from the observed limits on half-lives $T^{0\nu}_{1/2}$ of the 0ν $\beta^-\beta^-$ decay.

Finally, a number of necessary improvements that need to be incorporated into the PHFB model for a more reliable study of the $\beta\beta$ decay are discussed in Chapter 5.

LIST OF TABLES

Table 3.1: Theoretically calculated NTMEs $M_{2\nu}$ within the PHFB model with four different parametrizations and their average value $\overline{M}_{2\nu}$ along with experimental values [Barabash (2010)].

Table 3.2: Calculated NTMEs $M_{2\nu}(2^+)$ within the PHFB model and their average $\overline{M}_{2\nu}(2^+)$ along with standard deviation $\Delta\overline{M}_{2\nu}(2^+)$.

Table 3.3: Theoretically calculated NTME $M_{2\nu}(2^+)$ and half-life $T^{2\nu}_{1/2}(2^+)$ (in yr) for the $0^+ \rightarrow 2^+$ transition of ^{94,96}Zr, ^{100}Mo, ^{104}Ru, ^{110}Pd, ^{128,130}Te and ^{150}Nd nuclei along with experimental half-lives $T^{2\nu}_{1/2}(2^+)$ (in yr). The numbers corresponding to (a) and (b) are calculated for $g_A = 1.2701$ and 1.0 respectively. "*" denotes the present calculation.

Table 4.1: Calculated NTMEs M_α of ^{100}Mo for point case (P), with the inclusion of finites size of nucleons (FNS) and both the FNS and SRC (F+SRC).

Table 4.2: Combination of NTMEs $M^{(0\nu)}$ and $M_{i\pm}(i = 1, 2)$.

Table 4.3: Change in the NTME M_α of $0\nu\beta^-\beta^-$decay (in %) due to the exchange of light Majorana neutrino, and admixture of $V - A$ and $V + A$ currents, with the inclusion of FNS and SRC (SRC1, SRC2, SRC3) for all four parametrizations of the effective two-body interaction.

Table 4.4: Average values for NTMEs $\overline{M}_\alpha$ and uncertainty $\Delta\overline{M}_\alpha$ for the $0\nu\beta^-\beta^-$ decay of ^{94,96}Zr, ^{100}Mo, ^{110}Pd, ^{128,130}Te and ^{150}Nd isotopes.

Table 4.5: Phase space factor $G_{0k}(k = 1, 11)$ for ^{96}Zr,^{100}Mo, ^{110}Pd , ^{130}Te, and ^{150}Nd nuclei [Štefánik *et al.* (2015)].

Table 4.6: Calculated nuclear structure factors C_{mm}, $C_{m\lambda}$, $C_{m\eta}$, $C_{\lambda\lambda}$, $C_{\eta\eta}$ and $C_{\lambda\eta}$ in (a) PQQ1, (b) PQQHH1, (c) PQQ2 and (d) PQQHH2 parametrizations. In each parametrization, the three rows correspond to SRC1, SRC2 and SRC3, respectively.

Table 4.7: Average nuclear structure factors $\overline{C}_{mm}$, $\overline{C}_{m\lambda}$, $\overline{C}_{m\eta}$, $\overline{C}_{\lambda\lambda}$, and $\overline{C}_{\eta\eta}$ for the $0\nu\beta^-\beta^-$ decay of ^{96}Zr, ^{100}Mo, ^{110}Pd, ^{130}Te and ^{150}Nd isotopes.

Table 4.8: Experimental limits on half-lives $T^{0\nu}_{1/2}$ and the extracted on-axis limits on the effective mass of light neutrino $\langle m_\nu \rangle$, $\langle \lambda \rangle$, and $\langle \eta \rangle$ for the $0\nu\beta^-\beta^-$ decay of ^{96}Zr, ^{100}Mo, ^{110}Pd, ^{130}Te and ^{150}Nd isotopes. Predicted half-lives $T^{0\nu}_{1/2}$ of $0\nu\beta^-\beta^-$decay for two sets of parameters (i) $\langle m_\nu \rangle = 50$ meV (Case I) and (ii) $\langle m_\nu \rangle = 50$ meV, $\langle \lambda \rangle = 10^{-7}$ and $\langle \eta \rangle = 10^{-9}$ (Case II).

Table 5.1 : Calculated limits on effective light Majorana neutrino mass $\langle m_\nu \rangle$ (in eV) along with average NTMEs $\overline{M}^{(0\nu)}$, uncrtainties $\Delta\overline{M}^{(0\nu)}$ and the present half-life limits $T^{0\nu}_{1/2}$ (in yr) for the $0\nu\beta^-\beta^-$ decay.

TABLES OF CONTENTS

Chapter 1

Introduction

Neutrinos are quite fascinating particles due to their weird nature. They came into existence during the first three minutes of the Big Bang, in which the universe was created 13.7 ± 0.2 G yr ago. Although the neutrinos permeate most of the space all around us but they hardly interact with anything. Even they can pass through the entire Earth without being affected. The story of neutrinos is fairly exciting. In 1930, Wolfgang Pauli postulated the existence of electron neutrino ν_e - a chargeless, massless and spin 1/2 particle - to explain the continuous nature of the beta spectrum. Almost immediately Fermi gave the theory of beta decay assuming the electron neutrino to be a Dirac particle. In 1956, Cowan and Reines experimentally detected neutrinos at the Savannah river reactor site. In the same year, T. D. Lee and C. N. Yang suggested that parity is not conserved in weak interaction, and Madam C. S. Wu [Wu *et al.* (1957)] established experimentally that the weak interaction in fact violates the conservation of parity maximally. With this discovery, it became apparent that the neutrinos are Weyl particles, i.e. chargeless, massless and left-handed spin 1/2 fermions.

In the theory of Standard Model (SM), which asserts that the material universe consists of four fundamental forces and forty-five chiral fermions, the neutrinos are assumed to be massless particles. However, there is no valid reason for assuming neutrinos to be massless and it is an input rather than a prediction of the SM. Further, the SM has eighteen free parameters and it does not give an explanation of the quantization of electrical charges. In order to overcome these difficulties and to extend the unification scheme further to include strong interaction, Grand Unified theories (GUTs), Supersymmetric theories (SUSYs), Supergravity theories (SUGRAs) and String theories etc. have been developed. In most of these gauge field theories, which go beyond the SM, the neutrino turns out to be a Majorana particle. Thus, the mass and exact nature of neutrinos -Dirac or Majorana character- are not completely known till today.

The distinction between Dirac and Majorana character of neutrinos can be drawn on the basis of CPT invariance and Lorentz transformation. According to CPT invariance, there exists a right-handed antineutrino $\overline{\nu}_R$ for each left handed massive neutrino ν_L. There are four available states for a massive neutrino, namely ν_L , ν_R, $\overline{\nu}_L$, and $\overline{\nu}_R$. This set of states four states is called **Dirac Neutrino $\boldsymbol{\nu}^D$**. A Dirac neutrino can also be constructed from a pair of mass degenerate Majorana neutrinos. There are two types of Dirac neutrinos, namely *Ordinary Dirac Neutrino* (pair of neutrinos are in same flavor having definite lepton number which is conserved) and *Konopinski-Mahmood* **(KM)** *Dirac neutrino* (two or more flavors of neutrinos are involved). On the other hand, if ν_R is identical to $\overline{\nu}_R$, then the set of two states is called **Majorana Neutrino $\boldsymbol{\nu}^M$**. Thus, Majorana neutrino is identical to its antiparticle.

In 1967, Raymond Davis started looking for neutrinos produced by the nuclear reac-

tions in the Sun's core using a huge tank of cleaning fluid (HCl_4) placed deep underground to shield it from cosmic rays. However, he could only detect about half of what was expected. Other underground detectors found similar neutrino shortages. In 1957, Bruno Pontecarvo and independently, Maki, Nakagawa and Sakata in 1962 had already proposed that neutrinos might change from one flavor into another, a phenomenon called neutrino oscillation (ν-oscillation) [Pontecorvo (1957), Maki *et al.* (1962)] given by

$$|\nu_\alpha\rangle = \sum_{i=1}^{n} U_{\alpha i}\nu_i \tag{1.1}$$

Gradually, physicists started to suspect that oscillation could explain the shortfall of neutrinos detected from the Sun. The detectors could capture only one type of neutrino, and neutrinos during their journey from the Sun changed flavor and escaped detection. The quantum theory requires that neutrinos must have mass to change flavor. The confirmation of neutrino oscillations in solar, atmospheric, accelerator and reactor neutrino sources has established the fact that neutrinos have mass. However, the oscillation data provide only mass squared difference and the actual neutrino mass cannot be extracted. The study of tritium single β decay and $\beta^-\beta^-$ decay together has the potential to extract sharpest limits on the neutrino mass and explain the nature of the electron neutrinos. Further, these determining features of the elusive neutrinos through the observation of $0\nu\beta^-\beta^-$ decay could provide a deep insight into the nature of the universe during the earliest moments of the Big Bang.

1.1 The Nuclear $\beta\beta$ decay

The nuclear $\beta\beta$ decay is a rare second order weak transition between two isobars having even Z-even N configuration and differing in nuclear charge by two units. The $\beta\beta$ decay candidates are stable against single β decay either due to energy conservation or angular momentum mismatch. There are two modes of $\beta\beta$ decay, one involving the emission of two neutrinos ($2\nu\beta\beta$ decay) and the other neutrinoless double beta ($0\nu\beta\beta$) decay. The former conserves the lepton number L exactly and is an allowed process within SM. In the latter one, the lepton number is violated by two units and it has the potential to probe physics beyond the SM. The $2\nu\beta\beta$ decay can be regarded as a simultaneous transformation of two neutrons into two protons, which leads to the final state with emission of two electrons and two antielectron-neutrinos ($2\nu\beta^-\beta^-$ decay) i.e.,

$$ {}^{A}_{Z}X \rightarrow {}^{A}_{Z+2}Y + 2e^- + 2\overline{\nu}_e \tag{1.2} $$

There are 35 potential $\beta^-\beta^-$ emitters in nature and we present a list of them in Table 1.1 along with $Q_{\beta\beta}$, natural abundance and β_2 parameters related to the deformation of nucleus.

The three other processes through which $2\nu\beta\beta$ decay may occur involving the emission (capture) of one or two positrons (electrons) along with two neutrinos are

$$ \begin{aligned} &(i) \quad {}^{A}_{Z}X \rightarrow {}^{A}_{Z-2}Y + 2e^+ + 2\nu_e && \textit{positron emission} \\ &(ii) \quad e^- + {}^{A}_{Z}X \rightarrow {}^{A}_{Z-2}Y + e^+ + 2\nu_e && \textit{electron capture} \\ &(iii) \quad 2e^- + {}^{A}_{Z}X \rightarrow {}^{A}_{Z-2}Y + 2\nu_e && \textit{double electron capture} \end{aligned} \tag{1.3} $$

The half-life of such decays was expected to be fairly long since they are low energy processes of second order in weak interaction. Historically, the study of $2\nu\beta^-\beta^-$ decay was

motivated to understand the observed stability of even-even nuclei, which are otherwise candidates for β decay, over a geological time scale of billion years. Maria Goepert-Mayer (1935) at the suggestion of Eugene P. Wigner calculated the half-life for the $2\nu\beta^-\beta^-$ decay to be $> 10^{17}$ years, which is exceedingly slow even on the geological time scale and explained the observed stability of even Z-even N nuclei.

The $0\nu\beta^-\beta^-$ decay, one of the most interesting case of $\beta\beta$ decay, is given as

$$ {}^{A}_{Z}X \rightarrow {}^{A}_{Z+2}Y + 2e^- \tag{1.4} $$

and was considered first by Racah [Racah (1937)] and W. Furry [Furry (1939)] as a tool to distinguish whether the neutrino is of Majorana (particle≡antiparticle) [Majorana (1937)] or Dirac (particle≠antiparticle) nature. The mechanism of $0\nu\beta^-\beta^-$ decay is based on the emission of an electron antineutrino $\overline{\nu}_e$ on the first decay vertex ($n \rightarrow p + e^- + \bar{\nu}_e$) and its absorption in the second vertex. The absorption part is an inverse beta decay ($n + \nu_e \rightarrow p + e^-$), where electron neutrino instead of antineutrino is required. The emission and absorption processes yield to exchange of a virtual neutrino and the associated propagator produces a neutrino potential. Though, the conservation of energy and momentum required the emission of a neutrino in single β decay, there is no corresponding requirement for neutrinos in $0\nu\beta\beta$ decay. The energy and momentum could be conserved in this decay mode releasing two electrons only. Similar to the $2\nu\beta\beta$ decay, the $0\nu\beta\beta$ decay may also occur involving the emission (capture) of one or two positrons (electrons)

as

$$
\begin{aligned}
&(i) \quad {}^{A}_{Z}X \rightarrow {}^{A}_{Z-2}Y + 2e^{+} && \textit{positron emission} \\
&(ii) \quad e^{-} + {}^{A}_{Z}X \rightarrow {}^{A}_{Z-2}Y + e^{+} && \textit{electron capture} \\
&(iii) \quad 2e^{-} + {}^{A}_{Z}X \rightarrow {}^{A}_{Z-2}Y^{*} && \textit{double electron capture}
\end{aligned}
\tag{1.5}
$$

1.1.1 $2\nu\beta^{-}\beta^{-}$ decay and validity of nuclear models

The inverse half-life of the $2\nu\beta^{-}\beta^{-}$ decay for the $0^{+} \rightarrow 0^{+}$ transition is given by

$$
[T^{2\nu}_{1/2}(0^{+} \rightarrow 0^{+})]^{-1} = G_{2\nu} \left| M_{2\nu} \right|^{2} \tag{1.6}
$$

where $G_{2\nu}$ is the integrated kinematical factor and can be calculated with good accuracy. The nuclear transition matrix element (NTME) $M_{2\nu}$ is a model dependent quantity. The half-life $T^{2\nu}_{1/2}$ of $2\nu\beta^{-}\beta^{-}$ decay has been already measured for eleven nuclei out of 35 possible candidates. Using the experimental half-life $T^{2\nu}_{1/2}$ and accurately known integrated kinematical factor $G_{2\nu}$, the values of $M_{2\nu}$ can be extracted directly from Eq.(1.6). It is observed that in all cases of $2\nu\beta^{-}\beta^{-}$ decay, the NTMEs $M_{2\nu}$ are sufficiently quenched. The main motive of all theoretical calculations is to understand the physical mechanism responsible for the observed suppression of $M_{2\nu}$. Hence, the validity of different nuclear models can be tested through the calculation of $M_{2\nu}$.

The calculation of $M_{2\nu}$ requires the knowledge of a complete set of states of the intermediate nucleus in addition to the initial and final nuclear states. Therefore, the calculation of NTME $M_{2\nu}$ is quite complex. In solving this problem, different models and nuclear structure scenarios have been applied. Over the past few years, several nuclear models have been employed to calculate the $2\nu\beta^{-}\beta^{-}$ decay rate in 2n mechanism. They can be broadly classified into three categories, namely shell model and its variants,

quasiparticle random phase approximation (QRPA) and its extensions and alternative models. The details about these models -their advantages as well as shortcomings- have been discussed excellently by Suhonen and Civitarese (1998) and Faessler and Simkovic (1998). We briefly discuss in the below the relative applicability, success and failure of various models used so far to study the $\beta^-\beta^-$ decay processes for the sake of completeness.

Shell model and its variants

The shell model, which attempts to solve the nuclear many-body problem as exactly as possible, is the best choice for the calculation of the NTMEs for $\beta^-\beta^-$ decay. Beyond the *pf*-shell, the number of basis states increases so drastically that a few years back it was not possible to perform a conventional shell model calculation without imposing certain truncation schemes. In the following we discuss about them briefly.

1. Most of the $\beta^-\beta^-$ decay emitters are medium or heavy mass nuclei. Since a reliable shell-model calculation was difficult to perform, Vergados *et al.* (1976), Haxton *et al.* (1984) and Caurier *et al.* (1999) have studied the $\beta^-\beta^-$ decay of ^{48}Ca, ^{76}Ge, ^{82}Se and ^{128,130}Te nuclei in weak coupling limit (WCSM).

2. The large scale shell model (LSSM) calculations by Skouras *et al.* (1983), Zhao and coworkers [(1990), (1993)] and Strassbourg-Madrid collaboration [(1990), (1995), (1999)] are more promising in nature.

3. The $0\nu\beta^-\beta^-$ decay of ^{48}Ca has been studied by Retamosa *et al.* (1995) in lower *fp*-shell without any restriction.

4. Ogawa *et al.* [Ogawa *et al.* (1989)] and Caurier *et al.* [Caurier *et al.* (1990)] have studied $2\nu\beta^-\beta^-$ decay of ^{48}Ca in full *fp*-shell.

5. The calculations by Caurier *et al.* are more realistic in nature, in which the NTMEs of $2\nu\beta^-\beta^-$ as well as $0\nu\beta^-\beta^-$ decay of ^{82}Se is calculated exactly, and those of ^{76}Ge and ^{136}Xe are dealt with in a nearly exact manner [Caurier *et al.* (1996)]. Further, NTMEs of $2\nu\beta^-\beta^-$ and $0\nu\beta^-\beta^-$ decay have been calculated by Caurier *et al.* [Caurier *et al.* (1999)] for ^{48}Ca, ^{76}Ge, ^{82}Se , ^{124}Sn, ^{128,130}Te, ^{136}Xe nuclei.

6. The conventional shell model and Monte-Carlo shell model (MCSM) [Koonin *et al.* (1997) and Radha *et al.* (1996), (1997)] have been tested against each other for the case of ^{48}Ca in complete *pf*-shell and ^{76}Ge in upper *fpg*-shell, and the agreement is interestingly significant. Hence, the MCSM could turn out to be a good alternative to conventional shell model calculations in the near future.

7. A new method for accurate calculation of $M^{(0\nu)}$ for ^{76}Ge have been investigated by Sen'kov and Horoi (2014).

8. Caurier *et al.* (2008) and Menéndez *et al.* (2008) have calculated $M^{(0\nu)}$ of ^{48}Ca, ^{76}Ge, ^{82}Se, ^{124}Sn, ^{128,130}Te and ^{136}Xe nuclei in interacting shell model (ISM).

9. Recently the NTMEs due to light Majorana neutrino exchange $M^{(0\nu)}$ as well as heavy Majorana neutrino exchange $M^{(0N)}$ have been calculated for the $0\nu\beta^-\beta^-$ decay of ^{48}Ca, ^{76}Ge, ^{82}Se, ^{124}Sn, ^{130}Te and ^{136}Xe nuclei by Menéndez *et al.* (2018) in the shell model.

Thus, the mechanism responsible for the quenching of $2\nu\beta^-\beta^-$ decay strength is not well understood. The shell model calculations, besides being feasible for a limited number of nuclei due to a large number of basis states, fail to fulfil Ikeda sum rule by about 40 to 60 %.

QRPA and its extensions

Vogel and Zirnbauer (1986) were the first to explain the observed suppression of $M_{2\nu}$ in the QRPA model. It was observed that the suppression of $M_{2\nu}$ can be achieved by a proper inclusion of ground state correlations through the particle-particle interaction in the $S = 1$, $T = 0$ channel. The QRPA overestimates the ground state correlations. This results in an increase in the strength of attractive proton-neutron interaction and leads to the collapse of QRPA solutions. The physical value of this force is usually close to the point at which the QRPA solutions collapse. The origin of this unfortunate behavior is attributed to the quasi-boson approximation (QBA) of the QRPA operators violating the Pauli exclusion principle. With increase in ground state correlations, the violation of the exclusion principle is also increased. Many extensions of the QRPA has been proposed for solving some of the inherent problems. These extensions are as follows.

1. Inclusion of proton-neutron pairing (full QRPA) [Cheoun *et al.* (1993), (1995)]

2. Renormalized QRPA in which violation of Pauli exclusion principle is restored (RQRPA) [Toivanen *et al.* (1995), (1997), Simkovic *et al.* (1997), Krmpotic *et al.* (1997), Simkovic *et al.* (2010)]

3. Full RQRPA [Schwieger *et al.* (1996), Simkovic *et al.* (1997) and Stoica *et al.*

(2001)]

4. Higher QRPA (HQRPA) [Raduta *et al.* (1991), Sambarato *et al.* (1997)], SQRPA [Stoica *et al.* (1993), (1994), (1995), (1996), (2000), (2001)]

5. SRQRPA [Bobyk *et al.* (2001)]

6. Multiple commutator method (MCM) [Suhonen *et al.* (1993), Civitarese *et al.* (1994), Aunola *et al.* (1996)]

7. Particle number projection (PQRPA) [Civitarese *et al.* (1990) and (1991), Suhonen *et al.* (1992), Suhonen (1993), Krmpotic *et al.* (1993)]. The $2\nu\beta^-\beta^-$ decay of ^{76}Ge, ^{100}Mo and ^{128,130}Te nuclei [Civitarese *et al.* (1990) and (1991)] and $0\nu\beta^-\beta^-$ decay of ^{76}Ge isotope [Suhonen *et al.* (1992)] has been studied with particle number projection and it is noticed that the effect is negligible in case of medium-heavy and heavy mass nuclei.

8. pnQRPA [Civitarese and Suhonen (2009), Hyvarinen and Suhonen (2015)]

9. QRPA with isospin restoration [Simkovic *et al.* (2013)]

10. Deformed QRPA [Fang *et al.* (2010), (2011), Faessler *et al.* (2012), Mustonen *et al.* (2013)]

11. Deformed QRPA with isospin restoration [Fang *et al.* (2018)]

However, it is not clear which method is the best. Altogether, QRPA and its various extensions with the ability to adjust one free parameter are able to explain the observed $2\nu\beta^-\beta^-$ decay rates.

Alternative models

The shell model and its variants as well as the QRPA and its extensions, besides having their own limitations, fail to fulfil the Ikeda sum rule. In the QRPA approach, a larger uncertainty may occur in deformed nuclei as deformation is usually ignored. This has been shown for ^{100}Mo and ^{150}Nd isotopes using QRPA [Suhonen *et al.* (1994)] and pseudo SU(3) model [Hirsch *et al.* (1995)]. The small predictive power of QRPA and its extensions is the main motivation for seeking an alternative description which might result in a more reliable approach for the study of nuclear $\beta^-\beta^-$ decay processes. These attempts have been summarized as alternative models. Under alternative models, one has

1. Operator expansion method (OEM) [Ching *et al.* (1989), Simkovic (1989), Engel *et al.* (1992), Wu *et al.* (1991) and (1992), Hirsch *et al.* (1993), (1994), Muto (1993), Simkovic *et al.* (1998)]

2. Broken SU(4) symmetry [Bernabeu *et al.* (1990), Vladimirov *et al.* (1992), Moe and Vogel (1994) and Rumyantsev *et al.* (1995)]

3. Group theoretical studies in SU(2) [Hirsch *et al.* (1996)], SO(5) [Hirsch *et al.* (1997)], O(8) [Engel *et al.* (1997)] and the pseudo-SU(3) [Castanos *et al.* (1994) and Hirsch *et al.* (1995), (2002)]

4. Two-Vacua RPA (TVRPA) [Simkovic *et al.* (1994) and Teneva *et al.* (1995)]

5. Single state dominance hypothesis (SSDH) [Ejiri *et al.* (1996), Civitarese *et al.* (1998) and (1999)]

6. Energy Density Functional (EDF) theory [Rodríguez *et al.* (2010), Vaquero *et al.* (2013)]

7. Interacting Boson Model (IBM) [Barea and Iachello (2009), Barea *et al.* (2012)]

8. IBM2 [Iachello *et al.* (2011), Barea *et al.* (2013)]

9. IBM2 with isospin restoration [Barea *et al.* (2015)]

10. Covariant Density Functional Theory (CDFT) [Yao *et al.* (2015), Song *et al.* (2017)]

11. Projected Hartree-Fock-Bogoliubov (PHFB) method [Tomoda *et al.* (1985) and (1986)]

The NTMEs $M^{(0\nu)}$ calculated in theses models for $0\nu\beta^-\beta^-$ decay are complied in Table 1.2.

1.1.2 $0\nu\beta^-\beta^-$ decay and physics beyond the SM

In the SM, the neutrinos are massless due to the absence of the right-handed neutrinos and the existence of an exact global $B-L$ symmetry. The gauge theories beyond the *SM* fulfill the above mentioned requirements. The possible ways for breaking the $B-L$ symmetry are (i) explicit breaking of $B-L$ symmetry where Lagrangian contains terms that break $B-L$ symmetry, (ii) spontaneous breaking of local $B-L$ symmetry and (iii) spontaneous breaking of global $B-L$ symmetry. Thus, the study of $\beta\beta$ decay in general and $0\nu\beta^-\beta^-$ decay in particular is a convenient tool to test the following important ramifications vis-a-vis constraints on parameters of various gauge theoretical models beyond the SM,

namely (i) lepton number violation, (ii) mass and charge conjugation properties of the electron-neutrino and (iii) possible right handed admixtures in the weak leptonic current. The $0\nu\beta^-\beta^-$ decay can be studied mainly in three types of models, namely Left-right symmetric models (LRSM), Majoron models and R-parity violating Supersymmetric models (R_p-violating MSSM). Further, the $0\nu\beta^-\beta^-$ decay can verify issues like compositeness, leptoquarks, sterile neutrinos and violation of weak equivalence principle.

1.2 Experimental search for neutrinoless double beta decay

The experimental aspect of nuclear $\beta^-\beta^-$ decay has been reviewed over the years to update its experimental status [Avignone *et al.* (2005), Barabash (2010), (2013), (2015), (2018), Dell'Oro *et al.* (2015) and references there in]. In Tables 1.3–1.5, we have compiled the experimentally measured half-lives of $2\nu\beta^-\beta^-$decay and limits on half-lives of the $0\nu\beta^-\beta^-$decay for the $0^+ \rightarrow 0^+$ as well as $0^+ \rightarrow J^+$ transition.

Experiments on $\beta^-\beta^-$ decay can be divided into two broad categories namely (a) indirect experiments and (b) direct experiments.

1.2.1 Indirect experiments

Under indirect methods, the geochemical and the radiochemical methods are uncontrolled and controlled inclusive studies respectively in which neither the decay processes nor the final states are identified. We outline briefly the scope of different experimental methods in the below.

Geochemical method

In geochemical experiments, one measures the abundance of daughter isotope that has accumulated over the geological time of the order of 10^9 years in an ore sample rich in parent isotopes. In such indirect experiments, the investigation consists of

(i) the determination of the age of the sample if possible by more than one independent methods.

(ii) the extraction of the daughter nuclei from the sample and the determination of their concentration. This limits the applicability of the method to these cases where the daughter nucleus is a noble gas. There exists in nature only three systems namely ^{82}Se$\rightarrow$ ^{82}Kr and ^{128,130}Te$\rightarrow$ ^{128,130}Xe.

(iii) a mass spectroscopic isotopic analysis of the extracted gases and determination of the absolute concentration of ^{82}Kr and ^{128,130}Xe isotopes.

(iv) the determination of the coefficient of retention of the daughter nuclei in the sample during the time of their generation. Ideally, the system must be closed for both the parent and the daughter nucleus.

(v) a comprehensive and careful elimination of various background reactions, which may populate the daughter nucleus.

The signature for the production of a daughter isotope in $\beta^-\beta^-$ decay is an increase in the isotopic abundance relative to some reference isotopes of the same element not produced in $\beta^-\beta^-$ decay in the parent ore. State-of-the-art technique in mass spectrometry permits one to measure changes in the isotopic abundance of one part in 10^5 at the best. Thus, for accumulation time of 10^9 years and typical $\beta^-\beta^-$ decay rate of 10^{-21}

events per year, the initial concentration of the daughter isotope in the ore sample must be no more than 10^{-7} that of the parent. Essentially, this requirement limits studies to transitions involving noble gas daughter isotopes, as only in those cases is such strong fractionation between elements with $|\Delta Z| = 2$ likely. Of course, the three reactions that produce daughter nuclei not found naturally (^{146}Sm, ^{232}U and ^{238}Pu) are in principle exceptions to the general rule. However, the latter two isotopes are so short-lived ($\sim 10^2$ years) that they may be better subjects for radiochemical methods while the $\beta^-\beta^-$ reaction producing the first isotope $^{146}\mathrm{Nd} \rightarrow {}^{146}\mathrm{Sm}$ is enormously suppressed by phase space ($\mathrm{T_0} = 61$ keV). Manuel has reviewed in detail the geochemical methods and obtained experimental results [Manuel (1991)].

The inherent limitation of the geochemical method is that it can not distinguish the $0\nu\beta^-\beta^-$ and the $2\nu\beta^-\beta^-$ decay modes, as the energy information is long lost. However, information about the decay modes can be sometimes inferred from the geochemically measured half-life by resorting to a specific nuclear model. For example, when the geochemical value is shorter than the lower limits for the $0\nu\beta^-\beta^-$ and Majoron accompanied $0\nu\beta^-\beta^-$ decay half-lives determined for that isotope by an independent technique, a predominance of the $2\nu\beta^-\beta^-$ decay mode is implied. The latter can be used to set limits on the neutrino mass and Majoron coupling strength as the half-life of any mode can not be shorter than the geochemical value.

Radiochemical methods

Radiochemical methods are another version of indirect experiments in which the accumulation of the daughter nucleus occurs in a known interval of time under carefully controlled

environment. The sample should be purged of daughter atoms existing in the environment as the accumulation time is much shorter than the geological time. Hence, the most easily studied reactions by the radiochemical method are ^{232}Th$\rightarrow^{232}$U, ^{238}U$\rightarrow^{238}$Pu and ^{244}Pu$\rightarrow^{244}$Cm as the daughter isotopes are so short lived ($\sim 10^2$ years) that their abundance in the environment will be pretty low. The development of extremely sensitive resonance ionization techniques for noble gases suggest that radiochemical measurements of $\beta^-\beta^-$ decay for ^{82}Se and ^{128,130}Te may be practical [Hurst *et al.* (1980)]. In such single atom experiments, it must be established that the container holding the parent is free from the contamination of the daughter present in the environment.

1.2.2 Direct detection experiments

The direct methods began in the late 1940's at approximately of the same time as the geochemical experiments. Various approaches were attempted such as coincidence searches for two emitted electrons with Geiger tubes and scintillators, nuclear emulsion techniques, magnetic spectrometers, tracking chambers and calorimeters using Ge crystals and ionization chambers. An excellent historical review of all these unsuccessful attempts has been presented by Haxton *et al.* (1984) up to 1984.

The following conditions are necessary requirements for an effective experimental set up.

(i) The source, detector and shielding should be free from radioactive contaminants at the level of one part per 10^9 for maximum background suppression.

(ii) The reliable functioning of the equipments over a long period of time is required.

(iii) A maximum pure and large sample of optimum size has to be decided so that there is

an increase in the number of counts without increasing the background beyond a certain level.

(iv) Extraction of as many characteristics as possible of the $\beta^-\beta^-$ decay event such as tracking in addition to energy measurement so that the process can be discriminated against the background.

There are two different types of direct $\beta^-\beta^-$ decay experiments namely (a) active source - in which the source and the detector are identical and (b) passive source - in which the source and detector are not identical. The active source methods are more sensitive for the $0\nu\beta^-\beta^-$ decay mode and the passive source methods are the best suited for the $2\nu\beta^-\beta^-$ mode. In both types of experiments, attempt is made to measure the characteristic properties of $0\nu\beta^-\beta^-$ decay such as

(i) emission of two electrons from the same point inside the source

(ii) simultaneous emission of two electrons and

(iii) constancy of the energy of the two emitted electrons.

The experiments, which determine all the three characteristics are called "complete experiments" and those which measure only the second and the third are called "identification experiments".

The signature of $2\nu\beta^-\beta^-$ decay is the emission of two electrons from a common point free from other activity for some hours before and after the event. With the development of the tracking capabilities of the time projection chamber (TPC), it was possible ultimately to identify the long sought $\beta^-\beta^-$ decay event separating it from the background observed in the $2\nu\beta^-\beta^-$ decay of ^{82}Se [Elliott *et al.* [(1987), (1988)]. The $2\nu\beta^-\beta^-$ decay now has been observed for nearly 10 nuclei namely ^{48}Ca, ^{76}Ge, ^{82}Se, ^{96}Zr, ^{100}Mo, ^{116}Cd, ^{128,130}Te,

^{150}Nd and ^{238}U and for the rest of the isotopes lower limits have been set on the $2\nu\beta^-\beta^-$ decay. The experimentally deduced half-lives for the $2\nu\beta^-\beta^-$ decay are given in Table 1.2.

The $0\nu\beta^-\beta^-$ decay is not observed so far and all the present experimental activities are directed in this direction. As the broadly distributed sum energy spectra of $2\nu\beta^-\beta^-$, $0\nu\beta^-\beta^-$, $2\nu\beta^-\beta^-\phi$ and $2\nu\beta^-\beta^-\phi\phi$ yields to similar experimental tracks, the direct counting experiments reporting the $2\nu\beta^-\beta^-$ decay also give lower limits of half-lives for corresponding processes. Most of the recent activities, however refers to direct counting experiments which measure the energy of the $\beta^-\beta^-$ emitted electrons and so the spectral shapes of the $2\nu\beta^-\beta^-$, $0\nu\beta^-\beta^-$ and $0\nu\beta^-\beta^-\phi$ modes of decay. Some experimental devices track the electrons (and other charged particles) measuring the energy, angular distribution and topology of the events. The tracking capabilities are essential to discriminate the $\beta^-\beta^-$ signal from the background.

The experimental limit on $\langle m_\nu \rangle$ can be written as

$$\langle m_\nu \rangle = \left(2.50 \times 10^{-8}\ eV\right) \left[\frac{W}{fx\varepsilon F_N}\right]^{1/2} \left[\frac{B\Delta E}{MT}\right]^{1/4} \tag{1.7}$$

in the case of limited background and for zero background

$$\langle m_\nu \rangle = \left(2.67 \times 10^{-8}\ eV\right) \left[\frac{W}{fx\varepsilon F_N}\right]^{1/2} \left[\frac{1}{\sqrt{MT}}\right] \tag{1.8}$$

where W is the molecular weight of the source material, f is the isotopic abundance, x is the number of $\beta^-\beta^-$ atoms per molecule, ε is the detector efficiency, B is the background (counts/ kg-yr-keV), ΔE is the energy window in keV around $Q_{\beta\beta}$, M is the mass of the $\beta^-\beta^-$ emitter (kg), T *is* the time measurement in years and nuclear factor-of-merit F_N is

given by

$$F_N = G_{0\nu} \left| M_{0\nu} \right|^2 \tag{1.9}$$

where $G_{0\nu}$ is the kinematical factor and the nuclear transition matrix element (NTME) $M_{0\nu}$, is the likeliness of the transition. The Eqs. (1.19) and (1.20) suggest that the requirements of effective experimental set up are

(i) a $\beta^-\beta^-$ source having large factor-of-merit F_N

(ii) a large source mass

(iii) a low back ground preferably almost zero background

(iv) a high detector efficiency.

The types of detectors currently used are:

(i) Calorimeters in which the detector is also the $\beta^-\beta^-$ source (Ge diodes, scintillators-CaF_2, $CdWO_4$, thermal detectors, ionization chambers). They are calorimeters which measure the two electron sum energy and discriminate partially signals from the background by pulse shape analysis (PSD).

(ii) Tracking detectors of the source≠detector type (TPC, drift chambers, electronic detectors). In this case, the $\beta^-\beta^-$ source plane(s) is placed within the detector tracking volume, defining two or more detector sectors.

(iii) Tracking calorimeters: They are tracking devices where the tracking volume is also the $\beta^-\beta^-$ source. Only one of this type of device is operating (Xenon TPC), but there are others in project.

In the below we discuss about some completed, ongoing and future experiments of $0\nu\beta^-\beta^-$ decay.

Completed Experiments

CANDLES CANDLES was installed at Kamioka underground laboratory in Japan to observe $0\nu\beta^-\beta^-$ decay in ^{48}Ca. After successful first stage of setting up, the lower limit on half life of $0\nu\beta^-\beta^-$ decay found out to be 1.4×10^{22} years [Ogawa *et al.* (2004)], using ELEGANT VI detector system of Oto Cosmo Observatory. CANDLES proceeded with improved background reduction techniques. The choice of ^{48}Ca is due to its high Q value (4.3MeV) resulting in more number of decays, but the natural abundance of ^{48}Ca is $\backsim$0.2% which makes it quite challenging. CANDLES had number of R & D phase for the testing of CaF_2 crystal based detector's testing and in phase IV it came up with a 2 tons of CaF_2 detector system expected to drop down the background rate up to 5×10^{-5} counts/kg/year [Kishimoto *et al.* (2011)]

DCBA (Drift Chamber Beta-ray Analyzer) The DCBA is a device which can measure the momentum and position of β particles emitted in 0ν and $2\nu\beta^-\beta^-$ decay. In the presence of uniform magnetic field, it can reconstruct the three-dimensional track of the particals This device consists of a drift chamber having dimensions $464\times524\times680$ mm^3, a solenoidal coil and cosmic ray veto counters [Ishihara *et al.* (2000)]. If $0\nu\beta^-\beta^-$ decay occurs via Majorana mechanism, the energy distribution of $2\nu\beta^-\beta^-$ decay and $0\nu\beta^-\beta^-$ decay are plotted and the difference between these distribution would yield the required information. The additional cuts due to low energy electrons can improve the signal to noise ratio. Although the DCBA has number of phases for detecting $0\nu\beta^-\beta^-$ decay in ^{150}Nd and claiming the sensitivity up to 0.05-0.1 eV but unfortunately this method of separation could only improve the signal to noise ratio up to 3–4 times and it

does not solve the purpose [Barabash *et al.* (2001)].

GENIUS (Germanium Nitrogen Underground Setup) GENIUS is installed in GRAN SASSO Underground Laboratory. It is a high level multi-channel data acquisition system which can detect signals from 300 detectors simultaneously. In this setup crystals were placed on a special type of teflon plate in a thin-walled copper box filled with 70 liters of highly purified nitrogen. High purity Germanium detectors were used to detect the $0\nu\beta^-\beta^-$ decay in ^{76}Ge on the basis of the accumulated data obtained with Bayesian method. The half-life and effective neutrino masses corresponding to the matrix elements of [Staudt *et al.* (1990)] were 0.80-35.07$\times10^{25}$yr and 0.08-0.54 eV respectively [Klapdor-Kleingrothaus (2003)].

ELEGANT (ELectron GAmma-ray Neutrino Telescope) ELEGANT is a three segment detector system with plastic scintillator array and Sodium Iodide [NaI(TI)] detectors. Aim of the experiment is to search $0\nu\beta^-\beta^-$ decay in ^{48}Ca and ^{100}Mo nuclei. It is installed in Kamioka underground laboratory at Japan. The entire setup is packed in a air tight container [Fushimi *et al.* (2002)]. Each segment has a drift chamber to record the track of particles. Plastic scintillation detectors record the timing of radiation. The X-rays and γ rays are detected by NaI detectors array and $0\nu\beta^-\beta^-$ decay events are identified by rejecting the background radiations due to X-rays and γ rays. The half life limits achieved for ^{48}Ca and ^{100}Mo nuclei are $\geq1.4\times10^{22}$ yr [Ogawa *et al.* (2004)] and $>5.5\times10^{22}$ yr [Ejiri *et al.* (2001)], respectively.

The Heidelberg-Moscow Experiment Heidelberg-Moscow (HM) experiment is a German-Russian Collaborative work for the search of $0\nu\beta^-\beta^-$ decay in ^{76}Ge. The HM experiment operated with 10.9 kg of 86% enriched germanium in the Gran Sasso underground laboratory from August 1990 to May 2003. The final results that set the limit of $0\nu\beta^-\beta^-$ decay for ^{76}Ge to be $T_{1/2}^{(0\nu)} > 1.19 \times 10^{25}$yr [Klapdor-Kleingrothaus *et al.* (2004)].

LUCIFER (Low-background Underground Cryogenic Installation For Elusive Rates) LUCIFER is a calorimeters detectors with high energy resolution, comprises of an array of scintillating bolometer searching the $0\nu\beta^-\beta^-$ decay of highly pure and enriched ^{82}Se. The purpose of using scintillating bolometers was to detect the energy deposition of particles and electrons as they produce scintillations in ZnSe crystals used in detector. Discrimination between these energy deposition lead to the reduction of background radiation [Cardani *et al.* (2012), Beeman *et al.* (2015)].

CUORICINO The purpose of CUORICINO detector is to detect the $0\nu\beta^-\beta^-$ decay of ^{130}Te. The design of the detector is the extended version of Milano-Como-Gran-Sasso groups with MiDBD experiments. It is an array 44+18 of TeO_2 bolometer detectors arranged in 13 plane tower structure weighing 40.7 kg and having about 11 Kg of ^{130}Te. The suppression of the background radiation is taken in to care by growing crystals with very low contaminations and low radioactive content and the array is hanged inside the vacuum chamber and cooled. A lower bound of $T_{1/2}^{(0\nu)} > 1.8\times10^{24}$ at 90% C.L. has been obtained for ^{130}Te isotope [Arnaboldi *et al.* (2005)].

Ongoing Experiments

AMoRE (Advanced Mo based Rare process Experiment) AMoRE is a multiphase experiment of international collaboration. It is installed in a 700 meter depth Yangyang underground laboratory(Y2L) in South Korea. The aim of the experiment is to detect the $0\nu\beta^-\beta^-$ decay in ^{100}Mo using scintillating Mo crystals. The initial phase of the experiment started with 5, $^{40}Ca^{100}MoO_4$ crystals depleted with ^{48}Ca in the summer of 2015 [Kim *et al.* (2015)]. A 200 kg $^{40}Ca^{100}MoO_4$ was kept under observation and the upper limit of $T_{1/2}^{(0\nu)} > 9.5\times10^{22}$ yr [Alenkov *et al.* (2019)] for $0\nu\beta^-\beta^-$ decay in ^{100}Mo was attained.

CUORE (Cryogenic Underground Observatory for Rare Events) The CUORE is an array of 988 TeO_2 cryogenic bolometric detector arranged in a compact cylindrical and granular structure having 52 crystals which are further arranged in 13 floors having 4 detectors each. It is currently taking data in Gran Sasso National Laboratories (LNGS) situated within the mountains of Gran Sasso, Assergi, Italy. The achievements of the COURE is the successful detection of $2\nu\beta^-\beta^-$ decay in ^{130}Te and measuring the half life $T_{1/2}^{(2\nu)} = (7.9\pm0.1\pm0.2)\times10^{20}$ yr [Caminata *et al.* (2019)]. The half life limit of $0\nu\beta^-\beta^-$ decay achieved in ^{130}Te is $T_{1/2}^{(0\nu)} > 1.5 \times 10^{25}$ yr [Alduino *et al.* (2018)]. Further R&D is in process to increase the sensitivity of the detector to make measurements up to $T_{1/2}^{(0\nu)} > 9.5 \times 10^{25}$ yr.

CUPID (CUore upgrade with Particle Identification) CUPID is the advance version of CUORE experiment proposed to detect $0\nu\beta^-\beta^-$ decay in ^{82}Se isotope. Depending

on the results of COURE it may use either scintillation bolometers based on $ZNMoO_4$, $CdWO_4$ and Li_2MoO_4 crystals or TeO_2 with Cherenov light detection technology. The main aim of the experiment is to explore the Majorana nature of the neutrinos in the inverted hierarchy mass region. It is proposed to be built by deploying the check marks of COURE having improved detector and shielding technologies, enhanced purification and isotopic enrichment. Moreover the quantity of source will be greater than the CUORE and much lesser background radiation. The latest half life measure from the CUPID-0, which is the first pilot experiment of CUPID, is $T_{1/2}^{(0\nu)} > 2.4 \times 10^{24}$ yr for ^{82}Se [Azzolini *et al.* (2018)].

EXO (Enriched Xenon Observatory) EXO-200 detectors are based on Liquid xenon (LXe) time projection chamber(TPC) having two equal volumes, each part has a photoetched phosphor bronze cathode plane connected with large array of photodiodes. Observatory is located at the Waste Isolation Pilot Plant(WIPP) is carlsbad, NM, USA. It started taking data in June 2011, after two and a half years of successful operation got effected by the ground fire. The limits of $T_{1/2}^{(0\nu)} > 1.1{\times}10^{25}$ yr with 90% confidence level for $0\nu\beta^-\beta^-$ decay in ^{136}Xe was established, and precise measurements for $2\nu\beta^-\beta^-$ decay of ^{136}Xe have been published. The phase II of the experiment was started in 2016, and came up with the combine results for $0\nu\beta^-\beta^-$ decay of ^{136}Xe, $T_{1/2}^{(0\nu)} > 5.7{\times}10^{25}$ yr. At present the work is in progress to increasing the sensitivity up to $T_{1/2}^{(0\nu)} > 9.5 \times 10^{25}$yr [Albert *et al.* (2018)].

nEXO Promising results of EXO-200 have indicated that the LXe TPC technology can be a good choice of detection of $0\nu\beta^-\beta^-$ decay as the LXe TPC detectors can reach up

to the high sensitivity of $\backsim 6\times 10^{27}$ yrs. The R&D have been developing for more than a year and came up with the idea of $5\backsim$ton detectors having enriched Xe. Further work for the design and Barium tagging technique still need more focused efforts.

GERDA (GERmanium Detector Array) GERDA is located in Italy in a 3500 m underground Laboratory in LNGS of INFN. The purpose of the underground laboratory is to reduce the muon flux and other cosmic radiations and use other sophisticated measures to allow a bare Germanium detector to work inside a cryogenic liquid argon (LAr) covered by protective shield of water tank. It is a three phase experiment, the initial phase ran from November 2011 to June 2013. The aim of the first run was to verify the claims made by the Heidelberg-Moscow experiment. The second phase of the experiment [Agostini *et al.* (2018*a*)] is totally dedicated to the reduction of the background radiation as low as possible. GERDA phase I and GERDA phase II set the limits on half-life of $0\nu\beta^-\beta^-$ decay for ^{76}Ge as $T_{1/2}^{(0\nu)} > 5.8 \times 10^{25}$ yr and $T_{1/2}^{(0\nu)} > 8 \times 10^{25}$yr [Agostini *et al.* (2018*b*)], respectively. The third phase of GERDA is trying to increase the sensitivity up to $T_{1/2}^{(0\nu)} > 1.5 \times 10^{26}$yr.

KamLAND (Kamioka Liquid scintillator Anti-Neutrino Detector)-Zen This experiment is a modified version of KamLAND, which is in an underground laboratory in Kamioka Observatory near Toyama Japan. The purpose of the KamLAND was to detect the antineutrinos from the nuclear reactors but a decade later in the 2011 modification in the shape and size were made and the detectors were assigned to detect the $0\nu\beta^-\beta^-$ decay with a name KamLAND-Zen. It is a spherical detector with an inner balloon and an outer balloon. The inner balloon with a diameter of 3.08 m contains liquid scintillator

detector filled with 13 tons of Xe. The diameter of the outer balloon is about 13 m. The space in between both balloons is filled with 1 k ton of liquid scintilator which act as a shield for the inner detector against the external radiations. The scintillation light is detected by a series of photomultiplier tube. The energy resolution of these detectors is 9.9% at 2.458 MeV. The phase I and phase II of the detector result in $T_{1/2}^{(0\nu)} > 2.6{\times}10^{24}$ yr with 90% confidence level [Gando *et al.* (2012)] and $T_{1/2}^{(0\nu)} > 1.07{\times}10^{26}$ yr [Gando *et al.* (2016)] for the $0\nu\beta^{-}\beta^{-}$ decay of ^{136}Xe. R&D is in progress to increase the sensitivity up to $T_{1/2}^{(0\nu)} > 2.0 \times 10^{26}$ yr [Shirai *et al.* (2018)].

Majorana It located in an underground laboratory, Sanford Underground Research Facility (SURF) at South Dakota USA. This experiment is an array of isotopically enriched High Purity Germanium detector (HPGe) arranged mainly to reduce the background radiations to the minimum possible value to detect $0\nu\beta^{-}\beta^{-}$ decay in ^{76}Ge and also to calculate the mass and other relative parameters of neutrinos in the inverted-heirarchy mass region. Majorana experiment contains modular assembly of two cryostat having 35 detectors made up of ultra-pure electroformed copper. Each cryostat contains over 20 kg of P-type point-contact high purity germanium detector. The results of the experiment with exposure of 9.95 kg of enriched Ge show the suppression of the background up to $\backsim 1.6{\times}10^{-3}$ c/keV×Kg×yr and a lower limit of half life $T_{1/2}^{(0\nu)} > 1.9 \times 10^{25}$ yr [Aalseth *et al.* (2018)] was obtained. Recently, lower limit on half life $T_{1/2}^{(0\nu)} > 2.7 \times 10^{25}$yr with the exposure of 26 kg of enriched Ge [Alvis *et al.* (2019)] has been achieved.

NEMO (Neutrino Ettore Majorana Observatory) The NEMO collaboration worked on the research and development of the detectors since 1989 by developing two prototype

detectors from 1994 to 2001 and ended up with the construction of Nemo-3 detector. Nemo-3 is a cylindrical shaded detectors with 20 equal parts with a capacity up to 9 kg of seven different $0\nu\beta^-\beta^-$ decay isotopes. These isotopes are surrounded scintillators coupled with the photomultipliers which work as a calorimeter. The whole detector is covered with a 18 cm iron shield and 30 cm borated water to provide a protective shield against the external gamma rays and neutrons to discriminate between the events of $0\nu\beta^-\beta^-$ decay and the background radiation. The soul purpose of the NEMO-3 detectors is to detect and analyze the emitted e^-, e^+, γ and α particles through the tracking chambers and calometric calculations and to understand the $0\nu\beta^-\beta^-$ decay mechanism. The experiment started taking data in January 2003 and ^{96}Zr ,^{100}Mo and ^{150}Nd isotopes were put under the test. The limits on the half-lives were found to be $T_{1/2} > 9.2\times10^{21}$ yr [Argyriades *et al.* (2010)], $T_{1/2} > 1.1\times10^{24}$ yr [Arnold *et al.* (2015)] and $T_{1/2} > 2.2\times10^{22}$ yr [Arnold *et al.* (2016)] for ^{96}Zr ,^{100}Mo and ^{150}Nd isotopes, respectively.

NEXT (Neutrino Experiment with a Xenon TPC) NEXT uses time projection chamber(TPC) facilitated with elecrtoluminescent to detect $0\nu\beta^-\beta^-$ decay in ^{136}Xe. The improved features of the experiment are energy resolution up to 1% FWHM at Q-value and emphasis on reconstruction of tracks of particles that help in discriminating signals from the background radiation. The idea is to place 100 kg xenon gas at high pressure, the electrons liberated due to electroluminescence move towards TPC and accelerated to an array of PMTs and finally digitalized. The signals through the initial phase of the prototypes NEXT-DEMO and NEXT-DBDM have shown promising results of 1% FWHM at 662 keV [Alvarez *et at.* (2016)]. The current stage of experiment is R&D of

event selection simulations, calibration and reconstruction of available data [Martin-Ablo *et at.* (2016)].

SNO+ (Sudbury Neutrino Observatory +) SNO+ is an advancement of Sudbury Neutrino Observatory located as SNOLAB, Ontario, Canada. The sole purpose of the SNO was to study solar neutrinos where as the task assigned to the SNO+ is to search $0\nu\beta^-\beta^-$ decay in ^{130}Te. The detectors are acrylic spherical vessel filled with 780 tons of liquid scintillators with ^{130}Te and surrounded by thousands of photo multipliers. This entire setup is surrounded by an ultra-pure water which provide a shielding to the detector [Andringa *et at.* (2016)]. The phase I of the experiment is water phase which searches the decay of ^{16}O nucleons, next phase is Scintillator phase which measures the low energy solar neutrinos and the third phase is Tellurium phase which is dedicated to the detection of $0\nu\beta^-\beta^-$ decay in ^{130}Te. The current ongoing experimental data analysis claim to achieve the sensitivity of half life up to $T_{1/2}^{(0\nu)} > 2 \times 10^{26}$yr with 90% confidence level in years to come [Fischer *et at.*(2018), Paton *et at.* (2019)].

TGV (Telescope Germanium Vertical) TGV is a collaborative research project between Joint Institute for Nuclear Research, Dubna, Czech Technical University, Prague and CSNSM Orsay [Brudanin *et at.* (2000*a*)], to detect $0\nu\beta^-\beta^-$ decay in ^{48}Ca and $0\nu ECEC$ decay in ^{106}Cd nuclei. The aim of the experiment is to distinguish between β particles and γ rays using 16 HPGe multidetector spectrometer. The data can be helpful in the suppression of the background which is an important feature required for the detection of $0\nu\beta^-\beta^-$ decay. The estimation of half life of $0\nu\beta^-\beta^-$ decay in ^{48}Ca is found to be $T_{1/2}^{(0\nu)} > 1.5{\times}10^{21}$ yr with 90% confidence level [Brudanin *et at.* (2000*b*)].

Cadmium ^{106}Cd was also put under observation in modified version of the experiment (TGV-2) to detect the $0\nu ECEC$ decay and has provided a limit of $T_{1/2}^{(0\nu)} > 1.6{\times}10^{20}$ yr with 90% confidence level [Rukhadze *et al.* (2012)].

Future Experiment

SuperNemo SuperNemo is an extended and advanced version of Nemo-3, and currently working for the development of tracker. Maintaining the aspect of keeping the $\beta^-\beta^-$ source separate from the detector, Super Nemo could be used for other isotopes of $\beta^-\beta^-$ decay. The improved design of the detector would minimize the background by identifying and distinguishing the traces of the electrons, positron, gamma rays and alpha particles in magnetic field. The new features and measurements of the parameters like energy vertices, time of flight and electron tracks help to reconstruct and understand the kinematics of topology of an event. The SuperNEMO comprises of 20 identical detector modules and is ready to run with ^{82}Se as the baseline isotope [Barabash *et at.* (2017), Cascella (2016)]. The ^{150}Nd and ^{48}Ca are other possible candidates to be considered. A thin foil of the source will be placed inside the detector surrounded by a gas chamber and calorimeter walls which are divided in 712 blocks. The aim of SuperNEMO is to reach a sensitivity $T_{1/2}^{(0\nu)} {>}10^{26}$ yr, corresponding to an effective neutrino mass of 50-100 meV.

LEGEND (Large Enriched Germanium Experiment for Neutrinoless $\beta\beta$ Decay) LEGEND is an international collaboration to observe $0\nu\beta^-\beta^-$ decay in ^{76}Ge. After the successful background reduction of Majorana Demonstrator and GERDA experiment, LEGEND aims further to increase the sensitivity up to 10^{28} yr. It is a two phase exper-

iment which will use the infrastructure of Majorana Demonstrator and GERDA with several modification like ultra pure materials, more sensitive pulse shape discriminator and additional mass. The purpose of the experiment is to deploy 200 kg of detector in the cryostat to make the least background measurements of the $0\nu\beta^-\beta^-$ decay. In subsequent phases, the size of the detector will be increased up to 1000 kg to get more and more events and the sensitivity will be improved up to $T^{(0\nu)}_{1/2} \backsim 10^{28}$yr [Andringa *et al.* (2016), Abgrall *et at.* (2017)].

1.3 Present motivation

Our present aim is to study the $0\nu\beta^-\beta^-$ decay of some nuclei in the mass range $90 \leq A \leq 150$ for the $0^+ \rightarrow 0^+$ transition to extract various gauge-theoretical parameters, namely effective light neutrino mass $< m_\nu >$, the effective weak coupling constants $< \lambda >$ and $< \eta >$ for coupling of right-handed leptonic current with right-handed and left-handed nucleonic currents. The present aim of all theoretical calculations is to evaluate reliable NTMEs for the $0\nu\beta^-\beta^-$ decay so that the mentioned gauge-theoretical parameters can be extracted as accurately as possible from the observed limits on half-lives $T^{(0\nu)}_{1/2}$. There is no objective way to judge a priori the correctness of theoretical calculations. Since the $2\nu\beta^-\beta^-$ and $0\nu\beta^-\beta^-$ decay modes involve same set of initial and final wave functions, the usual practice is to first calculate $M_{2\nu}$ and compare with the experimentally extracted value. While the NTMEs of $2\nu\beta^-\beta^-$ decay is spin-isospin dependent, the NTMEs of $0\nu\beta^-\beta^-$ decay are energy-momentum dependent also. Hence, the reliability of NTMEs can be judged a priori only on the basis of the success of a nuclear model in explaining

various observed physical properties of nuclei in accordance with the basic philosophy of nuclear many-body theory.

Over the past years, experimental studies involving in-beam γ-ray spectroscopy have yielded a vast amount of data concerning the level energies as well as electromagnetic properties. Hence, the $\beta^-\beta^-$ decay is not an isolated nuclear process. Although the availability of data permits a rigorous and detailed critique of the ingredients of the microscopic framework that seeks to provide a description of these isotopes, most of the calculations of $\beta^-\beta^-$ decay matrix elements performed so far do not satisfy this criterion. Hence, we aim to calculate the yrast spectra, reduced $B(E2)$ transition probabilities and deformation parameters β_2 as well as $M_{2\nu}$, and compare them with the experimentally observed values to test the reliability of wave functions.

All the nuclei undergoing $\beta\beta$ decay are even-even type, in which the pairing degrees of freedom play an important role. Moreover, it has been already conjectured that the deformation can play a crucial role in the case of $2\nu\beta^-\beta^-$ decay of ^{100}Mo and ^{150}Nd [Suhonen *et al.* (1994), Griffiths *et al.* (1992)]. Hence, it is desirable to have a model which incorporates the pairing and deformation degrees of freedom on equal footing in its formalism. The PHFB model is a convenient choice in this sense, which fulfills these requirements.

Our aim is to study the $0\nu\beta^-\beta^-$ decay processes for the $0^+ \rightarrow 0^+$ transition for ^{94,96}Zr, ^{100}Mo, ^{104}Ru, ^{110}Pd, ^{128,130}Te and ^{150}Nd nuclei. It is well known that the pairing part of the two-body interaction is responsible for the reduction of collectivity, whereas the quadrupole-quadrupole (QQ) interaction enhances the collectivity in the nuclear intrinsic wave functions. In other words, the pairing interaction is responsible for the sphericity of

the nucleus, whereas the QQ interaction makes the nucleus deformed. Hence, to examine the explicit role of deformation degrees of freedom vis-à-vis the suppression of $M_{2\nu}$, the pairing plus quadrupole-quadrupole interaction (PQQ) [Baranger *et al.* (1968)] is the most appropriate choice. In the present work we use a pairing plus multipolar type of effective two-body interaction.

The present thesis is organized in following five chapters. In Chapter 1, we give introduction of the present work and related literature survey is presented. In Chapter 2, we test the reliability of PHFB wave functions by comparing the calculated yrast spectra, reduced $B(E2{:}0^+ \rightarrow 2^+)$ transition probabilities and deformation parameters β_2 of ^{94,96}Zr, ^{94,96,100}Mo, ^{100,104}Ru, ^{104,110}Pd, ^{110}Cd, ^{128,130}Te, ^{128,130}Xe, ^{150}Nd and ^{150}Sm nuclei participating in the $0\nu\beta^-\beta^-$ decay, with the available experimental data. Subsequently, the PHFB wave functions are employed to study the $2\nu\beta^-\beta^-$ decay for the $0^+ \rightarrow J^+$ transition in Chapter 3. In Chapter 4, we study the $0\nu\beta^-\beta^-$ decay of same nuclei in the mass range $90 \leq A \leq 150$ for the $0^+ \rightarrow 0^+$ transition and extract limits on effective gauge theoretical parameters $\langle m_\nu \rangle$, $\langle \lambda \rangle$ and $\langle \eta \rangle$. In Chapter 5, we intend to suggest and discuss a number of necessary improvements that need to be incorporated into the PHFB model for a more reliable study of the $\beta\beta$ decay.

Table 1.1: List of 35 naturally occuring $\beta^-\beta^-$ emitters along with $Q_{\beta\beta}$ for the $0^+ \rightarrow 0^+$ transition, natural abundance of the parent isotope (P) [Wapstra and Audi (1985), Lederer and Shirley (1978)] and deformation parameter β_2 [Raman *et al.* (2001)].

Nuclear	$Q_{\beta\beta}$	$P(\%)$	β_2	
Transition	(keV)		Parent	Daughter
$^{46}_{20}$Ca$\rightarrow^{46}_{22}$Ti	987.0±4.0	0.0035	0.153±0.005	0.317±0.008
$^{48}_{20}$Ca$\rightarrow^{48}_{22}$Ti	**4271.0±4.0**	0.187	0.106±0.018	0.269±0.007
$^{70}_{30}$Zn$\rightarrow^{70}_{32}$Ge	1001.0±3.0	0.62	0.228±0.010	0.2245±0.0026
$^{76}_{32}$Ge$\rightarrow^{76}_{34}$Se	**2039.6±0.9**	7.8	0.2623±0.0039	0.3090±0.0033
$^{80}_{34}$Se$\rightarrow^{80}_{36}$Kr	130.0±9.0	**49.8**	0.2318±0.0027	0.265±0.008
$^{82}_{34}$Se$\rightarrow^{82}_{36}$Kr	**2995.0±6.0**	9.2	0.1934±0.0027	0.2021±0.0045
$^{86}_{36}$Kr$\rightarrow^{86}_{38}$Sr	1256.0±5.0	17.3	0.145±0.006	0.140±0.008
$^{94}_{40}$Zr$\rightarrow^{94}_{42}$Mo	1145.3±2.5	17.4	0.090±0.010	0.1509±0.0015
$^{96}_{40}$Zr$\rightarrow^{96}_{42}$Mo	**3350.0±3.0**	2.8	0.080±0.017	0.1720±0.0016
$^{98}_{42}$Mo$\rightarrow^{98}_{44}$Ru	112.0±7.0	**24.1**	0.1683±0.0028	0.1947±0.0030
$^{100}_{42}$Mo$\rightarrow^{100}_{44}$Ru	**3034.0±6.0**	9.6	0.2309±0.0022	0.2148±0.0011
$^{104}_{44}$Ru$\rightarrow^{104}_{46}$Pd	1299.0±4.0	18.7	0.2707±0.0020	0.209±0.007
$^{110}_{46}$Pd$\rightarrow^{110}_{48}$Cd	**2013.0±19.0**	11.8	0.257±0.006	0.1770±0.0039
$^{114}_{48}$Cd$\rightarrow^{114}_{50}$Sn	534.0±4.0	**28.7**	0.1903±0.0035	0.121±0.013
$^{116}_{48}$Cd$\rightarrow^{116}_{50}$Sn	**2802.0±4.0**	7.5	0.1906±0.0034	0.1118±0.0016
$^{122}_{50}$Sn$\rightarrow^{122}_{52}$Te	364.0±4.0	4.56	0.1036±0.0011	0.1847±0.0008
$^{124}_{50}$Sn$\rightarrow^{124}_{52}$Te	**2288.1±1.6**	5.64	0.0953±0.0011	0.1695±0.0009

Table 1.1 continued

Nuclear Transition	$Q_{\beta\beta}$ (keV)	P(%)	β_2	
			Parent	Daughter
$^{128}_{52}$Te→$^{128}_{54}$Xe	868.0±4.0	**31.7**	0.1363±0.0011	0.1836±0.0049
$^{130}_{52}$Te→$^{130}_{54}$Xe	**2533.0±4.0**	**34.5**	0.1184±0.0014	0.169±0.007
$^{134}_{54}$Xe→$^{134}_{56}$Ba	847.0±10.0	10.4	0.119±0.011	0.1609±0.0009
$^{136}_{54}$Xe→$^{136}_{56}$Ba	**2479.0±8.0**	8.9	0.122±0.010	0.1258±0.0012
$^{142}_{58}$Ce→$^{142}_{60}$Nd	1417.6±2.5	11.1	0.1277±0.0008	0.0917±0.0010
$^{146}_{60}$Nd→$^{146}_{62}$Sm	56.0±5.0	17.2	0.1524±0.0025	-
$^{148}_{60}$Nd→$^{148}_{62}$Sm	1928.3±1.9	5.7	0.2013±0.0037	0.1423±0.0030
$^{150}_{60}$Nd→$^{150}_{62}$Sm	**3367.1±2.2**	5.6	0.2853±0.0021	0.1931±0.0021
$^{154}_{62}$Sm→$^{154}_{64}$Gd	1251.9±1.5	**22.6**	0.3410±0.0020	0.3120±0.0028
$^{160}_{64}$Gd→$^{160}_{66}$Dy	1729.5±1.4	**21.8**	0.3534±0.0020	0.3387±0.0036
$^{170}_{68}$Er→$^{170}_{70}$Yb	653.9±1.6	14.9	0.3363±0.0029	0.3258±0.0037
$^{176}_{70}$Yb→$^{176}_{72}$Hf	1078.8±2.7	12.6	0.305±0.005	0.2953±0.0028
$^{186}_{74}$W→$^{186}_{76}$Os	490.3±2.2	**28.6**	0.2257±0.0039	0.2000±0.0034
$^{192}_{76}$Os→$^{192}_{78}$Pt	417.0±4.0	**41.0**	0.1667±0.0012	0.1532±0.0016
$^{198}_{78}$Pt→$^{198}_{80}$Hg	1048.0±4.0	7.2	0.1141±0.0006	0.1065±0.0006
$^{204}_{80}$Hg→$^{204}_{82}$Pb	416.5±1.9	6.9	0.0686±0.0006	0.0412±0.0005
$^{232}_{90}$Th→$^{232}_{92}$U	858.0±6.0	**100**	0.2608±0.0014	0.264±0.013
$^{238}_{92}$U→$^{238}_{94}$Pu	1145.8±1.7	**99.275**	0.2863±0.0024	0.2861±0.0019

Table 1.2 : NTMEs $\left|M^{(0\nu)}\right|$ due to light neutrino exchange in different nuclear models.

Nuclie	Model	Ref.	g_A	Jastrow	UCOM	AV18	CD Bonn
^{48}Ca	SM	[Horoi *et al.*, (2010)]	1.25	0.570		0.845	0.779
	SM	[Coraggio *et al.*, (2020)]	1.2723				0.30
	ISM	[Caurier *et al.*, (2008)a]	1.25	0.59			
	ISM	[Caurier *et al.*, (2008)b]	1.25	0.67			
	ISM	[Menedez *et al.*, (2009)]	1.25	0.61	0.85		
	ShM	[Neacsu *et al.*, (2014)]	1.25	0.508		0.733	0.809
	ShM	[Neacsu *et al.*, (2014)]	1.275				0.800
	ShM	[Neacsu *et al.*, (2014)]	1.25	0.628		0.884	0.969
	ShM	[Neacsu *et al.*, (2014)]	1.275				0.960
	QRPA	[Simkovic *et al.*, (2009)]	1.27			0.541	0.594
	EDF	[Rodriguez *et al.*, (2010)]	1.254		2.37		
	EDF	[Vaquero *et al.*, (2013)]			2.229		
	REDF	[Yao *et al.*, (2015)]			2.94		
	IBM	[Barea *et al.*, (2012)]	1.269			2.28	
	IBM-2	[Barea *et al.*, (2013)]	1.269	1.98		2.28	2.38
	IBM-2	[Barea *et al.*, (2015)]	1.269			1.75	
	CDFT	[Song *et al.*, (2017)]	1.254	3.26		3.62	3.74
^{76}Ge	SM	[Senekov *et al.*, (2014)]	1.25	2.72		3.37	3.57
	SM	[Coraggio *et al.*, (2020)]	1.2723				2.66
	ISM	[Caurier *et al.*, (2008)a]	1.25	2.22			
	ISM	[Caurier *et al.*, (2008)b]	1.25	2.35			
	ISM	[Menedez *et al.*, (2009)]	1.25	2.30	2.81		
	ShM	[Neacsu *et al.*, (2014)]	1.25	2.378		2.979	3.177
	QRPA	[Simkovic *et al.*, (2009)]	1.254			5.81	6.32
	QRPA	[Faessler *et al.*, (2012)]	1.254	4.92	5.98	6.34	6.89
	QRPA	[Simkovic *et al.*, (2013)]	1.27			5.157	5.571
	pnQRPA	[Kortelainen *et al.*, (2007)]	1.254	5.811	7.734		
	pnQRPA	[Civitarese *et al.*, (2009)]	1.25	4.029	5.355		

Table 1.2 continued

Nuclie	Model	Ref.	g_A	Jastrow	UCOM	AV18	CD Bonn
	pnQRPA	[Fang *et al.*, (2011)]	1.25				4.69
	pnQRPA	[Hyvarinen *et al.*, (2015)]	1.26				5.26
	(R)QRPA	[Simkovic *et al.*, (2008)]	1.254	3.33–4.68	3.92–5.73		
	RQRPA	[Simkovic *et al.*, (2009)]	1.254			4.97	5.44
	RQRPA	[Rodriguez *et al.*, (2010)]	1.254	4.28	5.17	5.42	5.93
	DQRPA	[Mustonen *et al.*, (2013)]	1.25				
	DQRPA	[Fang *et al.*, (2018)]	1.27			3.12	3.40
	EDF	[Rodriguez *et al.*, (2010)]	1.25		4.60		
	EDF	[Vaquero *et al.*, (2013)]	1.25		5.551		
	IBM-2	[Barea *et al.*, (2009)]	1.25	5.465			
	IBM-2	[Barea *et al.*, (2012)]	1.269			5.98	
	IBM-2	[Barea *et al.*, (2013)]	1.269	5.42		5.98	6.16
	IBM-2	[Barea *et al.*, (2015)]	1.269			4.68	
	CDFT	[Yao *et al.*, (2015)]	1.254		6.13		
	CDFT	[Song *et al.*, (2017)]	1.254	6.36		7.48	7.84
^{82}Se	SM	[Coraggio *et al.*, (2020)]	1.2723				2.72
	ISM	[Caurier *et al.*, (2008)a]	1.25	2.11			
	ISM	[Caurier *et al.*, (2008)b]	1.25	2.26			
	ISM	[Menedez *et al.*, (2009)]	1.25	2.18	2.64		
	ShM	[Neacsu *et al.*, (2014)]	1.25	2.176		2.703	2.878
	QRPA	[Simkovic *et al.*, (2009)]	1.254			5.19	5.65
	QRPA	[Faessler *et al.*, (2012)]	1.254	4.39	5.32	5.66	6.16
	pnQRPA	[Civitarese *et al.*, (2009)]	1.25	2.771	3.722		
	pnQRPA	[Hyvarinen *et al.*, (2015)]	1.26			3.73	
	(R)QRPA	[Simkovic *et al.*, (2008)]	1.254	2.82-4.17	3.35-5.09		
	RQRPA	[Simkovic *et al.*, (2009)]	1.254			4.44	4.86
	RQRPA	[Faessler *et al.*, (2012)]	1.254	3.81	4.59	4.84	5.30
	DQRPA	[Neacsu *et al.*, (2014)]	1.27			2.86	3.13
	EDF	[Rodriguez *et al.*, (2010)]	1.25		4.22		

Table 1.2 continued

Nuclie	Model	Ref.	g_A	Jastrow	UCOM	AV18	CD Bonn
	EDF	[Vaquero *et al.*, (2013)]	1.25		4.674		
	IBM-2	[24][Barea *et al.*, (2009)]	1.25	4.412			
	IBM-2	[Barea *et al.*, (2012)]	1.269			4.84	
	IBM-2	[Barea *et al.*, (2013)]	1.269	4.37			
	IBM-2	[Barea *et al.*, (2015)]	1.269			3.73	
	CDFT	[Yao *et al.*, (2015)]	1.254		5.40		
	CDFT	[Song *et al.*, (2017)]	1.254	6.38		7.48	7.83
^{96}Zr	QRPA	[Faessler *et al.*, (2012)]	1.25	1.22	1.77	2.07	
	RQRPA	[Faessler *et al.*, (2012)]	1.25	1.31	1.77	2.01	2.19
	(R)QRPA	[Simkovic *et al.*, (2009)]	1.254	1.01-1.34			1.43-2.12
	RQRPA	[Simkovic *et al.*, (2009)]	1.254	1.01-1.34			1.31-1.79
	pnQRPA	[Civitarese *et al.*, (2009)]	1.25	-2.065	-3.117		
	pnQRPA	[Hyvarinen *et al.*, (2015)]	1.26				3.14
	EDF	[Rodriguez *et al.*, (2010)]	1.254		5.65		
	EDF	[Vaquero *et al.*, (2013)]	1.25		6.498		
	REDF	[Yao *et al.*, (2015)]	1.254		6.47		
	IBM	[Barea *et al.*, (2012)]	1.269			2.89	
	IBM-2	[Barea *et al.*, (2013)]	1.269	2.53		2.89	3.00
	IBM-2	[[Barea *et al.*, (2015)]	1.269			2.83	
	CDFT	[Song *et al.*, (2017)]	1.254	4.84		5.58	5.82
^{100}Mo	QRPA	[Faessler *et al.*, (2012)]	1.25	3.64	4.71	5.18	5.73
	QRPA	[Simkovic *et al.*, (2013)]	1.27			5.402	5.850
	(R)QRPA	[Simkovik *et al.*, (2008)]	1.254	2.22-3.53	2.77-4.58		
	(R)QRPA	[Simkovic *et al.*, (2009)]	1.254	2.22-3.53			2.91-5.56
	pnQRPA	[Civitarese *et al.*, (2009)]		-2.737	-3.931		
	pnQRPA	[Hyvarinen *et al.*, (2015)]	1.26				3.90
	EDF	[Rodriguez *et al.*, (2010)]	1.254		5.08		
	EDF	[Vaquero *et al.*, (2013)]	1.25		6.588		
	REDF	[Yao *et al.*, (2015)]	1.254		6.58		

Table 1.2 continued

Nuclie	Model	Ref.	g_A	Jastrow	UCOM	AV18	CD Bonn
	IBM	[Barea *et al.*, (2009)]	1.25	3.732			
	IBM	[Barea *et al.*, (2009)]	1.25	4.217			
	IBM	[Barea *et al.*, (2012)]	1.269			4.31	
	IBM-2	[Barea *et al.*, (2013)]	1.269	3.73		4.31	4.50
	IBM-2	[Barea *et al.*, (2015)]	1.269			4.22	
	CDFT	[Song *et al.*, (2017)]	1.254	9.38		10.80	11.27
^{116}Cd	QRPA	[Rodin *et al.*, (2003)]	1.25	2.99			
	QRPA	[Simkovic *et al.*, (2009)]	1.25	2.99	3.74	3.86	4.35
	QRPA	[Rodrıguez *et al.*, (2010)]	1.27			4.053	4.367
	QRPA	[Vaquero *et al.*, (2013)]	1.25	3.034	3.935		
	pnQRPA	[Civitarese *et al.*, (2009)]	1.254			-3.54	-3.99
	pnQRPA	[Hyvarinen *et al.*, (2015)]	1.26				4.26
	RQRPA	[Rodin *et al.*, (2003)]		2.64			
	RQRPA	[Simkovik *et al.*, (2008)]				3.06	3.41
	RQRPA	[Simkovic *et al.*, (2009)]		2.64	3.21	3.34	3.72
	(R)QRPA	[Rodrıguez *et al.*, (2010)]	1.254	1.83-2.93	2.18-3.54		
	EDF	[Rodrıguez *et al.*, (2010)]	1.254		4.72		
	EDF	[Vaquero *et al.*, (2013)]	1.25	5.348			
	EDF	[Rodríguez *et al.*, (2014)]	1.25		4.8		
	REDF	[Yao *et al.*, (2015)]			5.52		
	IBM-2	[Barea *et al.*, (2012)]	1.269			3.16	
	IBM-2	[Barea *et al.*, (2013)]	1.269	2.78		3.16	3.29
	IBM-2	[Barea *et al.*, (2015)]	1.269			3.10	
	CDFT	[Song *et al.*, (2017)]	1.254	5.18		6.08	6.37
	CDFT	[Meng *et al.*, (2017)]			6.18		
^{128}Te	ISM	[Caurier *et al.*, (2008)a]	1.25	2.26			
	ISM	[Caurier *et al.*, (2008)b]	1.254	2.67			
	QRPA	[Simkovic *et al.*, (2009)]	1.254			4.93	5.49

able 1.2 continued

Nuclie	Model	Ref.	g_A	Jastrow	UCOM	AV18	CD Bonn
	QRPA	[Rodrıguez *et al.*, (2010)]	1.25	3.97	5.04	5.38	5.99
	pnQRPA	[Civitarese *et al.*, (2009)]	1.25	-3.383	4.790		
	pnQRPA	[Hyvarinen *et al.*, (2015)]	1.26				4.92
	RQRPA	[Simkovic *et al.*, (2009)]				4.32	4.82
	RQRPA	[Rodrıguez *et al.*, (2010)]		3.52	4.45	4.71	5.26
	(R)QRPA	[Simkovik *et al.*, (2008)]	1.254	2.46-3.77	3.06-4.76		
	EDF	[Rodrıguez *et al.*, (2010)]	1.254		4.11		5.13
	EDF	[Vaquero *et al.*, (2013)]	1.25		5.687		
	IBM	[Barea *et al.*, (2009)]	1.25	4.517			
	IBM	[Barea *et al.*, (2009)]	1.25	3.845			
	IBM-2	[Barea *et al.*, (2012)]	1.269			4.97	
	IBM-2	[Barea *et al.*, (2013)]	1.269	4.48		4.97	5.13
	IBM-2	[Barea *et al.*, (2015)	1.269			4.10	
^{130}Te	SM	[Coraggio *et al.*, (2020)]	1.2723				3.16
	GCM	[Jiao[PRC *et al.*, (2018)]	1.254				2.52
	SM	[Neacsu *et al.*, (2015)]	1.254			1.80	1.94
	ISM	[Caurier *et al.*, (2008)a]	1.25	2.04			
	ISM	[Caurier *et al.*, (2008)b]	1.25	2.41			
	QRPA	[Simkovic *et al.*, (2009)]	1.254			4.37	4.92
	QRPA	[Rodrıguez *et al.*, (2010)]	1.25	3.56	4.53	4.77	5.37
	pnQRPA	[Civitarese *et al.*, (2009)]	1.25	-2.993	-4.221		
	pnQRPA	[Hyvarinen *et al.*, (2015)]	1.26				4.00
	RQRPA	[Simkovic *et al.*, (2009)]				3.91	4.40
	RQRPA	[Rodrıguez *et al.*, (2010)]		3.22	4.07	4.27	4.80
	(R)QRPA	[Simkovik *et al.*, (2008)]	1.254	2.27-3.38			
	DQRPA	[Mustonen *et al.*, (2013)]	1.25	1.37			
	DQRPA	[Fang *et al.*, (2018)]				2.90	3.22
	EDF	[Rodrıguez *et al.*, (2010)]	1.254		5.13		
	EDF	[Vaquero *et al.*, (2013)]	1.25		6.405		

Table 1.2 continued

Nuclie	Model	Ref.	g_A	Jastrow	UCOM	AV18	CD Bonn
	REDF	[Yao *et al.*, (2015)]	1.254		4.98		
	IBM	[Barea *et al.*, (2009)]	1.25	4.059			
	IBM	[Barea *et al.*, (2009)]		3.372			
	IBM-2	[Barea *et al.*, (2012)]	1.269			4.47	
	IBM-2	[Barea *et al.*, (2013)]	1.269	4.03		4.47	4.61
	IBM-2	[Barea *et al.*, (2015)]	1.269			3.70	
	CDFT	[Song *et al.*, (2017)]	1.254	8.03		9.38	9.82
^{136}Xe	SM	[Neacsu *et al.*, (2015)]	1.254			1.63	1.76
	SM	[Coraggio *et al.*, (2020)]	1.2723				2.39
	GCM	[Jiao[PRC *et al.*, (2018)]	1.254				2.35
	ISM	[Caurier *et al.*, (2008)a]	1.25	1.70			
	ISM	[Caurier *et al.*, (2008)b]	1.25	2.00			
	IS M	[Menedez *et al.*, (2009)]	1.25	1.76	2.19		
	QRPA	[Simkovic *et al.*, (2008)]	1.254	1.17	1.49		
	QRPA	[Rodrıguez *et al.*, (2010)]	1.25	2.16	2.73	2.88	3.23
	pnQRPA	[Civitarese *et al.*, (2009)]	1.25	-2.053	-2.802		
	pnQRPA	[Hyvarinen *et al.*, (2015)]	1.26				2.91
	(R)QRPA	[Simkovic *et al.*, (2009)]	1.254	1.17-2.22			1.57-3.24
	RQRPA	[Rodrıguez *et al.*, (2010)]	1.25	2.02	2.54	2.68	3.00
	DQRPA	[Mustonen *et al.*, (2013)]	1.25	1.55			
	DQRPA	[Fang *et al.*, (2018)]	1.27			1.11	1.18
	EDF	[Rodrıguez *et al.*, (2010)]	1.254		4.20		
	EDF	[Vaquero *et al.*, (2013)]	1.25		4.773		
	REDF	[Yao *et al.*, (2015)]	1.254		4.32		
	IBM-2	[Barea *et al.*, (2012)]	1.269			3.67	
	IBM-2	[Barea *et al.*, (2013)]	1.269	3.33		3.67	3.79
	IBM-2	[Barea *et al.*, (2015)]	1.269			3.06	
	CDFT	[Meng *et al.*, (2017)]			6.59		
	CDFT	[Song *et al.*, (2017)]	1.254	5.58		6.51	6.80

Table 1.2 continued

Nuclie	Model	Ref.	g_A	Jastrow	UCOM	AV18	CD Bonn
^{150}Nd	QRPA	[Terasaki *et* at., (2015)]	1.25				3.604
	pnQRPA	[Fang *et al.*, (2011)]	1.25	3.34			6.12
	DQRPA	[Mustonen *et al.*, (2013)]	1.25	2.71			
	EDF	[Rodrıguez *et al.*, (2010)]	1.254		1.71		
	E D F	[Vaquero *et al.*, (2013)]	1.25		2.190		
	REDF	[Song *et al.*, (2017)]	1.254	5.60			
	REDF	[Song *et al.*, (2017)]	1.254	4.68			
	IBM	[Barea *et al.*, (2009)]	1.25	2.321			
	IBM	[Barea *et al.*, (2009)]	1.25	2.888			
	IBM-2	[Iachello *et al.*, (2011)]	1.25	2.321			
	IBM-2	[Barea *et al.*, (2012)]	1.269			2.74	
	IBM-2	[Barea *et al.*, (2013)]	1.269	2.32		2.74	2.88
	IBM-2	[Barea *et al.*, (2015)]	1.269			2.67	

Table 1.3: Experimental half lives $T^{2\nu}_{1/2}$ of $2\nu\beta^-\beta^-$ decay of A = 48, 76, 82, 94, 96, 100, 110, 116, 128, 130, 136, 150, 238 and 244 nuclei for the $0^+ \rightarrow 0^+$ transition. †denotes all modes.

Transition	$T^{2\nu}_{1/2}$ (yr)	Project	Reference
^{48}Ca→^{48}Ti	$(6.4^{+0.7}_{-0.6})\times10^{19}$	NEMO 3	[Arnold.*et al.*(2016)]
	$(4.4^{+0.5}_{-0.4}\pm0.4)\times10^{19}$	NEMO 3	[Barabash *et al.*(2011)]
	9.0×10^{19}	ITEP+CSNS+ JINR+FNSPE	[Bakalyarov *et al.* (2002)]
	$(4.2^{+3.3}_{-1.3})\times10^{19}$	TGV	[Brudanin *et al.* (2000)]
	$(4.3^{+2.4}_{-1.1}\pm1.4)\times10^{19}$	UC Irvine	[Balysh *et al.*(1996)]
	$>3.6\times10^{19}$		[Bardin *et al.* (1970)]
	$(5.3^{+1.2}_{-0.8})\times10^{19}$	Average	[Barabash (2019)]
^{76}Ge→^{76}Se	$(1.925\pm0.094)\times10^{21}$	GERDA	[Agostini *et al.* (2015)]
	$(1.84^{+0.14}_{-0.10})\times10^{21}$	GERDA	[Agostini *et al.* (2013)]
	$(1.74\pm0.01^{+0.18}_{-0.16})\times10^{21}$		[Dorr *et al.*(2003)]
	$(1.55\pm0.01^{+0.19}_{-0.15})\times10^{21}$	HM	[Klapdor *et al.* (2001)]
	$(1.45\pm0.15)\times10^{21}$	IGEX	[Morales (1999)]
	$(1.77^{+0.01\ +0.13}_{-0.01\ -0.11})\times10^{21}$	HM	[Gunther *et al.* (1997)]
	$(1.1\pm0.2)\times10^{21}$	IGEX	[Aalseth *et al.* (1996)]
	$(1.2^{+0.2}_{-0.1})\times10^{21}$		[Avignone (1994)]
	$(8.4^{+1.0}_{-0.8})\times10^{20}$	IGEX	[Brodzinski *et al.* (1993)]
	$(9.2^{+0.7}_{-0.4})\times10^{20}$	USC+PNL+ ITEP+YPI	[Avignone *et al.* (1991)]
	$(1.1^{+0.6}_{-0.3})\times10^{21}$	PNL+USC	[Miley *et al.* (1991)]
	$(0.9\pm0.1)\times10^{21}$	ITEP+Yerevan	[Vasenko *et al.* (1990)]
	$>5.0\times10^{20}$		[Vuilleumier *et al.* (1988)]
	$>3.0\times10^{20}$	USC+PNL	[Avignone *et al.* (1986)]
	$(1.88\pm0.08)\times10^{21}$	Average	[Barabash (2019)]

Table 1.3 continued

Transition	$T^{2\nu}_{1/2}$ (yr)	Project	Reference
^{82}Se→^{82}Kr	$(0.939\pm0.017)\times10^{20}$	NEMO 3	[Arnold *et al.* (2018)]
	$(9.6\pm0.3\pm1.0)\times10^{19}$	NEMO 3	[Arnold *et al.* (2005)]
	$(10.3\pm0.2\pm1.0)\times10^{19}$	NEMO 3	[Lalanne (2005)]
	$(0.83\pm0.09\pm0.06)\times10^{20}$	NEMO 2	[Piquemal *et al.* (1999)]
	$(8.3\pm1.0\pm0.7)\times10^{19}$	NEMO 2	[Arnold *et al.* (1998)]
	$(1.08^{+0.26}_{-0.06})\times10^{20}$	UC Irvine	[Elliott *et al.* (1992)]
	1.0×10^{20}	Geochemical	[Manuel *et al.* (1991)]
	$(1.2\pm0.1)\times10^{20}$	Geochemical	[Lin *et al.* (1988)]
	$(1.1^{+0.8}_{-0.3})\times10^{20}$	UC Irvine	[Elliott *et al.* (1987)]
	$(1.3\pm0.05)\times10^{20}$	Geochemical	[Kirsten *et al.* (1986)]
	$(0.93\pm0.05)\times10^{20}$	Average	[Barabash (2019)]
^{94}Zr→^{94}Mo	$>1.1\times10^{17}$	NEMO 2	[Arnold *et al.* (1999)]
^{96}Zr→^{96}Mo	$(2.35\pm0.14\pm0.16)\times10^{19}$	NEMO 3	[Argyriades *et al.* (2010)]
	$(2.0\pm0.3\pm0.2)\times10^{19}$	NEMO 3	[Lalanne (2005)]
	$(9.4\pm3.2)\times10^{18}$	Geochemical	[Wieser *et al.* (2001)]
	$(2.1^{+0.8}_{-0.4}\pm0.2)\times10^{19}$	NEMO 2	[Arnold *et al.* (1999)]
	$(2.0^{+0.9}_{-0.5}\pm0.5)\times10^{19}$	NEMO 2	[Barabash (1998)]
	$(3.9\pm0.9)\times10^{19}$	Geochemical	[Kawashima *et al.* (1993)]
	$(2.3\pm0.2)\times10^{19}$	Average	[Barabash (2019)]
^{100}Mo→^{100}Ru	$(6.81\pm0.01)\times10^{18}$	NEMO 3	[Arnold *et al.* (2019)]
	$(7.12^{+0.18}_{-0.14}\pm0.10)\times10^{18}$	CUPID	[Armengaud *et al.* (2019)]
	$(6.90\pm0.15\pm0.37)\times10^{18}$	CUPID	[Armengaud *et al.* (2017)]
	$(7.15\pm0.37\pm0.66)\times10^{18}$	INFN	[Cardani *et al.* (2014)]
	$(7.11\pm0.02\pm0.54)\times10^{18}$	NEMO 3	[Arnold *et al.* (2005)]

Table 1.3 continued

Transition	$T^{2\nu}_{1/2}$ (yr)	Project	Reference
	$(7.72\pm0.02\pm0.54)\times10^{18}$	NEMO 3	[Lalanne (2005)]
	$(2.1\pm0.3)\times10^{18}$	Geochemical	[Hidaka *et al.* (2004)]
	$(7.2\pm0.9\pm1.8)\times10^{18}$	ITEP+INFN	[Ashitkov *et al.* (2001)]
	8.5×10^{18}	ITEP+INFN	[Ashitkov *et al.* (1999)]
	$(6.82^{+0.38}_{-0.53}\pm0.68)\times10^{18}$	UC Irvine	[De Silva *et al.* (1997]
	$(7.6^{+2.2}_{-1.4})\times10^{18}$	LBL+MHC+ UNM+INEL	[Alston-Garnjost *et al.* (1997)]
	$(9.5\pm0.4\pm0.9)\times10^{18}$	NEMO 2	[Dassie *et al.* (1995)]
	$(11.6^{+3.4}_{-0.8})\times10^{18}$	UC Irvine	[Elliot *et al.,* (1991)]
	$(11.5^{+3.0}_{-2.0})\times10^{18}$	ELEGANT V	[Ejiri *et al.*(1991)]
	$(3.3^{+2.0}_{-1.0})\times10^{18}$	INS Baksan	[Vasilev *et al.* (1990)]
	$(6.88\pm0.25)\times10^{18}$	Average	[Barabash (2019)]
^{110}Pd$\rightarrow^{110}$Cd	$>6.0\times10^{16}$		[Winter (1952)]
^{116}Cd$\rightarrow^{116}$Sn	$(2.63^{+0.11}_{-0.12})\times10^{19}$	Aurora	[Barabash *et al.* (2018)]
	$(2.74\pm0.04\pm0.18)\times10^{19}$	NEMO 3	[Arnold *et al.* (2017)]
	$(2.80\pm0.05\pm0.4)\times10^{19}$	INR	[Poda *et al.* (2014)]
	$(2.88\pm0.04\pm0.16)\times10^{19}$	-	[Barabash (2011)]
	$(2.8\pm0.1\pm0.3)\times10^{19}$	NEMO 3	[Lalanne (2005)]
	$(2.9\pm0.1^{+0.4}_{-0.3})\times10^{19}$	INR	[Danevich *et al.* (2003)]
	$(2.6\pm0.1^{+0.7}_{-0.4})\times10^{19}$	INR+INFN	[Danevich *et al.* (2000)]
	$(3.75\pm0.35\pm0.21)\times10^{19}$	NEMO 2	[Arnold *et al.* (1996)]
	$(2.7^{+0.5}_{-0.4}\pm0.9)\times10^{19}$	INR	[Danevich *et al.* (1995)]
	$(2.6^{+0.9}_{-0.5})\times10^{19}$	Osaka	[Ejiri *et al.* (1995)]
	$(2.6^{+0.9}_{-0.5}\pm0.35)\times10^{19}$		[Kume *et al.,* (1994)]
	$(2.69\pm0.09)\times10^{19}$	Average	[Barabash (2019)]

Table 1.3 continued

Transition	$T^{2\nu}_{1/2}$ (yr)	Methods	Reference
^{128}Te$\rightarrow^{128}$Xe	$(2.41\pm0.39)\times10^{24}$	Geochemical	[Meshik *et al.*(2008)]
	$(2.3\pm0.3)\times10^{24}$	Geochemical	[Thomas *et al.*(2008)]
	$(2.2\pm0.3)\times10^{24}$	Geochemical	[Takaoka *et al.* (1996)]
	$(7.7\pm0.4)\times10^{24}$	Geochemical	[Bernatovicz *et al.* (1993)]
	2.2×10^{24}	Geochemical	[Manuel (1991)]
	$(1.8\pm0.7)\times10^{24}$	Geochemical	[Lin *et al.* (1988)]
	$>5\times10^{24}$	Geochemical	[Kirsten *et al.* (1986)]
	$(2.25\pm0.09)\times10^{24}$	Recommended	[Barabash (2019)]
^{130}Te$\rightarrow^{130}$Xe	$(7.9\pm0.1\pm0.2)\times10^{20}$	CUORE	[Caminata *et al.* (2019)]
	$(8.2\pm0.2\pm0.6)\times10^{20}$	CUORE 0	[Alduino *et al.* (2017)]
	$(7.0\pm0.9\pm1.1)\times10^{20}$	NEMO 3	[Arnold *et al.* (2011)]
	$6.1\pm1.4^{+2.9}_{-3.5}$	INFN+LNGS	[Arnaboldi *et al.* (2003)]
	$>3.0\times10^{20}$	INFN+LNGS	[Alessandrello *et al.* (2000)]
	$(7.9\pm1.0)\times10^{20}$	Geochemical	[Takaoka *et al.* (1996)]
	$(2.7\pm0.1)\times10^{21}$	Geochemical	[Bernatovicz *et al.* (1993)]
	0.8×10^{21}	Geochemical	[Manuel (1991)]
	$>8.0\times10^{20}$		[Bellotti *et al.* (1987)]
	$(2.7\pm0.1)\times10^{21}$	Recommended	[Elliott *et al.* (2002)]
	$(7.19\pm0.21)\times10^{20}$	Average	[Barabash (2019)]
^{136}Xe$\rightarrow^{136}$Ba	$(2.21\pm0.02\pm0.07)\times10^{21}$	KamLAND Zen	[Gando *et al.* (2016)]
	$(2.165\pm0.016\pm0.0059)\times10^{21}$	EXO-200	[Albert *et al.*(2014)]
	$(2.30\pm0.02\pm0.12)\times10^{21}$	KamLAND-Zen	[Gando *et al.*(2012)]
	$>1.0\times10^{22}$	INFN	[Bernabei *et al.* (2002)]
	$>8.1\times10^{20}$	INR	[Gavriljuk *et al.* (2000)]
	$>5.5\times10^{20}$	Gotthard tunnel	[Busto *et al.*,(1996)]

Table 1.3 continued

Transition	$T^{2\nu}_{1/2}$ (yr)	Project	Reference
	$(2.18\pm0.05)\times10^{21}$	Average	[Barabash (2019)]
^{150}Nd→^{150}Sm	$(9.34\pm0.22\pm0.63)\times10^{18}$	NEMO 3	[Arnold *et al.*(2016)]
	$(9.11^{+0.25}_{-0.22}\pm0.63)\times10^{18}$	NEMO 3	[Argyriades *et al.* (2009)]
	$(9.7\pm0.7\pm1.0)\times10^{18}$	NEMO 3	[Lalanne (2005)]
	$(6.75^{+0.37}_{-0.42}\pm0.68)\times10^{18}$	UC Irvine	[De Silva *et al.* (1997)]
	$(18.8^{+6.9}_{-3.9}\pm1.9)\times10^{18}$	ITEP +INR	[Artemiev *et al.* (1995)]
	$(17^{+10}_{-5.0}\pm3.5)\times10^{18}$	ITEP +INR	[Artemiev *et al.* (1993)]
	9.0×10^{18}	UC Irvine	[Elliott *et al.* (1993)]
	$>11.0\times10^{18}$	INS Baksan	[Vasilev *et al.* (1993)]
	$>18\times10^{18}$	INR	[Klimenko *et al.* (1986)]
	$(8.4\pm1.1)\times10^{18}$	Average	[Barabash (2019)]
^{238}U→^{238}Pu	$\geq8.1\times10^{10}$	INR	[Tretyak *et al.* (2005)]
	$(2.0\pm0.6)\times10^{21}$	Radiochemical	[Turkevich *et al.* (1991)]
^{244}Pu→^{244}Cm	$\geq1.1\times10^{18\dagger}$	Radiochemical	[Moody *et al.* (1992)]

Table 1.4: Experimental half lives $T^{2\nu}_{1/2}(2^+)$ of $2\nu\beta^-\beta^-$ decay of A = 48, 76, 82, 94, 96, 100, 110, 116, 124, 128, 130, 136, 148, 150, 154, 160, 170, 176 and 186 nuclei for the $0^+ \rightarrow 2^+$ transition.

Transition	$T^{2\nu}_{1/2}(2^+)$ (y)	Project	Reference
^{48}Ca$\rightarrow^{48}$Ti	$> 1.8 \times 10^{20}$	RRCKI+ITEP+FNSPE+JINP	[Bakalyarov *et al.* (2002)]
^{76}Ge$\rightarrow^{76}$Se	$> 3.7 \times 10^{22}$	ITEP+PNPI	[Beck *et al.* (1992)]
	$> 1.1 \times 10^{21}$	IETP	[Barabash *et al.* (1995)]
	$> 1.6 \times 10^{23}$	GERDA	[Agostini *et al.* (2015)]
^{82}Se$\rightarrow^{82}$Kr	$> 1.4 \times 10^{21}$	DPUJ+ITEP	[Suhonen *et al.* (1997)]
	$> 1.0 \times 10^{22}$	LUCIFER	[Beeman *et al.* (2015)]
^{94}Zr$\rightarrow^{94}$Mo	$> 1.3 \times 10^{19}$	NSDLBL	[Norman *et al.* (1987)]
	$> 3.4 \times 10^{19}$	DNAP+INO+DPUL+HBNI	[Dokania *et al.* (2017)]
^{96}Zr$\rightarrow^{96}$Mo	$> 2.0 \times 10^{19}$	NSDLBL	[Norman *et al.* (1987)]
	$> 4.1 \times 10^{19}$	INFN+IETP	[Arpesella *et al.* (1994)]
	$> 7.9 \times 10^{19}$	IETP	[Barabash *et al.* (1996)]

Table 1.4 continued

Transition	$T^{2\nu}_{1/2}(2^+)$(y)	Project	Reference
^{100}Mo$\rightarrow^{100}$Ru	$> 2.3 \times 10^{21}$	-	[Kudomi *et al.* (1992)]
	$> 2.3 \times 10^{21}$	-	[Blum *et al.* (1992)]
	$> 2.3 \times 10^{21}$	ITEP	[Barabash *et al.* (1993)]
	$> 1.6 \times 10^{21}$	ITEP	[Barabash et al (1995)]
	$> 2.5 \times 10^{21}$	NEMO-3	[Arnold *et al.* (2014)]
^{110}Pd$\rightarrow^{110}$Cd	$> 2.9 \times 10^{20}$	-	[Lehnert *et al.* (2016)]
^{116}Cd$\rightarrow^{116}$Sn	$> 2.3 \times 10^{21}$	MPIK+ITEP+INFN	[Piepke *et al.* (1994)]
^{124}Sn$\rightarrow^{124}$Te	$> 4.1 \times 10^{19}$	-	[Smolnikov *et al.*(1985)]
	$> 9.1 \times 10^{20}$	ITEP	[Barabash *et al.* (2009)]
^{128}Te$\rightarrow^{128}$Xe	$> 4.7 \times 10^{21}$	DFU+INFN	[Bellotti *et al.*(1987)]
^{130}Te$\rightarrow^{130}$Xe	$> 4.5 \times 10^{21}$	DFU+INFN	[Bellotti *et al.*(1987)]
	$> 2.8 \times 10^{21}$	INFN	[Bellotti *et al.* (1987)]
	$> 1.6 \times 10^{21}$	ITEP	[Barabash et al (2001)]
^{136}Xe$\rightarrow^{136}$Ba	$> 6.5 \times 10^{21}$	DFU+INFN	[Bellotti *et al.* (1991)]
	$> 4.6 \times 10^{23}$	KamLAND-Zen	[Asakura *et al.* (2016)]

Table 1.4 continued

Transition	$T^{2\nu}_{1/2}(2^+)$(y)	Project	Reference
^{148}Nd$\rightarrow^{148}$Sm	$> 3.0 \times 10^{18}$	IFU+INFN	[Bellotti *et al.* (1982)]
^{150}Nd$\rightarrow^{150}$Sm	$> 8.0 \times 10^{18}$	LNGS+INFN+ITEP+LPI	[Arpesella *et al.* (1994)]
	$> 9.1 \times 10^{19}$	INFN+DFU	[Arpesella *et al.* (1999)]
	$> 2.2 \times 10^{20}$	ITEP	[Barabash *et al.*(2009)]
^{154}Sm$\rightarrow^{154}$Gd	$> 2.3 \times 10^{18}$	-	[Derbin *et al.* (1996)]
^{160}Gd$\rightarrow^{160}$Dy	$> 1.2 \times 10^{17}$	-	[Burachas *et al.*(1993)]
	$> 2.1 \times 10^{19}$	INR	[Danevich et al (2001)]
^{170}Er$\rightarrow^{170}$Yb	$> 3.2 \times 10^{17}$	-	[Derbin *et al.* (1996)]
^{176}Yb$\rightarrow^{176}$Hf	$> 1.6 \times 10^{17}$	-	[Derbin *et al.* (1996)]
^{186}W$\rightarrow^{186}$Os	$> 2.4 \times 10^{20}$	-	[Georgadze *et al.* (1995)]

Table 1.5: Experimental half-life limits $T^{0\nu}_{1/2}$ of $0\nu\beta^-\beta^-$ decay of A = 48, 76, 82, 94, 96, 98, 100, 116, 128, 130, 136, 150 and 238 nuclei for the $0^+ \rightarrow 0^+$ transition.

Transition	$T^{0\nu}_{1/2}$ (yr)	C.L.(%)	Project	Reference
^{48}Ca→^{48}Ti	>1.3 × 10^{22}	90	NEMO 3	[Barabash *et al.*(2011)]
	>2.7×10^{22}	90	GSS+GSE+RCNS	[Umehara *et al.* (2008)]
	≥1.4×10^{22}	90	ELEGANT VI	[Ogawa *et al.* (2004)]
	>1.5×10^{21}	90	TGV	[Brudanin *et al.* (2000)]
	>9.5×10^{21}	76	HEP Beijing	[You *et al.* (1991)]
	>2.0×10^{21}	80		[Bardin *et al.* (1970)]
^{76}Ge→^{76}Se	>9.0×10^{25}	90	GERDA-II	[Agostini *et al.* (2019)]
	>8.0×10^{25}	90	GERDA	[Agostini *et al.* (2018)]
	>1.9×10^{25}	90	MAJORANA	[Aalseth *et al.* (2018)]
	>3.0×10^{25}	90	GERDA	[Agostini *et al.* (2013)]
	>1.57×10^{25}	90	IGEX	[Aalseth *et al.* (2002)]
	>1.9×10^{25}	90	HM	[Klapdor *et al.* (2001)]
	>1.6×10^{25}	90	IGEX	[Gonzalez *et al.* (2000)]
	>1.6×10^{25}	90	HM	[Baudis *et al.* (1999)]
	>1.2×10^{25}	90	MPIH+KIAE	[Morales (1999)]
	>1.1×10^{25}	90	HM	[Baudis *et al.* (1997)]
	>7.4×10^{24}	90	HM	[Gunther *et al.* (1997)]
	>5.6×10^{24}	90	HM	[Balysh *et al.* (1995)]
	>1.4×10^{24}	90	HM	[Balysh *et al.* (1992)]
	>2.5×10^{23}	68	UC+LBL	[Caldwell *et al.* (1986)]
	>1.0×10^{23}	68	PNL+USC	[Avignone *et al.* (1985)]
	>2.0×10^{22}	68		[Forster *et al.* (1984)]
	>1.2×10^{23}	68		[Bellotti *et al.* (1984)]
	>3.0×10^{22}	68		[Simpson *et al.* (1984)]
	>4.0×10^{21}	68		[Leccia *et al.* (1983)]

Table 1.5 continued

Transition	$T^{0\nu}_{1/2}$ (yr)	C.L.(%)	Project	Reference
^{82}Se$\rightarrow^{82}$Kr	$>2.4\times10^{24}$	90	CUPID-0	[Azzolini *et al.* (2018)]
	$>1.0\times10^{23}$	90	NEMO 3	[Arnold *et al.* (2005)]
	$>1.9\times10^{23}$	90	NEMO 3	[Lalanne (2005)]
	$\geq9.5\times10^{21}$	90	NEMO 2	[Arnold *et al.* (1998)]
	$>5.0\times10^{21}$	90	NEMO 2	[Barabash *et al.* (1998)]
	$>2.7\times10^{22}$	68	UC Irvine	[Elliott *et al.* (1992)]
	$>1.8\times10^{22}$			[Moe *et al.* (1988)]
^{94}Zr$\rightarrow^{94}$Mo	$>1.9\times10^{19}$	90	NEMO 2	[Arnold *et al.* (1999)]
^{96}Zr$\rightarrow^{96}$Mo	$>9.2\times10^{21}$	90	NEMO 3	[Barabash *et al.* (2011)]
	$>9.2\times10^{21}$	90	NEMO 3	[Argyriades *et al.* (2010)]
	$>1.0\times10^{21}$	90	NEMO 2	[Arnold *et al.* (1999)]
	$>8.0\times10^{20}$	90	NEMO 2	[Barabash *et al.* (1998)]
^{98}Mo$\rightarrow^{98}$Ru	$>1.0\times10^{14}$			[Fremlin *et al.* (1952)]
^{100}Mo$\rightarrow^{100}$Ru	$>1.1\times10^{24}$	90	NEMO 3	[Arnold *et al.* (2015)]
	$>4.6\times10^{23}$	90	NEMO 3	[Arnold *et al.* (2005)]
	$>3.5\times10^{23}$	90	NEMO 3	[Lalanne (2005)]
	$>5.5\times10^{22}$	90	ELEGANT V	[Ejiri *et al.* (2001)]
	$>4.9\times10^{21}$	90	ITEP+INFN	[Ashitkov *et al.* (2001)]
	$>2.2\times10^{22}$	90	ELEGANT V	[Kudomi *et al.* (2000)]
	$>2.3\times10^{21}$	90	ITEP+INFN	[Ashitkov *et al.* (1999)]
	$>5.2\times10^{22}$	68	ELEGANT V	[Kudomi *et al.* (1998)]
	$>2.2\times10^{22}$	68	LBL+UNM	[Garnjost *et al.* (1997)]
	$>1.23\times10^{23}$	90	UC Irvine	[De Silva *et al.* (1997]
	$>5.2\times10^{22}$	68	ELEGANT V	[Ejiri *et al.* (1996)]

Table 1.5 continued

Transition	$T^{0\nu}_{1/2}$ (yr)	C.L.(%)	Project	Reference
	$>6.4\times10^{21}$	90	NEMO 2	[Dassie *et al.* (1995)]
	$>4.4\times10^{22}$	68	LBL+UNM	[Garnjost *et al.* (1993)]
	$>4.7\times10^{21}$	68	ELEGANT V	[Ejiri *et al.* (1991)]
	$>7.1\times10^{20}$	68	INS Baksan	[Vasilev *et al.* (1990)]
	$>4.0\times10^{21}$	68	LBL+UNM	[Garnjost *et al.* (1989)]
	$>1.0\times10^{19}$	68	UC Irvine	[Elliott *et al.* (1987)]
^{116}Cd$\rightarrow^{116}$Sn	$>7.0\times10^{22}$	90	INR+INFN	[Danevich *et al.* (2000)]
	$>3.2\times10^{22}$	90	INR+INFN	[Danevich *et al.* (1999)]
	$>5.0\times10^{21}$	90	NEMO 2	[Arnold *et al.* (1996)]
	$>2.9\times10^{22}$	90	INR	[Danevich *et al.* (1995)]
	$>2.9\times10^{21}$	90	Osaka	[Ejiri *et al.* (1995)]
	$>5.4\times10^{21}$	68		[Kume *et al.* (1994)]
	$>2.6\times10^{18}$	90	ITEP+INFN	[Pipke *et al.* (1994)]
^{128}Te$\rightarrow^{128}$Xe	$>1.1\times10^{23}$	90	INFN+LNGS	[Arnaboldi *et al.* (2003)]
	$>8.6\times10^{22}$	90	INFN+LNGS	[Allessandrello *et al.* (2000)]
	$>7.7\times10^{24}$		Geochemical	[Bernatowicz *et al.* (1993)]
^{130}Te$\rightarrow^{130}$Xe	$>1.5\times10^{25}$	90	CUORE	[Alduino *et al.* (2018)]
	$>4.0\times10^{24}$	90	CUORE-0	[Alduino *et al.* (2016)]
	$>7.0\times10^{20}$	90	NEMO 3	[Arnold *et al.*(2015)]
	$>1.8\times10^{24}$	90	CUORICINO	[Arnaboldi *et al.* (2005)]
	$>5.5\times10^{23}$	90	CUORICINO	[Arnaboldi *et al.* (2004)]
	$>2.1\times10^{23}$	90	INFN+LNGS	[Arnaboldi *et al.* (2003)]
	$>1.4\times10^{23}$	90	INFN+LNGS	[Allessandrello *et al.* (2000)]
	$>7.7\times10^{22}$	90	Milano	[Morales (1999)]
	$>5.6\times10^{22}$	90	INFN+LNGS	[Allessandrello *et al.* (1998)]

Table 1.5 continued

Transition	$T^{0\nu}_{1/2}$ (yr)	C.L.(%)	Project	Reference
^{136}Xe$\rightarrow^{136}$Ba	$>2.1\times10^{23}$	90	PANDAX-II	[Kaixiang *et al.* (2019)]
	$>1.8\times10^{25}$	90	EXO-200	[Albert *et al.* (2018)]
	$>1.07\times10^{26}$	90	KamLAND-Zen	[Gando *et al.* (2016)]
	$>1.1\times10^{25}$		EXO-200	[Albert *et al.* (2014)]
	$>1.6\times10^{25}$	90	EXO	[Auger *et al.* (2012)]
	$>2.6\times10^{24}$	90	KamLAND-Zen	[Gando *et al.* (2012)]
	$>1.2\times10^{24}$	90	INFN	[Bernabei *et al.* (2002)]
	$>4.4\times10^{23}$	90	Caltech+PSI+UN	[Luescher *et al.* (1998)]
	$>4.2\times10^{23}$		Gotthard tunnel	[Busto *et al.* (1996)]
	$>2.6\times10^{23}$	90	Gotthard tunnel	[Vuilleumier *et al.* (1993)]
	$>3.0\times10^{21}$	68	ITEP+INR	[Barabash *et al.* (1989)]
	$>1.0\times10^{21}$	90	Milano+INFN	[Alessandrello *et al.* (1988)]
	$>2.0\times10^{21}$	68		[Barabanov *et al.* (1986)]
^{150}Nd$\rightarrow^{150}$Sm	$>2.0\times10^{22}$	90	NEMO-3	[Arnold *et al.* (2016)]
	$>1.8\times10^{22}$	90	NEMO 3	[Barabash *et al.*(2011)]
	$>1.8\times10^{22}$	90	NEMO-3	[Argyriades *et al.* (2009)]
	$>1.2\times10^{21}$	90	UC Irvine	[De Silva *et al.* (1997]
	$>2.1\times10^{20}$	90	ITEP +INR	[Artemiev *et al.* (1995)]
	$>2.1\times10^{21}$			[Moe *et al.* (1994)]
	$>1.7\times10^{21}$		INR	[Klimenko *et al.* (1986)]
^{238}U$\rightarrow^{238}$Pu	$>1.0\times10^{12}$	68	INR	[Tretyak *et al.* (2005)]

Chapter 2

Reliability of PHFB wave functions of some nuclei in the mass range $90 \leq A \leq 150$ participating in $\beta^-\beta^-$ decay

The half-life of $2\nu\beta^-\beta^-$ decay is a product of an accurately known phase space factor and an appropriate NTME $M_{2\nu}$, and it has been already measured for eleven nuclei for the $0^+ \rightarrow 0^+$ transition. Consequently, the values of NTMEs $M_{2\nu}$ can be extracted directly. Hence, the validity of different models employed for nuclear structure calculations can be tested by calculating the NTMEs $M_{2\nu}$. Further, the requirement of calculating reliable NTMEs relevant to the $0\nu\beta^-\beta^-$ decay is usually tested by reproducing the experimentally extracted NTMEs $M_{2\nu}$. However, there are a number of other processes operating inside the nucleus, regarding which a vast amount of experimentally observed data already

exist. Hence, our aim is to calculate nuclear spectroscopic properties, namely sub-shell occupation numbers, excited energies E_{2^+} of yrast 2^+ state, reduced $B(E2{:}0^+ \rightarrow 2^+)$ transition probabilities and deformation parameters β_2 of nuclei involved in the $\beta^-\beta^-$ decay as a test of the reliability of the wave function prior to calculating NTMEs relevant to $0\nu\beta^-\beta^-$ decay.

The present chapter is organized as follows. A detailed derivation of the HFB method has been given by Baranger (1963), Villars (1966) and Goodman (1979). The projection technique in the context of HFB method was developed by Onishi and Yosida (1966). In Section 2.1, we present a brief outline of the PHFB model in order to define various quantities and make the discussion self-contained. In Section 2.2, the formalism to calculate the spectroscopic properties has been presented [Dixit *et al.* (2002)]. We compare the calculated E_{2^+} and electromagnetic properties with available experimental data for ^{94,96}Zr, ^{94,96,100}Mo,^{100,104}Ru, ^{104,110}Pd, ^{110}Cd, ^{128,130}Te, ^{128,130}Xe, ^{150}Nd and ^{150}Sm nuclei in Section 2.3. Finally, the conclusions are given in Section 2.4.

2.1 The PHFB model

The nuclear many-body problem is complex and numerically difficult to solve in practice. The many-body Hamiltonian H is given by

$$\begin{aligned} H &= \sum_{\alpha\beta} \langle\alpha|\ T\ |\beta\rangle a^+_\alpha a_\beta + \frac{1}{4}\sum_{\alpha\beta\gamma\delta} \langle\alpha\beta|\ V\ |\gamma\delta\rangle a^+_\alpha a^+_\beta a_\delta a_\gamma \\ &= \sum_{\alpha} \varepsilon_\alpha a^+_\alpha a_\alpha + \frac{1}{4}\sum_{\alpha\beta\gamma\delta} \langle\alpha\beta|\ V\ |\gamma\delta\rangle a^+_\alpha a^+_\beta a_\delta a_\gamma \end{aligned} \tag{2.1}$$

The standard procedure for the solution of the many-body problem is a perturbative approach with accompanying problems of convergence. In the shell model, one attempts to solve the many-body Schroedinger equation as exactly as possible. Beyond the pf-shell, the number of basis states increases so drastically that it is not possible to perform a conventional shell model calculation without imposing certain truncation scheme. On the other hand, most of the $\beta\beta$ decay emitters are medium or heavy mass nuclei. Moreover, most of the nuclei are reasonably or heavily deformed. Hence, it is necessary to have the mixing of a large number configurations to study these nuclei. On the other hand, the PHFB model is the most convenient choice to study the medium and heavy mass deformed nuclei.

The essential idea behind the HFB theory is to transform particle coordinates to quasiparticle coordinates through general Bogoliubov transformation such that the quasiparticles are relatively weakly interacting. Essentially, the Hamiltonian H is expressed as

$$H = E_0 + H_{qp} + H_{qp-int} \tag{2.2}$$

where E_0 is the energy of the quasiparticle vacuum, H_{qp} is the Hamiltonian of quasiparticles and H_{qp-int} is the interaction between the quasiparticles, which is generally weak. In HFB theory, the interaction between the quasiparticles is usually neglected and the Hamiltonian H is approximated by an independent quasiparticle Hamiltonian. In time dependent HFB (TDHFB) or the quasiparticle random phase approximation (QRPA), some effects of quasiparticle interaction can be included.

The HFB equations are obtained by equating to zero the off diagonal bilinear qua-

siparticle part of the transformed Hamiltonian after making a canonical transformation from a_α's to quasi-fermions q_α's through

$$q_k^+ = \sum_\alpha \left(u_{k\alpha} a_\alpha^+ + v_{k\alpha} a_{\overline{\alpha}}\right) \tag{2.3}$$

$$q_{\overline{k}}^+ = \sum_\alpha \left(u_{k\alpha} a_{\overline{\alpha}}^+ - v_{k\alpha} a_\alpha\right) \tag{2.4}$$

The transformation coefficients are real and satisfy appropriate orthonormality conditions. Henceforward, we use time reversal symmetry as we are concerned with even-even nuclei only. The HFB equations are given by

$$\begin{aligned} E_k u_{k\alpha} &= \sum_\gamma h'_{\alpha\gamma} u_{\alpha\gamma} + \Delta_{\alpha\overline{\gamma}} v_{\alpha\gamma} \\ E_k v_{k\alpha} &= \sum_\gamma \Delta_{\alpha\overline{\gamma}} u_{\alpha\gamma} - h'_{\alpha\gamma} v_{\alpha\gamma} \end{aligned} \tag{2.5}$$

where E_k is the quasiparticle energy. Further

$$h'_{\alpha\gamma} = T_{\alpha\gamma} - \lambda\delta_{\alpha\gamma} + \Gamma_{\alpha\gamma} \tag{2.6}$$

where

$$\Gamma_{\alpha\gamma} = \sum_{\beta\delta} \left[\langle\alpha\beta|\ V\ |\gamma\delta\rangle + \langle\alpha\overline{\beta}|\ V\ |\gamma\overline{\delta}\rangle\right] \sum_{k=1}^{n} v_{k\beta} v_{k\delta} \tag{2.7}$$

$$= \sum_{\beta\delta} \left[\langle\alpha\beta|\ V\ |\gamma\delta\rangle + \langle\alpha\overline{\beta}|\ V\ |\gamma\overline{\delta}\rangle\right] \rho_{\beta\delta} \tag{2.8}$$

with

$$\rho_{\beta\delta} = \sum_k v_{k\beta} v_{k\delta} \tag{2.9}$$

and

$$\Delta_{\alpha\overline{\gamma}} = \sum_{\beta\delta} \langle \alpha\overline{\gamma}| \ V \ |\beta\overline{\delta}\rangle \sum_{k=1}^{n} v_{k\beta} u_{k\delta} \tag{2.10}$$

The coupled HFB equations can be written in a simplified form using the Bloch-Messiah theorem [Bloch and Messiah (1962)]. We define transformations

$$b_k^+ = \sum_{\alpha} C_{k,\alpha} a_\alpha^+ \qquad and \qquad b_{\overline{k}}^+ = \sum_{\alpha} C_{k,\alpha}^* a_{\overline{\alpha}}^+ \tag{2.11}$$

where the expansion coefficients appearing in Eq. (2.11) can be obtained by diagonalizing the HF like potential h' in spherical basis which includes the appropriate density $\rho_k = v_k^2$,

$$h_{\alpha\beta}^{'} = \langle \alpha | T - \lambda_\pi N_\pi - \lambda_\nu N_\nu | \beta \rangle + \sum_k \langle \alpha k| \ V \ |\beta k\rangle v_k^2 \tag{2.12}$$

The occupation probabilities v_k^2 are obtained by solving the BCS equation

$$\Delta_k = \Delta_{k\overline{k}} = \sum_{k'} \langle k\overline{k}| \ V \ |k'\overline{k'}\rangle u_{k'} v_{k'} \tag{2.13}$$

The calculation involves iteration between Eqs. (2.12) and (2.13) until a reasonable convergence is achieved in terms of both the expansion coefficients $C_{k,\alpha}$ and v_k^2. The probability amplitudes u_k and v_k in Eqs. (2.3-2.4) are given by

$$u_k^2 = \frac{1}{2}\left[1 + \frac{\theta_k}{E_k}\right] \tag{2.14}$$

with

$$u_k^2 + v_k^2 = 1 \tag{2.15}$$

where θ_k is the eigenvalue of $h'_{\alpha\beta}$ given by Eq. (2.12). Finally, one obtains

$$v_k^2 = \frac{1}{2}\left[1 - \frac{\theta_k}{E_k}\right] \tag{2.16}$$

where

$$E_k = \sqrt{\theta_k^2 + \Delta_k^2} \tag{2.17}$$

and

$$\Delta_{k\overline{k}} = \frac{1}{2}\sum_{k'}\langle k\overline{k}|\ V\ |k'\overline{k'}\rangle \left(\frac{\Delta_{k\overline{k'}}}{\sqrt{\theta_{k'}^2 + \Delta_{k'\overline{k'}}^2}}\right) \tag{2.18}$$

The chemical potential λ is determined from the equation

$$\sum_{k=1}^{n}\left[1 - \frac{\theta_k}{\sqrt{\theta_k^2 + \Delta_k^2}}\right] = N \tag{2.19}$$

Here N is the number of particles in the system. The ground state energy E_{HFB} is given by

$$E_{HFB} = \sum_{k=1}^{n}(T_{kk} + \lambda - E_k)v_k^2 \tag{2.20}$$

where

$$T_{kk} = \sum_{\alpha\gamma} T_{\alpha\gamma}\ C_{k\alpha}\ C_{k\gamma} \tag{2.21}$$

The quadrupole moment of the axially symmetric HFB intrinsic state is given by

$$Q_{HFB} = 2\sum_{k=1}^{n} Q_0^2\ v_k^2 \tag{2.22}$$

where

$$Q_0^2 = \left(\frac{16\pi}{5}\right)^{1/2}\ r^2\ Y_0^2 \tag{2.23}$$

is the quadrupole moment operator.

The axially symmetric HFB intrinsic state with $K = 0$ can be written as

$$|\Phi_0\rangle = \prod_{im} \left(u_{im} + v_{im} b^\dagger_{im} b^\dagger_{\overline{im}} \right) |0\rangle \tag{2.24}$$

where the creation operators $b^\dagger_{im}$ and $b^\dagger_{\overline{im}}$ are given by

$$b^\dagger_{im} = \sum_\alpha C_{i\alpha,m} a^\dagger_{\alpha m} \qquad and \qquad b^\dagger_{\overline{im}} = \sum_\alpha (-1)^{l+j-m} C_{i\alpha,m} a^\dagger_{\alpha,-m} \tag{2.25}$$

The wave function $|\Phi_0\rangle$ can be recast into the form

$$|\Phi_0\rangle = N \; exp \left(\frac{1}{2} \sum_{\alpha\beta} f_{\alpha\beta} a^\dagger_\alpha a^\dagger_\beta |0\rangle \right) \tag{2.26}$$

with

$$f_{\alpha\beta} = \sum_i C_{im_\alpha, j_\alpha} C_{im_\beta, j_\beta} \left(\frac{v_{im_\alpha}}{u_{im_\alpha}} \right) \delta_{m_\alpha - m_\beta} \tag{2.27}$$

where N is a normalization constant. A state with good angular momentum $\mathbf{J}$ is obtained from the HFB intrinsic state using the standard projection technique [Onishi *et al.* (1966)] through the following relation.

$$\begin{aligned} \left| \Psi^J_0 \right\rangle &= P^J_{00} \left| \Phi_0 \right\rangle \\ &= \left[\frac{(2J+1)}{8\pi^2} \right] \int D^J_{00}(\Omega) R(\Omega) \left| \Phi_0 \right\rangle d\Omega \end{aligned} \tag{2.28}$$

2.2 Spectroscopic properties of yrast states

In the below, we have presented expressions to calculate various nuclear spectroscopic properties, namely yrast energy spectra, reduced $B(E2{:}0^+ \rightarrow 2^+)$ transition probabilities and deformation parameters β_2 [Dixit *et al.* (2002)].

(1) Sub-shell occupation number

The sub-shell occupation numbers η_J in a yrast state J is given by

$$\begin{aligned} \eta_J &= \frac{\left\langle \Phi_0 \left| \left(\sum_m C^\dagger_{jm} C_{jm} \right) P^J_{00} \right| \Phi_0 \right\rangle}{\langle \Phi_0 \left| P^J_{00} \right| \Phi_0 \rangle} \\ &= \frac{\int_0^\pi P(\theta) d^J_{00}(\theta) \sin\theta d\theta}{\int_0^\pi n(\theta) d^J_{00}(\theta) \sin\theta d\theta} \end{aligned} \tag{2.29}$$

where

$$P(\theta) = n(\theta) \left[\sum_m \left(\frac{M}{1+M} \right)_{jm,jm} \right] \tag{2.30}$$

An approximate estimate of the subshell occupation numbers can be easily obtained in terms of the expectation value of the operator η_J with respect to the intrinsic state $|\Phi_0\rangle$

$$\eta_J^{intrinsic} = \langle \Phi_0 \left| \widehat{\eta}_J \right| \Phi_0 \rangle = \sum_{i,m} \left| c^m_{Ji} \right|^2 (V^m_i)^2 \tag{2.31}$$

(2) Yrast spectra

The energy E_J of a state with angular momentum $\mathbf{J}$ can be written as

$$\begin{aligned} E_J &= \frac{\left\langle \Psi^J_0 | H | \Psi^J_0 \right\rangle}{\langle \Psi^J_0 | \Psi^J_0 \rangle} \\ &= \frac{\int_0^\pi d\theta \sin\theta d^J_{00}(\theta) \left\langle \Phi_0 | H e^{-i\theta J_y} | \Phi_0 \right\rangle}{\int_0^\pi d\theta \sin\theta d^J_{00}(\theta) \langle \Phi_0 | e^{-i\theta J_y} | \Phi_0 \rangle} \\ &= \frac{\int_0^\pi h(\theta) d^J_{00}(\theta) \sin\theta \ d\theta}{\int_0^\pi n(\theta) d^J_{00}(\theta) \sin\theta \ d\theta} \end{aligned} \tag{2.32}$$

The Hamiltonian kernel $h(\theta)$ for a $PPQQ$ type of two-body interaction is given by

$$
\begin{aligned}
h(\theta) &= \left\langle \Phi_0 | H e^{-i\theta J_y} | \Phi_0 \right\rangle \\
&= n(\theta) \left[\sum_{\alpha} \varepsilon_\alpha \rho_{\alpha\alpha} - \frac{G}{4} \sum_{\alpha\tau_3} S_\alpha \left[\frac{f}{1+M} \right]^{\tau_3}_{\alpha\overline{\alpha}} \sum_{\beta\tau_3} S_\beta \left[\frac{F}{1+M} \right]^{\tau_3}_{\beta\overline{\beta}} \right. \\
&\quad \left. -\frac{1}{2} \sum_{\tau_3\tau_3'\mu} (-1)^\mu \chi_{\tau_3\tau_3'} \sum_{\alpha\gamma} \left\langle \alpha \left| q^2_\mu \right| \gamma \right\rangle \rho^{\tau_3}_{\gamma\alpha} \sum_{\beta\delta} \left\langle \beta \left| q^2_{-\mu} \right| \delta \right\rangle \rho^{\tau_3'}_{\delta\beta} \right]
\end{aligned} \tag{2.33}
$$

and the normalization kernel $n(\theta)$ is given by

$$
\begin{aligned}
n(\theta) &= \left\langle \Phi_0 | e^{-i\theta J_y} | \Phi_0 \right\rangle \\
&= \sqrt{\det[1 + M(\theta)]}
\end{aligned} \tag{2.34}
$$

where

$$
M(\theta) = f^\dagger F(\theta) \tag{2.35}
$$

with

$$
F_{\alpha\beta}(\theta) = \sum_{m'_\alpha m'_\beta} d^{j_\alpha}_{m_\alpha, m'_\alpha}(\theta) d^{j_\beta}_{m_\beta, m'_\beta}(\theta) f_{j_\alpha m'_\alpha, j_\beta m'_\beta} \tag{2.36}
$$

and

$$
\begin{aligned}
\rho_{\alpha\beta}(\theta) &= \left[\frac{M(\theta)}{1+M(\theta)} \right]_{\alpha\beta} \\
&= \delta_{\alpha\beta} - \left[\frac{1}{1+M(\theta)} \right]_{\alpha\beta}
\end{aligned} \tag{2.37}
$$

(3) Reduced $B(E2{:}J_i \to J_f)$ transition probabilities

The reduced $B(E2{:}J_i \to J_f)$ transition probability is given by

$$
B(E2{:}J_i \to J_f) = \left(\frac{5}{16\pi} \right) \left[e_\pi \left\langle Q^2_0 \right\rangle_\pi + e_\nu \left\langle Q^2_0 \right\rangle_\nu \right]^2 \tag{2.38}
$$

where

$$\begin{aligned}\left\langle Q_0^2 \right\rangle_{\tau_3} &= \left\langle \Psi_K^{J_i} \left| Q_0^2 \right| \Psi_K^{J_f} \right\rangle \\ &= \left[n^{J_i} n^{J_f} \right]^{-1/2} \int_0^\pi \sum_\mu \begin{pmatrix} J_i & 2 & J_f \\ -\mu & \mu & 0 \end{pmatrix} \\ &\quad \times d^{J_i}_{-\mu 0}(\theta) n(\theta) \left[b^2 \sum_{\tau_3 \alpha\beta} e_{\tau_3} \left\langle \alpha \left| Q_\mu^2 \right| \beta \right\rangle \rho^{\tau_3}_{\alpha\beta}(\theta) \right] \sin\theta \; d\theta \end{aligned} \tag{2.39}$$

with

$$n^J = \int_0^\pi n(\theta) d^J_{00}(\theta) \sin\theta \; d\theta \tag{2.40}$$

$$\rho^{\tau_3}_{\alpha\beta}(\theta) = \left[\frac{M(\theta)}{1 + M(\theta)} \right]^{\tau_3}_{\alpha\beta} \tag{2.41}$$

and

$$Q^2_\mu = \sqrt{\frac{16\pi}{5}} \frac{r^2}{b^2} Y^2_\mu(\theta, \phi) \tag{2.42}$$

The deformation parameter β_2 is given by

$$\beta_2 = \frac{4\pi}{3ZR_0^2} \left[\frac{B(E2)}{e^2} \right]^{1/2} \tag{2.43}$$

where $R_0 = 1.2 \; A^{1/3}$ and $B(E2)$ is in units of $\mathrm{e^2b^2}$.

2.3 Results and discussions

In this section, we present the results for the theoretically calculated sub-shell occupation numbers, excited energies E_{2^+} of yrast 2^+ state, reduced $B(E2{:}0^+ \rightarrow 2^+)$ transition probabilities and deformation parameters β_2 for ^{94,96}Zr, ^{94,96,100}Mo,^{100,104}Ru, ^{104,110}Pd,

^{110}Cd, ^{128,130}Te, ^{128,130}Xe, ^{150}Nd and ^{150}Sm nuclei and compare them with the available observed experimental data.

2.3.1 Model space, single particle energies and parameters of effective two-body interaction

We use the doubly even ^{76}Sr (N=Z=38) nucleus as an inert core for ^{94,96}Zr, ^{94,96,100}Mo, ^{100,104}Ru, ^{104,110}Pd and ^{110}Cd nuclei with the valence space spanned by $1p_{1/2}$, $2s_{1/2,}$ $1d_{3/2}$, $1d_{5/2}$, $0g_{7/2}$, $0g_{9/2}$ and $0h_{11/2}$ orbits for protons and neutrons. We have included the $1p_{1/2}$ orbit in the valence space to examine the explicit role of the Z=40 proton core vis-a-vis the onset of deformation in highly neutron rich isotopes. In case of ^{128,130}Te, ^{128,130}Xe, ^{150}Nd and ^{150}Sm nuclei, the doubly even ^{100}Sn (N=Z=50) nucleus has been taken as an inert core with the valence space spanned by $2s_{1/2,}1d_{3/2}$, $1d_{5/2}$, $1f_{7/2}$, $0g_{7/2}$, $0h_{9/2}$ and $0h_{11/2}$ orbits for protons and neutrons.

The single particle energies (SPEs) have been calculated from Woods-Saxon potential as proposed by Blomqvist and Wahlborn (1960). In the below we give the expression for Woods-Saxon potential along with parameters.

$$V(r) = -V_0 \frac{1}{1+\exp((r-R_0)/a)} - \lambda \left(\frac{\hbar}{2Mc}\right)^2 \mathbf{l}.\boldsymbol{\sigma}\ \frac{1}{r}\frac{d}{dr}\left(\frac{V_0}{1+\exp((r-R_0)/a)}\right) + V_C(r) \tag{2.44}$$

where $\lambda = 32.0$ is a dimensionless parameter, $a = 0.67$ is diffusitivity and V_C is the coulomb potential given as

$$V_C(r) = \begin{cases} Ze^2(3 - r^2/R_0^2)/2R_0 & , \quad r \leqslant R_0 \\ Ze^2/r & , \quad r \geqslant R_0 \end{cases} \tag{2.45}$$

with $R_0 = r_0 A^{1/3}$ and $r_0 = 1.2$ fm. The potential V_0 for neutron and proton is taken as 47.0 MeV and 57.0 MeV, respectively. In Table 2.1 and 2.2, we present the calculated SPEs.

We use a Hamiltonian with Pairing plus Quadrupole-Quadrupole plus Hexadecapole-Hexadecapole (*PQQHH)* type of effective two-body interaction. The Hamiltonian is explicitly written as

$$H = H_{sp} + V(P) + \zeta_{qq}\left[V(QQ) + V(HH)\right] \tag{2.46}$$

where ζ_{qq} is an arbitrary parameter and the final results are obtained by setting $\zeta_{qq} = 1$. The purpose of introducing ζ_{qq} is to study the role of deformation by varying the strength of $QQHH$ interaction. Further, H_{sp} denotes the single particle Hamiltonian. The pairing part of the effective two-body interaction $V(P)$ is given by

$$V(P) = -\left(\frac{G}{4}\right)\sum_{\alpha\beta}(-1)^{j_\alpha + j_\beta - m_\alpha - m_\beta} a^\dagger_\alpha a^\dagger_{\bar{\alpha}} a_{\bar{\beta}} a_\beta, \tag{2.47}$$

where α denotes the quantum numbers $(nljm)$. The state $\bar{\alpha}$ is same as α but with the sign of m reversed. For $A \leq 110$ nuclei, the strengths of the pairing interaction is fixed through the relation $G_p = 30/A$ MeV and $G_n = 25/A$ MeV. For ^{94}Zr and ^{94}Mo, we have used $G_n = 20/A$ MeV. The strengths of the pairing interaction fixed for $A \geq 128$ nuclei are $G_p = G_n = 35/A$ MeV.

The QQ part of the effective interaction $V(QQ)$ is expressed as

$$V(QQ) = -\left(\frac{\chi_2}{2}\right)\sum_{\alpha\beta\gamma\delta}\sum_{\mu}(-1)^\mu \langle\alpha|q_{2\mu}|\gamma\rangle\langle\beta|q_{2-\mu}|\delta\rangle \; a^\dagger_\alpha a^\dagger_\beta \; a_\delta \; a_\gamma \tag{2.48}$$

with

$$q_{2\mu} = \left(\frac{16\pi}{5}\right)^{1/2} r^2 Y_{2\mu}(\theta, \phi) \tag{2.49}$$

The HH part of the effective interaction $V(HH)$ is given as

$$V(HH) = -\left(\frac{\chi_4}{2}\right) \sum_{\alpha\beta\gamma\delta} \sum_{\nu} (-1)^{\nu} \langle\alpha|q_{4\nu}|\gamma\rangle\langle\beta|q_{4-\nu}|\delta\rangle \; a^{\dagger}_{\alpha} a^{\dagger}_{\beta} \; a_{\delta} \; a_{\gamma} \tag{2.50}$$

with

$$q_{4\nu} = r^4 Y_{4\nu}(\theta, \phi) \tag{2.51}$$

The parameters of the HH part of the two-body interaction were calculated as suggested by Bohr and Mottelson [Bohr and Mottelson (1975)]. For isospin $T = 0$, the approximate magnitude of these constants is given by

$$\chi_\lambda = \frac{4\pi}{2\lambda + 1} \frac{m\omega_0^2}{A \left\langle r^{2\lambda-2} \right\rangle} \qquad \text{for } \lambda = 1, 2, 3, 4 \cdots \tag{2.52}$$

and for the $T = 1$ case, the parameters are approximately half of their $T = 0$ counterparts. Using $b = 1.0032A^{1/6}$, one obtains

$$\begin{aligned} \chi_4 &= \left[\left(\frac{16}{25}\right)\left(\frac{2}{3}\right)^{2/3}\right] \chi_2 A^{-2/3} b^{-4} \\ &= 0.4884 \chi_2 A^{-2/3} b^{-4} \end{aligned} \tag{2.53}$$

We use four parametrizations of the effective two-body interaction give by a Hamiltonian in Eq. (2.46). Details of these parametrizations are as follows:

PQQ1 and PQQHH1

In PQQ1 parametrization, the hexadecapole-hexadecapole term is not included in the Hamiltonian while in PQQHH1 the hexadecapole-hexadecapole term is added in the Hamiltonian of effective two-body interaction. In both the parametrizations, strengths of the like particle components of the QQ interaction are taken as $\chi_{2pp} = \chi_{2nn} = -0.0105$ MeV b^{-4}, where b is oscillator parameter. For a given model space, SPE's, G_p, G_n and

χ_{2pp}, χ_{2pn} was varied to get optimum yrast spectra of nuclei. The theoretical yrast spectra was considered to be the optimum when the excitation energy of the 2^+ state E_{2^+} is reproduced as closely as possible in comparison to the experimental values.

PQQ2 and PQQHH2

The PQQ2 and PQQHH2 are also with and without hexadecapole-hexadecapole term in the Hamiltonian of effective two-body interaction but in these parametrizations χ_{2pn} is taken as twice of χ_{2pp}. The three parameters χ_{2pn}, χ_{2pp} and χ_{2nn} were varied together with the condition $\chi_{2pn} = 2\chi_{2pp} = 2\chi_{2nn}$ to get an optimum yrast spectra.

2.3.2 The yrast spectra and electromagnetic properties

The spectroscopic properties of ^{94,96}Zr, ^{94,96,100}Mo, ^{100,104}Ru, ^{104,110}Pd, ^{110}Cd, ^{128,130}Te, ^{128,130}Xe, ^{150}Nd and ^{150}Sm nuclei have been calculated in PHFB model using above four parametrizations. All these input parameters were kept fixed to calculate other nuclear spectroscopic properties.

The experimental sub-shell occupation numbers in case of ^{100}Mo, ^{100}Ru [Freeman *et al.* (2017)], ^{128,130}Te and ^{130}Xe [Kay *et al.* (2013)] are available. In Tables 2.3, the calculated sub-shell occupation numbers in PQQ1 parametrization are compared with the experimental data. From Table 2.3 we observed that the calculated values are in quite well agreement with the experimental values. The other three parametrizations give the similar results.

In Table 2.4, we present the theoretically calculated E_{2^+}, $B(E2{:}0^+ \rightarrow 2^+)$ and β_2 of the nuclei under study in all four parametrizations along with the experimental ones

[Sakai (1984)]. From Table 2.4 it can be seen that there is a quite good agreement between the calculated values and experimental results. We have succeeded to reproduce the experimental E_{2^+} within about 2% accuracy in either of the four parametrizations. The $B(E2{:}0^+ \rightarrow 2^+)$ and β_2 are calculated for effective charges $e_{eff} = 0.40$, 0.50 and 0.60. The presented values for ^{94}Zr, ^{96}Mo, ^{100}Ru and ^{150}Sm isotopes are at $e_{eff} = 0.40$. In case of ^{96}Zr, ^{104,110}Pd, ^{110}Cd, ^{128,130}Xe, ^{130}Te and ^{150}Nd isotopes, $e_{eff} = 0.50$. For ^{94,100}Mo, ^{104}Ru and ^{128}Te isotopes, $e_{eff} = 0.60$.

2.4 Conclusions

To summarize, as a test of the reliability of the wave functions, we have calculated the sub-shell occupation numbers, excitation energy of the 2^+ state E_{2^+} , reduced $B(E2 : 0^+ \rightarrow 2^+)$ transition probabilities and deformation parameters β_2 of some nuclei undergoing $\beta^-\beta^-$ decay in the mass range A=90 – 150 and compared with the available experimental data. The overall agreement between the theoretically calculated and experimentally observed values makes us confident to apply the same PHFB wave functions to study the nuclear 2ν $\beta^-\beta^-$ decay of the nuclei under consideration.

Table 2.1 : Single particle energies for ^{94,96}Zr, ^{94,96,100}Mo, ^{100,104}Ru, ^{104}Pd, ^{110}Pd and ^{110}Cd isotopes derived from Woods-Saxon potential.

Orbits	^{94}Zr	^{94}Mo	^{96}Zr	^{96}Mo	^{100}Mo	^{100}Ru	^{104}Ru	^{104}Pd	^{110}Pd	^{110}Pd
Proton										
$2s_{1/2}$	7.881	7.815	8.002	7.994	8.144	9.999	9.408	9.806	8.480	8.673
$1p_{1/2}$	-1.076	-1.043	-1.052	-1.008	-0.938	-0.112	-0.178	-0.177	-0.820	-0.788
$1d_{3/2}$	7.390	7.329	9.453	9.451	7.670	9.747	9.645	9.149	9.570	9.528
$1d_{5/2}$	5.615	5.385	5.67	5.676	5.841	7.451	7.878	7.175	5.905	5.888
$0g_{7/2}$	9.021	9.011	8.903	8.922	8.760	8.680	8.305	8.407	8.115	8.106
$0g_{9/2}$	0.0	0.0	0.0	0.0	0.0	0.0	0.0	0.0	0.0	0.0
$0h_{11/2}$	9.076	9.037	9.032	9.009	8.959	8.885	8.542	8.743	8.636	9.071
Neutron										
$2s_{1/2}$	6.559	6.587	6.540	6.690	10.567	9.998	9.859	9.920	6.033	7.043
$1p_{1/2}$	-1.276	-1.270	-2.269	-2.235	-1.560	-1.174	-1.153	-1.426	-2.286	-2.079
$1d_{3/2}$	7.949	5.978	7.878	5.530	7.950	8.210	8.806	8.983	7.063	8.058
$1d_{5/2}$	4.700	4.715	4.681	4.767	5.980	7.656	7.840	8.379	4.350	4.929
$0g_{7/2}$	7.811	7.827	7.640	7.727	6.997	7.677	8.442	8.968	6.417	6.964
$0g_{9/2}$	0.0	0.0	0.0	0.0	0.0	0.0	0.0	0.0	0.0	0.0
$0h_{11/2}$	9.099	9.108	9.013	9.062	8.250	8.878	8.924	9.999	8.354	8.688

Table 2.2: Single particle energies for ^{128,130}Te, ^{128,130}Xe, ^{150}Nd and ^{150}Sm nuclei derived from Woods-Saxon potential.

Orbits	^{128}Te	^{128}Xe	^{130}Te	^{130}Xe	^{150}Nd	^{150}Sm
Proton						
$2s_{1/2}$	2.763	2.742	2.779	2.751	2.774	2.722
$1d_{3/2}$	3.465	3.445	3.444	3.416	3.119	3.069
$1d_{5/2}$	0.0	0.0	0.0	0.0	0.0	0.0
$1f_{7/2}$	12.444	10.373	12.459	10.374	10.190	10.064
$0g_{7/2}$	3.195	3.198	3.098	3.101	3.288	1.791
$0h_{9/2}$	12.208	12.154	12.072	12.005	10.568	10.462
$0h_{11/2}$	6.131	6.112	6.084	6.068	3.634	5.631
Neutron						
$2s_{1/2}$	4.080	2.118	2.972	3.102	2.210	2.201
$1d_{3/2}$	4.765	2.801	3.310	4.955	2.584	2.575
$1d_{5/2}$	0.0	0.0	0.0	0.0	0.0	0.0
$1f_{7/2}$	12.997	10.073	12.963	11.522	10.045	10.027
$0g_{7/2}$	1.152	3.147	0.499	1.066	3.359	1.861
$0h_{9/2}$	11.467	11.725	11.196	10.256	10.244	10.229
$0h_{11/2}$	4.342	6.320	2.850	3.286	3.851	5.857

Table 2.3: Calculated (Theo.) and observed (Exp.) sub-shell occupation numbers for protons and neutrons along with experimental results for ^{100}Mo, ^{100}Ru [Freeman *et al.* (2017)] and ^{128,130}Te, ^{130}Xe isotopes [Kay *et al.* (2013)] in PQQ1 parametrization. $1d$ represents $1d_{3/2} + 1d_{5/2}$.

Nuclei			$2s_{1/2}$	$1p_{1/2}$	$1d$	$0g_{7/2}$	$0g_{9/2}$	$0h_{11/2}$
^{100}Mo	p	Theo.	0.035	0.013	0.544	0.019	3.380	0.008
		Exp.	–	–	–	–	4.06±0.30	–
	n	Theo.	0.309	1.986	3.677	2.558	9.666	1.804
		Exp.	0.33±0.02	–	3.40±0.17	2.48±0.19	–	1.89±0.13
^{100}Ru	p	Theo.	0.079	0.044	0.858	0.105	4.969	-0.056
		Exp.	–	–	–	–	5.56±0.22	–
	n	Theo.	0.535	1.989	2.814	2.336	9.112	1.214
		Exp.	0.23±0.01	–	2.50±0.12	2.19±0.15	–	1.13±0.08

			$2s_{1/2}$	$1d$	$1f_{7/2}$	$0g_{7/2}$	$0h_{9/2}$	$0h_{11/2}$
^{128}Te	p	Theo.	0.382	1.563	0.000	0.055	0.000	0.000
		Exp.	–	–	–	–	–	–
	n	Theo.	1.329	7.973	0.264	7.635	0.201	8.597
		Exp.	1.28±0.2	7.94±0.2	–	8.00	–	8.66±0.3
^{130}Te	p	Theo.	0.385	1.553	0.000	0.062	0.000	0.000
		Exp.	–	–	–	–	–	–
	n	Theo.	1.517	8.626	0.207	7.707	0.139	9.803
		Exp.	1.50±0.2	8.55±0.2	–	8.00	–	9.79±0.3
^{130}Xe	p	Theo.	0.465	2.767	0.010	0.791	0.004	-0.037
		Exp.	–	–	–	–	–	–
	n	Theo.	1.251	7.353	0.538	7.490	0.403	8.964
		Exp.	1.44±0.2	7.29±0.2	–	8.00	–	9.01±0.3

Table 2.4: Comparison of theoretically calculated and experimentally observed excitation energies E_{2^+} (MeV) [Sakai (1984)], reduced $B(E2{:}0^+ \rightarrow 2^+)$ transition probabilities, deformation parameters β_2 [Ramen *et al.* (2001)] and g factors $g(2^+)$ [Raghavan (1989)] ^{94,96}Zr, ^{94,96,100}Mo, ^{100,104}Ru, ^{104,110}Pd, ^{110}Cd, ^{128,130}Te, ^{128,130} Xe, ^{150}Nd and ^{150}Sm isotopes.

Nuclei		$PQQ1$	$PQQHH1$	$PQQ2$	$PQQHH2$	Experiment
^{94}Zr	χ_{2pp}	0.0105	0.0105	0.015798	0.0132	
	χ_{2pn}	0.032122	0.03095	0.031596	0.0264	
	E_{HFB}	11.5512	11.6760	10.3745	11.6550	
	Q_{HFB}	24.5837	23.0302	39.1223	20.6325	
	E_{2^+}	0.9192	0.9183	0.9184	0.9159	0.9183
	$B(E2{:}0^+ \rightarrow 2^+)$	0.065	0.058	0.173	0.065	0.066±0.014
	β_2	0.090	0.085	0.146	0.090	0.090±0.010
^{94}Mo	χ_{2pp}	0.0105	0.0105	0.01195	0.011727	
	χ_{2pn}	0.02511	0.02445	0.0239	0.023454	
	E_{HFB}	0.1558	0.1019	0.0009	0.0017	
	Q_{HFB}	31.5209	31.8086	31.7552	31.8953	
	E_{2^+}	0.8714	0.8708	0.8790	0.8811	0.8711
	$B(E2{:}0^+ \rightarrow 2^+)$	0.225	0.230	0.227	0.230	0.230±0.040
	β_2	0.159	0.144	0.159	0.144	0.1509±0.0015
^{96}Zr	χ_{2pp}	0.0105	0.0105	0.01022	0.01016	
	χ_{2pn}	0.026	0.02603	0.02044	0.02032	
	E_{HFB}	19.3916	19.3404	19.2733	19.2672	
	Q_{HFB}	2.5893	2.6300	0.4081	0.3933	
	E_{2^+}	1.7553	1.7567	1.7508	1.7876	1.7507
	$B(E2{:}0^+ \rightarrow 2^+)$	0.060	0.062	0.056	0.057	0.055±0.022
	β_2	0.085	0.086	0.082	0.082	0.080±0.017
^{96}Mo	χ_{2pp}	0.0105	0.0105	0.011779	0.01171	
	χ_{2pn}	0.02473	0.0245	0.023558	0.02342	
	E_{HFB}	5.2814	5.3053	5.1103	5.1520	
	Q_{HFB}	44.2408	43.2944	44.7574	43.8116	
	E_{2^+}	0.7758	0.7774	0.7781	0.7753	0.7782
	$B(E2{:}0^+ \rightarrow 2^+)$	0.284	0.274	0.287	0.277	0.271±0.005
	β_2	0.176	0.172	0.176	0.174	0.1720±0.0016

Table 2.4 continued

Nuclei		$PQQ1$	$PQQHH1$	$PQQ2$	$PQQHH2$	Experiment
^{100}Mo	χ_{2pp}	0.0105	0.0105	0.010505	0.0104	
	χ_{2pn}	0.02102	0.020717	0.02101	0.0208	
	E_{HFB}	34.7380	34.8100	34.7247	34.8261	
	Q_{HFB}	51.2172	51.2645	51.1874	51.1959	
	E_{2^+}	0.5306	0.5321	0.5329	0.5347	0.5355
	$B(E2{:}0^+ \rightarrow 2^+)$	0.466	0.469	0.465	0.468	0.516±0.010
	β_2	0.219	0.220	0.219	0.220	0.2309±0.0022
^{100}Ru	χ_{2pp}	0.0105	0.0105	0.01362	0.01349	
	χ_{2pn}	0.0313	0.0306	0.02724	0.02698	
	E_{HFB}	21.7229	22.1349	22.1605	22.2494	
	Q_{HFB}	60.2840	58.4752	60.0208	58.5762	
	E_{2^+}	0.5385	0.5399	0.5399	0.5320	0.5396
	$B(E2{:}0^+ \rightarrow 2^+)$	0.534	0.512	0.518	0.503	0.490±0.005
	β_2	0.224	0.219	0.221	0.218	0.2148±0.0011
^{104}Ru	χ_{2pp}	0.0105	0.0105	0.01135	0.01142	
	χ_{2pn}	0.0238	0.0240	0.0227	0.02284	
	E_{HFB}	55.8788	55.4580	55.8676	55.4490	
	Q_{HFB}	64.6017	65.1667	64.4541	64.9618	
	E_{2^+}	0.3578	0.3573	0.3578	0.3574	0.35799
	$B(E2{:}0^+ \rightarrow 2^+)$	0.898	0.913	0.889	0.902	0.820±0.012
	β_2	0.283	0.285	0.282	0.284	0.2707±0.0020
^{104}Pd	χ_{2pp}	0.0105	0.0105	0.01035	0.0104	
	χ_{2pn}	0.02054	0.0207	0.02070	0.0208	
	E_{HFB}	48.4522	48.4397	48.4667	48.4514	
	Q_{HFB}	55.8686	56.2952	55.8584	56.2814	
	E_{2^+}	0.5582	0.5555	0.5582	0.5556	0.5558
	$B(E2{:}0^+ \rightarrow 2^+)$	0.575	0.582	0.575	0.582	0.535±0.035
	β_2	0.217	0.218	0.217	0.212	0.209±0.007

Table 2.4 continued

Nuclei		$PQQ1$	$PQQHH1$	$PQQ2$	$PQQHH2$	Experiment
^{110}Pd	χ_{2pp}	0.0105	0.0105	0.011273	0.01085	
	χ_{2pn}	0.023299	0.02230	0.022546	0.02170	
	E_{HFB}	54.3496	55.3412	54.3884	55.4540	
	Q_{HFB}	66.9156	62.6100	66.8010	62.3623	
	E_{2^+}	0.3733	0.3733	0.3748	0.3739	0.3738
	$B(E2{:}0^+ \rightarrow 2^+)$	0.850	0.746	0.841	0.739	0.870±0.040
	β_2	0.254	0.238	0.2523	0.237	0.257±0.006
^{110}Cd	χ_{2pp}	0.0105	0.0105	0.00957	0.00951	
	χ_{2pn}	0.01704	0.01849	0.01914	0.019020	
	E_{HFB}	55.5796	54.6336	54.9926	55.0943	
	Q_{HFB}	48.7175	53.2976	51.1335	50.1360	
	E_{2^+}	0.6574	0.6585	0.6576	0.6645	0.6577
	$B(E2{:}0^+ \rightarrow 2^+)$	0.451	0.534	0.496	0.481	0.450±0.020
	β_2	0.177	0.193	0.186	0.183	0.1770±0.0039
^{128}Te	χ_{2pp}	0.0105	0.0105	0.01037	0.01045	
	χ_{2pn}	0.0206	0.02082	0.02074	0.02090	
	E_{HFB}	50.7831	50.6258	50.7241	50.6009	
	Q_{HFB}	37.4959	37.5739	37.4785	37.5923	
	E_{2^+}	0.7451	0.7432	0.7440	0.7424	0.7432
	$B(E2{:}0^+ \rightarrow 2^+)$	0.392	0.403	0.393	0.403	0.383±0.006
	β_2	0.138	0.140	0.138	0.140	0.1363±0.0011
^{128}Xe	χ_{2pp}	0.0105	0.0105	0.0117	0.0112	
	χ_{2pn}	0.025458	0.02453	0.0234	0.0224	
	E_{HFB}	51.1383	52.3971	51.6475	52.7784	
	Q_{HFB}	61.8537	59.7865	61.6242	59.2707	
	E_{2^+}	0.4389	0.4510	0.4473	0.4484	0.4429
	$B(E2{:}0^+ \rightarrow 2^+)$	0.771	0.739	0.761	0.733	0.750±0.040
	β_2	0.186	0.182	0.185	0.182	0.1836±0.0049

Table 2.4 continued

Nuclei		$PQQ1$	$PQQHH1$	$PQQ2$	$PQQHH2$	Experiment
^{130}Te	χ_{2pp}	0.0105	0.0105	0.01271	0.01057	
	χ_{2pn}	0.026	0.0204	0.02542	0.02114	
	E_{HFB}	35.8669	37.2704	35.5374	36.9659	
	Q_{HFB}	32.9693	27.1567	34.3438	28.3824	
	E_{2^+}	0.8397	0.8339	0.8366	0.8345	0.8395
	$B(E2{:}0^+ \rightarrow 2^+)$	0.277	0.226	0.289	0.239	0.295±0.007
	β_2	0.114	0.104	0.117	0.106	0.1184±0.0014
^{130}Xe	χ_{2pp}	0.0105	0.0105	0.01200	0.010504	
	χ_{2pn}	0.0237	0.02200	0.02400	0.021008	
	E_{HFB}	34.2376	35.9352	32.8358	36.5554	
	Q_{HFB}	55.0921	52.3544	57.3170	51.0835	
	E_{2^+}	0.5370	0.5322	0.5344	0.5425	0.5361
	$B(E2{:}0^+ \rightarrow 2^+)$	0.665	0.620	0.702	0.596	0.65±0.05
	β_2	0.171	0.165	0.176	0.162	0.169±0.007
^{150}Nd	χ_{2pp}	0.0105	0.0105	0.01042	0.01057	
	χ_{2pn}	0.02085	0.0212	0.02084	0.02114	
	E_{HFB}	153.6883	152.9843	153.6278	152.9235	
	Q_{HFB}	85.8091	85.9210	85.8360	85.9738	
	E_{2^+}	0.1303	0.1301	0.1302	0.1306	0.13012
	$B(E2{:}0^+ \rightarrow 2^+)$	2.667	2.692	2.670	2.696	2.760±0.040
	β_2	0.280	0.282	0.280	0.282	0.2853±0.0021
^{150}Sm	χ_{2pp}	0.0105	0.0105	0.0093	0.00933	
	χ_{2pn}	0.01745	0.01730	0.01860	0.01866	
	E_{HFB}	170.7875	170.0885	171.1474	171.0907	
	Q_{HFB}	73.4117	73.5946	72.9427	73.8965	
	E_{2^+}	0.333	0.336	0.333	0.332	0.3339
	$B(E2{:}0^+ \rightarrow 2^+)$	1.460	1.538	1.421	1.500	1.350±0.030
	β_2	0.201	0.206	0.198	0.203	0.1931±0.0021

Chapter 3

Two neutrino double beta decay of ^{94,96}Zr, ^{100}Mo, ^{104}Ru, ^{110}Pd, ^{128,130}Te and ^{150}Nd isotopes for the $0^+ \rightarrow J^+$ transition

Our aim is to predict half-lives $T^{2\nu}_{1/2}(0^+ \rightarrow 2^+)$ of $2\nu\beta^-\beta^-$ decay for the $0^+ \rightarrow 2^+$ transition. This decay mode has not been experimentally observed so far. Therefore, a reliable theoretical prediction can be helpful in designing and planning of future experiments. For a reliable prediction of the $T^{2\nu}_{1/2}(0^+ \rightarrow 2^+)$, the relevant wave functions of the participating nuclei should be as realistic as possible. The $2\nu\beta^-\beta^-$ decay is not an isolated process of the nucleus. There are a number of other processes operating inside the nucleus, regarding which a vast amount of experimentally observed data already exist. Further, the study of $2\nu\beta^-\beta^-$ decay for the $0^+ \rightarrow 0^+$ transition is very interesting as far as nuclear structure

point of view is concerned. The $2\nu\beta^-\beta^-$ decay for the $0^+ \rightarrow 0^+$ transition has been experimentally confirmed in case of ^{48}Ca, ^{76}Ge, ^{82}Se, ^{96}Zr, ^{100}Mo, ^{116}Cd, ^{128,130}Te, ^{136}Xe, ^{150}Nd and ^{238}U nuclei [Tretyak and Zdesenko (1995), (2002)] and the NTMEs $M_{2\nu}(0^+)$ extracted from the observed experimental half-lives are available. Hence, to establish the validity of PHFB model, we have calculated the spectroscopic properties of nuclei as well as $M_{2\nu}(0^+)$ and compared with available experimental data.

The present chapter has been organized in following three sections. In Section 3.1, the theoretical formalism to calculate the half life $T^{2\nu}_{1/2}(J^+)$ of $2\nu\beta^-\beta^-$ decay is given. In Section 3.2, the results of $2\nu\beta^-\beta^-$ decay of ^{94,96}Zr, ^{100}Mo, ^{104}Ru, ^{110}Pd, ^{128,130}Te and ^{150}Nd nuclei are presented and discussed. The conclusions are given in Section 3.3.

3.1 Theoretical framework

The theoretical formalism to calculate the half-life $T^{2\nu}_{1/2}(J^+)$ of $2\nu\beta^-\beta^-$ decay for the $0^+ \rightarrow J^+$ transition in 2n mechanism has been given by Tomoda (1991), Haxton and Stephenson Jr. (1984), Doi *et al.* (1985). We briefly outline steps to derive the $2\nu\beta^-\beta^-$ decay rate formula following the notations of Doi *et al.* (1985).

3.1.1 Effective Hamiltonian for β^- decay

In left-right symmetric models, the charged-current interaction Lagrangian L_{LR} due to the addition of extra gauge boson W_R is given by

$$L_{LR} = \frac{g}{2\sqrt{2}} \left[j^{\mu}_{L} W_{L\mu} + j^{\mu}_{R} W_{R\mu} \right] + h.c. \tag{3.1}$$

where the left and right handed weak leptonic $V \pm A$ currents are written as

$$j_L^\mu = \overline{e}\gamma^\mu \left(1-\gamma_5\right)\nu_{eL} \qquad\qquad j_R^\mu = \overline{e}\gamma^\mu \left(1+\gamma_5\right)\nu_{eR}^{'} \tag{3.2}$$

with

$$\nu_{eL} = \sum_i U_{ei} N_{ji} \qquad \nu_{eR}^{'} = \sum_i V_{ei} N_{iR} \tag{3.3}$$

The mixing matrices U and V satisfy the following orthonormality conditions.

$$\sum_i |U_{ei}|^2 = 1 \qquad \sum_i |V_{ei}|^2 = 1 \qquad \sum_i U_{ei} V_{ei} = 0 \tag{3.4}$$

The gauge bosons W_L and W_R are related to mass eigenstates W_1 and W_2 with masses M_1 and M_2 respectively by

$$\begin{pmatrix} W_L \\ W_R \end{pmatrix} = \begin{pmatrix} \cos\zeta & \sin\zeta \\ -\sin\zeta & \cos\zeta \end{pmatrix} \begin{pmatrix} W_1 \\ W_2 \end{pmatrix} \tag{3.5}$$

Including hadronic currents, the Lagrangian L_{LR} leads to the weak interaction effective Hamiltonian H_W given by

$$H_W = \left(\frac{G}{\sqrt{2}}\right)\left[j_{L\mu} J_L^{\mu\dagger} + \kappa j_{L\mu} J_R^{\mu\dagger} + \eta j_{R\mu} J_L^{\mu\dagger} + \lambda j_{R\mu} J_R^{\mu\dagger}\right] + h.c. \tag{3.6}$$

where

$$\frac{G}{\sqrt{2}} = \frac{g^2}{8M_1^2}\left[\cos^2\zeta + \left(\frac{M_1}{M_2}\right)^2 \sin^2\zeta\right] \tag{3.7}$$

$$\lambda = \frac{\left[\left(\frac{M_1}{M_2}\right)^2 + \tan^2\zeta\right]}{\left[1 + \left(\frac{M_1}{M_2}\right)^2 \tan^2\zeta\right]} \tag{3.8}$$

and

$$\eta = \kappa = \frac{\left[1 - \left(\frac{M_1}{M_2}\right)^2\right]\tan\zeta}{\left[1 + \left(\frac{M_1}{M_2}\right)^2 \tan^2\zeta\right]} \tag{3.9}$$

Here, the coupling constants κ, η and λ are small ($\ll 1$) parameters and $G = 1.16637\times10^{-5}$ GeV^{-2}. The left and right handed weak $V \pm A$ hadronic currents are given by

$$J_L^{\mu\dagger} = g_V \overline{u}\gamma^\mu (1-\gamma_5)\, d \qquad J_R^{\mu\dagger} = g'_V \overline{u}\gamma^\mu (1+\gamma_5)\, d \tag{3.10}$$

where

$$g_V = \cos\theta_c \qquad g'_V = e^{i\alpha}\cos\theta'_c \tag{3.11}$$

In Eq. (3.11), the θ_c and θ'_c are the Cabibbo-Kobayashi-Maskawa (CKM) mixing angles for the left- and right-handed d and s quarks. The CP violating phase α is due to both the mixing of right handed quarks and the mixing of left and right gauge bosons.

In the nonrelativistic impulse approximation, the left and right handed hadronic currents for nuclear $\beta^-\beta^-$ decay in $V \pm A$ forms are given by

$$J_L^{\mu\dagger}(x) = \sum_{n=1}^{A} \left[(g_V - g_A C_n) g^{\mu 0} + (g_A \sigma_n^k - g_V \mathbf{D}_n^k) g^{\mu k}\right] \delta(\mathbf{x} - \mathbf{r}_n)\, \tau_n^+ \tag{3.12}$$

$$J_R^{\mu\dagger}(x) = \sum_{n=1}^{A} \left[(g_V + g_A C_n) g^{\mu 0} + (-g_A \sigma_n^k - g_V \mathbf{D}_n^k) g^{\mu k}\right] \delta(\mathbf{x} - \mathbf{r}_n)\, \tau_n^+ \tag{3.13}$$

The nuclear recoil terms C_n and $\mathbf{D}_n$ are defined as follows

$$C_n = \frac{1}{2M}\left[(\mathbf{P}_n + \mathbf{P}'_n)\cdot\boldsymbol{\sigma}_n - \left(\frac{g_P}{g_A}\right)(E_n - E'_n)\,\boldsymbol{\sigma}_n\cdot\mathbf{Q}_n\right] \tag{3.14}$$

$$\mathbf{D}_n = \frac{1}{2M}\left[(\mathbf{P}_n + \mathbf{P}'_n) - i\left(1 - 2M\left(\frac{g_W}{g_V}\right)\right)\boldsymbol{\sigma}_n \times \mathbf{Q}_n\right] \tag{3.15}$$

where $\mathbf{Q}_n = \mathbf{P}_n - \mathbf{P}'_n$. The g_V, g_A, g_P and g_W are vector, axial vector, pseudoscalar and weak magnetism terms. At $q^2 = 0$,

$$g_V(0) = 1.0 \qquad g_A(0) = 1.25 \qquad \frac{g_p}{g_A} = \frac{2M_P}{m_\pi^2} \tag{3.16}$$

where M_P and m_π are the proton and pion masses. By the CVC hypothesis $g_W(0) = \kappa_\beta/2M$ and $\kappa_\beta = 3.70$, where M and κ_β are the mass and isovector anomalous magnetic moment of nucleons respectively.

3.1.2 Decay rate of $2\nu\beta^-\beta^-$ mode for the $0^+ \rightarrow J^+$ transition

The half life for the $0^+ \rightarrow J^+$ transition of $2\nu\beta^-\beta^-$ decay $T^{2\nu}_{1/2}(J^+)$ in 2n mechanism is given by

$$\left[T^{2\nu}_{1/2}(J^+)\right]^{-1} = G_{2\nu}(J^+)\left|M_{2\nu}(J^+)\right|^2 \tag{3.17}$$

where the integrated kinematical factor $G_{2\nu}(J^+)$ has been calculated with good accuracy [Stoica and Mirea (2013), Pahomi *et al.* (2014)]. The model dependent NTME $M_{2\nu}(J^+)$ is given by

$$M_{2\nu}(J^+) = \sqrt{\frac{1}{s}}\sum_N \frac{\left\langle J^+_F \left\| \sigma\tau^+ \right\| 1^+_N \right\rangle \left\langle 1^+_N \left\| \sigma\tau^+ \right\| 0^+_I \right\rangle}{\left[E_0 + E_N - E_I\right]^s} \tag{3.18}$$

where $s = \{1 + 2\delta_{J2}\}$ and

$$E_0 = \frac{1}{2}(E_I - E_F) = \frac{1}{2}Q_{\beta\beta} + m_e \tag{3.19}$$

Presently, the summation over the intermediate states is performed using the summation method [Civitarese and Suhonen (1993)]. Using summation method given by Civitarese and Suhonen (1993), the Eq. (3.18) can be written as

$$\begin{aligned} M_{2\nu}(0^+) &= \frac{1}{E_0}\left\langle 0^+_F \left| \sum_\mu (-1)^\mu \Gamma_{-\mu} F_\mu \right| 0^+_I \right\rangle \\ M_{2\nu}(2^+) &= \sqrt{\frac{1}{3}}\frac{1}{E_0^3}\left\langle 2^+_F \left| \sum_\mu (-1)^\mu \Gamma_{-\mu} F_\mu \right| 0^+_I \right\rangle \end{aligned} \tag{3.20}$$

where Γ_μ is given by

$$\Gamma_\mu = \sigma_\mu \tau^+ \tag{3.21}$$

and

$$F_\mu = \sum_{\lambda=0}^{\infty} \frac{(-1)^\lambda}{E_0^\lambda} D_\lambda \Gamma_\mu \tag{3.22}$$

with

$$D_\lambda \Gamma_\mu = [H, [H, ..., \ [H, \Gamma_\mu] .....]^{(\lambda \text{ times})} \tag{3.23}$$

The Eq. (3.20) can be further simplified, when the GT operator commutes with the effective two-body interaction. In the case of pseudo-SU(3) model [Castaños *et al.*(1994), Hirsch *et al.*(1995), Ceron *et al.*(1999)], the GT operator commutes with the two-body interaction and the energy denominator is a well-defined quantity without any free parameter. It has been evaluated exactly for the $2\nu\beta^-\beta^-$ of ^{150}Nd [Hirsch *et al.*(1995*a*)] in the context of pseudo-SU(3) scheme.

3.1.3 NTME $M_{2\nu}(J^+)$ in the PHFB model

In the present work, we use a Hamiltonian with PQQHH type of effective two-body interaction, which does not commute with the GT operator. Hence, the energy denominator is not a well-defined quantity. However, the violation of isospin symmetry for the QQHH part of our model Hamiltonian is negligible as is evident from the parameters of the two-body interaction given in Section 2.3. Further, the violation of isospin symmetry for the pairing part of the two-body interaction is presumably small. With these assumptions, the NTME $M_{2\nu}(J^+)$ of $2\nu\beta^-\beta^-$ decay for the $0^+ \rightarrow J^+$ transition in the PHFB model in conjunction with the summation method can be derived as follows. Using

$$\begin{aligned} \left[H, a_\pi^\dagger a_\nu\right] &= \left[H_\pi + H_\nu, a_\pi^\dagger a_\nu\right] \\ &= \sum_{nljm} \left(\varepsilon_\pi - \varepsilon_\nu\right) a_\pi^\dagger a_\nu \end{aligned} \tag{3.24}$$

where H_α consists of one-body part of the Hamiltonian only,

$$H_\alpha = \sum_{nljm} \varepsilon_\alpha(n,l,j) a_\alpha^\dagger(nljm) a_\alpha(nljm) \tag{3.25}$$

one obtains

$$\begin{aligned} D_\lambda \Gamma_\mu &= [H_\pi + H_\nu, [H_\pi + H_\nu, ..., [H_\pi + H_\nu, \Gamma_\mu] .....]]^{(\lambda \text{ times})} \\ &= \sum_{nljm} \left[\varepsilon(n_\pi, l_\pi, j_\pi) - \varepsilon(n_\nu, l_\nu, j_\nu)\right]^\lambda \sigma_\mu \tau^+ \end{aligned} \tag{3.26}$$

and F_μ is written as

$$\begin{aligned} F_\mu &= \sum_{\lambda=0}^{\infty} \frac{(-1)^\lambda}{E_0^\lambda} D_\lambda \Gamma_\mu \\ &= \sum_{\pi\nu} \sum_{\lambda=0}^{\infty} \left(\frac{-1}{E_0}\right)^\lambda \left[\varepsilon(n_\pi, l_\pi, j_\pi) - \varepsilon(n_\nu, l_\nu, j_\nu)\right]^\lambda \sigma_\mu \tau^+ \\ &= \sum_{\pi\nu} \frac{E_0^s}{\left[E_0 + \varepsilon(n_\pi, l_\pi, j_\pi) - \varepsilon(n_\nu, l_\nu, j_\nu)\right]^s} \sigma_\mu \tau^+ \end{aligned} \tag{3.27}$$

and the Eq. (3.20) can be further simplified to

$$M_{2\nu}(0^+) = \sum_{\pi,\nu} \frac{\langle 0_F^+ || \boldsymbol{\sigma} \cdot \boldsymbol{\sigma} \tau^+ \tau^+ || 0_I^+ \rangle}{E_0 + \varepsilon(n_\pi, l_\pi, j_\pi) - \varepsilon(n_\nu, l_\nu, j_\nu)} \tag{3.28}$$

$$M_{2\nu}(2^+) = \sqrt{5} \sum_{\pi,\nu} \frac{\left\langle 2_F^+ \left\| [\boldsymbol{\sigma} \otimes \boldsymbol{\sigma}]^{(2)} \tau^+ \tau^+ \right\| 0_I^+ \right\rangle}{\left[E_0 + \varepsilon(n_\pi, l_\pi, j_\pi) - \varepsilon(n_\nu, l_\nu, j_\nu)\right]^3} \tag{3.29}$$

and this expression is the same as that of Hirsch *et al.* [1995*a*]. We have evaluated the energy denominator as follows. With the assumption that the difference in single particle energies of protons in the intermediate nucleus and neutrons in the parent nucleus is mainly due to the difference in Coulomb energies, one obtains

$$\varepsilon(n_\pi, l_\pi, j_\pi) - \varepsilon(n_\nu, l_\nu, j_\nu) = \begin{cases} \Delta_C & for \quad n_\nu = n_\pi, l_\nu = l_\pi, j_\nu = j_\pi \\ \Delta_C + \Delta E_{s.o.splitting} & for \quad n_\nu = n_\pi, l_\nu = l_\pi, j_\nu \neq j_\pi \end{cases}, \tag{3.30}$$

where the Coulomb energy difference Δ_C is given by Bohr and Mottelson (1998).

$$\Delta_C = \frac{0.70}{A^{1/3}} \left[(2Z+1) - 0.76 \left\{(Z+1)^{4/3} - Z^{4/3}\right\}\right] \text{ MeV} \tag{3.31}$$

Finally, one obtains the following expression for the NTME $M_{2\nu}(0^+)$ of $2\nu\beta^-\beta^-$ decay for the $0^+ \rightarrow 0^+$ transition

$$\begin{aligned} M_{2\nu}(0^+) &= \sum_{\pi,\nu} \frac{\langle \Psi_{00}^{J_f=0} || \boldsymbol{\sigma} \cdot \boldsymbol{\sigma} \tau^+ \tau^+ || \Psi_{00}^{J_i=0} \rangle}{E_0 + \varepsilon(n_\pi, l_\pi, j_\pi) - \varepsilon(n_\nu, l_\nu, j_\nu)} \\ &= \left[n_{(Z,N)}^{Ji=0} n_{(Z+2,N-2)}^{J_f=0} \right]^{-1/2} \int_0^\pi n_{(Z,N),(Z+2,N-2)}(\theta) \\ &\times \sum_{\alpha\beta\gamma\delta} \frac{\langle \alpha\beta \left| \boldsymbol{\sigma}_1 . \boldsymbol{\sigma}_2 \tau^+ \tau^+ \right| \gamma\delta \rangle}{E_0 + \varepsilon_\alpha(n_\pi, l_\pi, j_\pi) - \varepsilon_\gamma(n_\nu, l_\nu, j_\nu)} \\ &\times \sum_{\varepsilon\eta} \left[\left(1 + F_{Z,N}^{(\pi)}(\theta) f_{Z+2,N-2}^{(\pi)*} \right) \right]_{\varepsilon\alpha}^{-1} \left(f_{Z+2,N-2}^{(\pi)*} \right)_{\varepsilon\beta} \\ &\times \left[\left(1 + F_{Z,N}^{(\nu)}(\theta) f_{Z+2,N-2}^{(\nu)*} \right) \right]_{\gamma\eta}^{-1} \left(F_{Z,N}^{(\nu)*} \right)_{\eta\delta} sin\theta d\theta \end{aligned} \tag{3.32}$$

and $M_{2\nu}(2^+)$ of $2\nu\beta^-\beta^-$ decay for the $0^+ \rightarrow 2^+$ transition.

$$\begin{aligned} M_{2\nu}(J^+) &= \sum_{\pi,\nu} \frac{\langle \Psi_{00}^{J_f=2} || [\boldsymbol{\sigma} \otimes \boldsymbol{\sigma}]^{(2)} \tau^+ \tau^+ || \Psi_{00}^{J_i=0} \rangle}{[E_0 + \varepsilon(n_\pi, l_\pi, j_\pi) - \varepsilon(n_\nu, l_\nu, j_\nu)]^3} \\ &= \left[n_{(Z,N)}^{Ji=2} n_{(Z+2,N-2)}^{J_f=0} \right]^{-1/2} \int_0^\pi n_{(Z,N),(Z+2,N-2)}(\theta) \sum_\mu \begin{bmatrix} J_i & 2 & J_f \\ -\mu & \mu & 0 \end{bmatrix} d_{\mu 0}^{J_i}(\theta) \\ &\times \sum_{\alpha\beta\gamma\delta} \frac{\left\langle \alpha\beta \left| [\boldsymbol{\sigma} \otimes \boldsymbol{\sigma}]^{(2)} \tau^+ \tau^+ \right| \gamma\delta \right\rangle}{[E_0 + \varepsilon_\alpha(n_\pi, l_\pi, j_\pi) - \varepsilon_\gamma(n_\nu, l_\nu, j_\nu)]^3} \\ &\times \sum_{\varepsilon\eta} \left[\left(1 + F_{Z,N}^{(\pi)}(\theta) f_{Z+2,N-2}^{(\pi)*} \right) \right]_{\varepsilon\alpha}^{-1} \left(f_{Z+2,N-2}^{(\pi)*} \right)_{\varepsilon\beta} \\ &\times \left[\left(1 + F_{Z,N}^{(\nu)}(\theta) f_{Z+2,N-2}^{(\nu)*} \right) \right]_{\gamma\eta}^{-1} \left(F_{Z,N}^{(\nu)*} \right)_{\eta\delta} sin\theta d\theta \end{aligned} \tag{3.33}$$

where

$$n^J = \int_0^\pi \left[det \left(1 + F^{(\pi)} f^{(\pi)\dagger} \right) \right]^{1/2} \left[det \left(1 + F^{(\nu)} f^{(\nu)\dagger} \right) \right]^{1/2} d_{00}^J(\theta) sin(\theta) d\theta \tag{3.34}$$

and

$$n_{(Z,N),(Z+2,N-2)}(\theta) = \left[det \left(1 + F_{Z,N}^{(\nu)} f_{Z+2,N-2}^{(\nu)\dagger} \right) \right]^{1/2} \times \left[det \left(1 + F_{Z,N}^{(\pi)} f_{Z+2,N-2}^{(\pi)\dagger} \right) \right]^{1/2} \tag{3.35}$$

The $\pi(\nu)$ represents the proton (neutron) of nuclei involved in the $2\nu\beta^-\beta^-$ decay process. The matrices $f_{Z,N}$ and $F_{Z,N}(\theta)$ are given by

$$f_{Z,N} = \sum_i C_{ij_\alpha,m_\alpha} C_{ij_\beta,m_\beta} \left(v_{im_\alpha}/u_{im_\alpha}\right) \delta_{m_\alpha,-m_\beta} \tag{3.36}$$

$$F_{Z,N}(\theta) = \sum_{m'_\alpha m'_\beta} d^{j_\alpha}_{m_\alpha,m'_\alpha}(\theta) d^{j_\beta}_{m_\beta,m'_\beta}(\theta) f_{j_\alpha m'_\alpha, j_\beta m'_\beta} \tag{3.37}$$

The results of PHFB calculations are summarized by amplitudes (u_{im}, v_{im}) and expansion coefficients $C_{ij,m}$. The required NTME $M_{2\nu}(J^+)$ is calculated as follows. In the first step, matrices $f_{Z,N}$ and $F_{Z,N}(\theta)$ given by Eqs. (3.36) and (3.37) are setup for the nuclei involved in the $2\nu\beta^-\beta^-$ decay making use of 20 Gaussian quadrature points in the range (0, π). Finally, the required NTME can be calculated in a straightforward manner using the Eqs. (3.32,3.33). As each proton-neutron excitation is considered according to its spin-flip or non–spin-flip character, the use of the summation method in the present context goes beyond the closure approximation. The spin-orbit splitting is explicitly included in the energy denominator, and hence, the PHFB formalism in conjunction with the summation method goes beyond that previously employed in the pseudo SU(3) model [Hirsch *et al.* (1995), (1995*a*)].

3.1.4 Phase space factors for $2\nu\beta^-\beta^-$ decay the for $0^+ \rightarrow 2^+$ transition

In the following, we give a brief discussion of the theoretical formalism to calculate the phase space factors of $2\nu\beta^-\beta^-$ decay for $0^+ \rightarrow 2^+$ transitions. The detailed derivation of these formulae are given by Doi *et al.* (1985), (1992), Suhonen and Civitarese (1998) and references there in.

The phase space factors of $2\nu\beta^-\beta^-$ decay for the $0^+ \rightarrow 2^+$ transition is given by

$$\begin{aligned} G_{2\nu}(2^+) &= \frac{2(Gg_A)^4}{448\pi^7 m_e^2 \ln(2)} \int_{m_e}^{T+m_e} F_0\left(Z,\varepsilon_1\right) p_1\varepsilon_1 I^{(2)}\left(T,\varepsilon_1\right) d\varepsilon_1 \\ &= g_{2\nu}(2^+) \int_{m_e}^{T+m_e} F_0\left(Z,\varepsilon_1\right) p_1\varepsilon_1 I^{(2)}\left(T,\varepsilon_1\right) d\varepsilon_1 \end{aligned} \tag{3.38}$$

where g_A is the axial vector coupling constant and

$$g_{2\nu}(2^+) = \frac{2(Gg_A)^4}{448\pi^7 m_e^2 \ln(2)} \tag{3.39}$$

$$I^{(2)}\left(T,\varepsilon_1\right) = \int_{m_e}^{T+2m_e-\varepsilon_1} F_0\left(Z,\varepsilon_2\right) p_2\varepsilon_2 \left(\varepsilon_1-\varepsilon_2\right)^2 \left(T+2-\varepsilon_1-\varepsilon_2\right)^7 d\varepsilon_2 \tag{3.40}$$

with $G = 1.16637 \times 10^{-5}\ GeV^{-2}$ and $\alpha = 1/137.06$. Here $\varepsilon_k = \sqrt{p_k^2 + m_e^2}$ is the energy of k^{th} electron. The Fermi function $F_0\left(Z,\varepsilon\right)$ can be approximated as

$$F_0\left(Z,\varepsilon\right) = \frac{4}{\left[\Gamma\left(2\gamma_1+1\right)\right]^2} \left(2pR_A\right)^{2(\gamma_1-1)} \left|\Gamma\left(\gamma_1+iy\right)\right|^2 e^{\pi y} \tag{3.41}$$

where

$$\gamma_k = \sqrt{k^2-\left(\alpha Z\right)^2} \qquad\qquad y = \alpha Z\varepsilon/p \tag{3.42}$$

and the complex gamma function is evaluated using the relation

$$\left|\Gamma\left(\alpha+i\beta\right)\right| = \frac{\Gamma\left(1+\alpha\right)}{\alpha} \prod_{n=0}^{\infty} \left[1+\frac{\beta^2}{\left(\alpha+n\right)^2}\right]^{-\frac{1}{2}} \tag{3.43}$$

Recently the phase space factors $G_{2\nu}(2^+)$ for excited state transition have been calculated by Pahomi *et al.* (2014) using exact Dirac wave functions of electron including finite nuclear size and screening effects.

3.2 Results and discussions

As discussed earlier that the $0^+ \rightarrow 2^+$ transition of $2\nu\beta^-\beta^-$ decay has not been observed experimentally and only half-life limits are available. As a test of reliability of the wave function, in Table 3.1, the NTMEs $M_{2\nu}(0^+)$ calculated with four different parametrization of effective two-body interactions, namely PQQ1, PQQHH1, PQQ2, PQQHH2, are presented along with experimental values for comparison. It is observed that theoretically calculated NTMEs agree well with the experimental values within error bar except for the case ^{130}Te and ^{150}Nd. The estimated average (mean) NTMEs $\overline{M}_{2\nu}(J^+)$ and uncertainties (standard deviation) $\Delta\overline{M}_{2\nu}(J^+)$ has been calculated as follows:

$$\overline{M}_i = \frac{\sum_{k=1}^{N} M_i^k}{N} \tag{3.44}$$

and

$$\Delta\overline{M}_i = \frac{1}{\sqrt{N-1}} \left[\sum_{k=1}^{N} \left(\overline{M}_i - M_i^k \right)^2 \right]^{1/2} \tag{3.45}$$

The Eqs. (3.44) and (3.45) define the best estimate of the mean and standard deviation for a Gaussian distribution. In Table 3.2, we present the presently calculated results of $M_{2\nu}(2^+)$ along with average values and uncertainties. The maximum uncertainty in NTMEs turns out to be about 45%, which implies that the NTMEs $M_{2\nu}(2^+)$ are highly sensitive to the deformation. In the present work, the phase space factors $G_{2\nu}(2^+)$ have been taken from Pahomi *et al.* (2014) and rescaled at $g_A = 1.2701$ (Beringer *et al.* (2012)). The $G_{2\nu}(2^+)$ of ^{94}Zr and ^{104}Ru nuclei are not available and these have been calculated by following the prescription of Suhonen and Civitarese (1998) using axial vector coupling constant $g_A = 1.2701$ in the present work. The $G_{2\nu}(2^+)$ (in yr^{-1}) used in the present work are 6.801×10^{-30}, 1.494×10^{-18}, 1.460×10^{-18}, 9.625×10^{-25}, 1.228×10^{-20},

1.429×10^{-24}, 4.632×10^{-19} and 3.253×10^{-17} for ^{94,96}Zr, ^{100}Mo, ^{104}Ru, ^{110}Pd, ^{128,130}Te and ^{150}Nd isotopes, respectively.

A large number of theoretical and experimental studies have been done for the $0^+ \rightarrow 2^+$ transition of $2\nu\beta^-\beta^-$ decay. Over the past years, the experimentally investigated isotopes for this particular decay mode are ^{94}Zr [Norman and Meekhof (1987), Dokania *et al.* (2017)], ^{96}Zr [Barabash *et al.* (1996), Arpesella *et al.* (1994)], ^{100}Mo [N. Kudomi *et al.* (1992), Blum *et al.* (1992), Barabash *et al.* (1993), Barabash *et al.* (1995), Arnold *et al.* (2014)], ^{110}Pd [Lehnert *et al.* (2016)], ^{128}Te [Bellotti *et al.* (1987)], ^{130}Te [Bellotti *et al.* (1987), Barabash *et al.* (2001)] and ^{150}Nd [Arpesella *et al.* (1994),(1999), Barabash *et al.* (2009)]. All the available theoretical and experimental results are compiled in Table 3.3 for the nuclei under study. We present only the theoretical $T^{2\nu}_{1/2}(2^+)$ for those models for which no direct or indirect information about $M_{2\nu}(2^+)$ is available to us. In case of heavy nuclei, it is more justified to use g_A around 1.0. Hence, the theoretical $T^{2\nu}_{1/2}(2^+)$ are calculated both for $g_A = 1.2701$ and 1.0.

From the Table 3.4 it can be observed that there is a remarkable spread in the calculated NTMEs $M_{2\nu}(2^+)$ within different nuclear models. Specifically, the NTMEs $M_{2\nu}(2^+)$ calculated with the QRPA model without and with deformation vary by a factor of about 2–341, corresponding to ^{130}Te and ^{96}Zr isotopes, respectively. The average NTMEs $\overline{M}_{2\nu}(2^+)$ evaluated using the PHFB approach are suppressed by a factor between 1 – 450 approximately with respect to those of Raduta *et al.* (2007) corresponding to ^{96}Zr and ^{104}Ru isotopes, respectively. Considering all the available experimental and theoretical results, it can be observed that the ^{96}Zr, ^{100}Mo, ^{110}Pd, ^{130}Te and ^{150}Nd are the probable nuclei for the observation of the $0^+ \rightarrow 2^+$ transition of $2\nu\beta^-\beta^-$ decay. Moreover, once

the the $0^+ \rightarrow 2^+$ transition of $2\nu\beta^-\beta^-$ decay is observed, it can constrain the validity of different nuclear models employed in the calculation of NTMEs.

3.3 Conclusions

Sets of four NTMEs $M_{2\nu}(2^+)$ have been calculated with in PHFB model using four different parametrization of the pairing plus multipolar type of effective two-body interaction namely, PQQ1, PQQHH1, PQQ2 and PQQHH2 to study the $2\nu\beta^-\beta^-$ decay of ^{94,96}Zr, ^{100}Mo, ^{104}Ru, ^{110}Pd, ^{128,130}Te and ^{150}Nd isotopes for the $0^+ \rightarrow 2^+$ transition. The observation of Raduta *et al.* (2007) that the inclusion of deformation in the mean field can reduce the NTMEs $M_{2\nu}(2^+)$ calculated within pnQRPA up to a factor of 341, motivated us to study the $0^+ \rightarrow 2^+$ transition of $2\nu\beta^-\beta^-$ decay within PHFB approach treating the pairing and deformation degrees of freedom simultaneously on equal footing. It is noticed that with respect to NTMEs $M_{2\nu}(2^+)$ of Raduta *et al.* (2007), the average NTMEs $\overline{M}_{2\nu}(2^+)$ calculated using the PHFB approach are further suppressed by a factor between 1 – 450 approximately corresponding to ^{96}Zr and ^{128}Te isotopes, respectively. In spite of the fact that the $0^+ \rightarrow 2^+$ transition of $2\nu\beta^-\beta^-$ decay is highly suppressed in comparison to the $0^+ \rightarrow 0^+$ transition, the available theoretical and experimental results suggest that the observation of the $0^+ \rightarrow 2^+$ transition of $2\nu\beta^-\beta^-$ decay may be possible in ^{96}Zr, ^{100}Mo, ^{110}Pd, ^{130}Te and ^{150}Nd isotopes.

Table 3.1: Theoretically calculated NTMEs $M_{2\nu}$ within the PHFB model with four different parametrizations and their average value $\overline{M}_{2\nu}$ along with experimental values [Barabash (2010)].

Nuclei	$M_{2\nu}(0^+)$				$\overline{M}_{2\nu}(0^+)$	$\Delta\overline{M}_{2\nu}(0^+)$	$M_{2\nu}(0^+)$(Exp.)
	PQQ1	PQQHH1	PQQ2	PQQHH2			
^{94}Zr	0.064	0.060	0.133	0.058	0.079	0.036	–
^{96}Zr	0.055	0.056	0.053	0.054	0.054	0.001	$0.048^{+0.002}_{-0.002}$
^{100}Mo	0.127	0.128	0.127	0.127	0.127	0.001	$0.123^{+0.004}_{-0.003}$
^{104}Ru	0.020	0.021	0.023	0.022	0.021	0.001	–
^{110}Pd	0.085	0.124	0.105	0.115	0.107	0.017	–
^{128}Te	0.026	0.022	0.027	0.021	0.024	0.003	$0.024^{+0.003}_{-0.002}$
^{130}Te	0.047	0.044	0.041	0.050	0.045	0.004	$0.017^{+0.002}_{-0.001}$
^{150}Nd	0.010	0.008	0.010	0.008	0.009	0.001	$0.031^{+0.002}_{-0.002}$

Table 3.2: Calculated NTMEs $M_{2\nu}(2^+)$ within the PHFB model and their average $\overline{M}_{2\nu}(2^+)$ along with standard deviation $\Delta\overline{M}_{2\nu}(2^+)$.

Nuclei	$M_{2\nu}(2^+)$				$\overline{M}_{2\nu}(2^+)$	$\Delta\overline{M}_{2\nu}(2^+)$
	PQQ1	PQQHH1	PQQ2	PQQHH2		
^{94}Zr	1.49×10^{-4}	1.49×10^{-4}	1.01×10^{-4}	1.45×10^{-4}	1.360×10^{-4}	0.234×10^{-4}
^{96}Zr	1.23×10^{-4}	1.34×10^{-4}	1.18×10^{-4}	1.27×10^{-4}	1.255×10^{-4}	0.067×10^{-4}
^{100}Mo	1.57×10^{-5}	1.47×10^{-5}	1.80×10^{-5}	1.14×10^{-5}	1.495×10^{-5}	0.274×10^{-5}
^{104}Ru	8.18×10^{-6}	8.66×10^{-6}	8.24×10^{-6}	8.85×10^{-6}	8.483×10^{-6}	0.325×10^{-6}
^{110}Pd	1.31×10^{-4}	2.03×10^{-4}	1.48×10^{-4}	2.01×10^{-4}	1.708×10^{-4}	0.367×10^{-4}
^{128}Te	1.82×10^{-6}	2.62×10^{-6}	1.90×10^{-6}	2.84×10^{-6}	2.295×10^{-6}	0.511×10^{-6}
^{130}Te	5.39×10^{-6}	6.01×10^{-6}	5.01×10^{-6}	6.06×10^{-6}	5.617×10^{-6}	0.506×10^{-6}
^{150}Nd	1.43×10^{-7}	1.71×10^{-7}	1.13×10^{-7}	1.37×10^{-7}	1.410×10^{-7}	0.238×10^{-7}

Table 3.3: Theoretically calculated NTME $M_{2\nu}(2^+)$ and half-life $T^{2\nu}_{1/2}(2^+)$ (in yr) for the $0^+ \rightarrow 2^+$ transition of ^{94,96}Zr, ^{100}Mo, ^{104}Ru, ^{110}Pd, ^{128,130}Te and ^{150}Nd nuclei along with experimental half-lives $T^{2\nu}_{1/2}(2^+)$ (in yr). The numbers corresponding to (a) and (b) are calculated for $g_A = 1.2701$ and 1.0 respectively. "*" denotes the present calculation.

Nuclei	Theory					Experiment	
	Model	Ref.	$\lvert M_{2\nu}(2^+)\rvert$		$T^{2\nu}_{1/2}(2^+)$	$T^{2\nu}_{1/2}(2^+)$	Ref.
^{94}Zr	PHFB	*	1.49×10^{-4}	(a)	7.950×10^{36}	$>1.3\times 10^{19}$	[1]
				(b)	2.069×10^{37}	$>3.4\times 10^{19}$	[3]
	QRPA†	[2]	0.0170	(a)	5.088×10^{32}		
				(b)	1.324×10^{33}		
	QRPA‡	[2]	0.0155	(a)	6.120×10^{32}		
				(b)	1.593×10^{33}		
^{96}Zr	PHFB	*	1.23×10^{-4}	(a)	4.250×10^{25}	$>2.0\times 10^{18}$	[1]
				(b)	1.106×10^{26}	$>4.1\times 10^{19}$	[5]
	QRPA	[4]	(0.005-0.038)	(a)	2.677×10^{22}	$>7.9\times 10^{19}$	[4]
				(a)	4.635×10^{20}		
				(b)	6.967×10^{22}		
				(b)	1.206×10^{21}		
	QRPA	[6]	1.113×10^{-4}	(a)	5.403×10^{25}		
				(b)	1.406×10^{26}		
	QRPA	[7]	0.011	(a)	5.532×10^{21}		
				(b)	1.440×10^{22}		
	RQRPA†	[8]	0.011	(a)	5.532×10^{21}		
				(b)	1.440×10^{22}		
	RQRPA‡	[8]	0.010	(a)	6.693×10^{21}		
				(b)	1.742×10^{22}		
	RQRPA	[9]			$(1.1\text{-}1.4)\times10^{21}$		
	SRPA	[10]	3.117×10^{-4}	(a)	6.889×10^{24}		
				(b)	1.793×10^{25}		

Table 3.3 continued

Nuclei	Theory					Experiment	
	Model	Ref.	$\lvert M_{2\nu}(2^+)\rvert$		$T^{2\nu}_{1/2}(2^+)$	$T^{2\nu}_{1/2}(2^+)$	Ref.
^{100}Mo	PHFB	*	1.57×10^{-5}	(a)	3.065×10^{27}	$>1.5\times 10^{20}$	[11]
				(b)	7.975×10^{27}	$>5.0\times 10^{20}$	[13]
	QRPA	[12]	0.033	(a)	6.290×10^{20}	$>2.3\times 10^{21}$	[14]
				(b)	1.637×10^{21}	$>1.6\times 10^{21}$	[15]
	QRPA	[6]	1.814×10^{-4}	(a)	2.081×10^{25}		
				(b)	5.417×10^{25}		
	QRPA	[7]	0.0078	(a)	1.126×10^{22}		
				(b)	2.930×10^{22}		
	RQRPA	[9]			$(1.0\text{-}1.1)\times10^{22}$		
	SRPA	[10]	1.482×10^{-3}	(a)	3.119×10^{23}		
				(b)	8.115×10^{23}		
	SU(3)$^{+}$	[16]	7.3×10^{-5}	(a)	1.285×10^{26}		
				(b)	3.345×10^{26}		
	SU(3)$^{++}$	[16]	1.53×10^{-4}	(a)	2.926×10^{25}		
				(b)	7.614×10^{25}		
	MCM	[17]			$(5.3\text{-}13)\times10^{20}$		
^{104}Ru	PHFB	*	8.18×10^{-6}	(a)	1.444×10^{34}		
				(b)	3.758×10^{34}		
	QRPA	[6]	3.736×10^{-3}	(a)	7.444×10^{28}		
				(b)	1.937×10^{29}		
	QRPA†	[2]	0.00792	(a)	1.656×10^{28}		
				(b)	4.310×10^{28}		
	QRPA‡	[2]	0.00811	(a)	1.580×10^{28}		
				(b)	4.111×10^{28}		
^{110}Pd	PHFB	*	1.31×10^{-4}	(a)	2.793×10^{27}	$>2.9\times10^{20}$	[18]
				(b)	7.268×10^{28}		
	QRPA	[6]	6.671×10^{-3}	(a)	1.830×10^{24}		
				(b)	4.762×10^{24}		

Table 3.3 continued

Nuclei	Theory					Experiment	
	Model	Ref.	$\lvert M_{2\nu}(2^+)\rvert$		$T^{2\nu}_{1/2}(2^+)$	$T^{2\nu}_{1/2}(2^+)$	Ref.
	QRPA†	[2]	0.0112	(a)	6.492×10^{23}		
				(b)	1.689×10^{24}		
	QRPA‡	[2]	0.00766	(a)	1.388×10^{24}		
				(b)	3.612×10^{24}		
	SRPA	[19]	5.621×10^{-3}	(a)	2.577×10^{24}		
				(b)	6.707×10^{24}		
^{128}Te	PHFB	*	1.82×10^{-6}	(a)	1.329×10^{35}	$>4.7\times 10^{21}$	[20]
				(b)	3.457×10^{35}		
	QRPA	[6]	3.055×10^{-4}	(a)	7.498×10^{30}		
				(b)	1.951×10^{31}		
	QRPA	[7]	0.00287	(a)	8.496×10^{28}		
				(b)	2.211×10^{29}		
	SRPA	[19]	1.022×10^{-3}	(a)	6.700×10^{29}		
				(b)	1.743×10^{30}		
^{130}Te	PHFB	*	5.39×10^{-6}	(a)	6.841×10^{28}	$>4.5\times 10^{21}$	[20]
				(b)	1.780×10^{29}	$>1.6\times 10^{21}$	[21]
	QRPA	[6]	8.272×10^{-5}	(a)	3.155×10^{26}		
				(b)	8.210×10^{26}		
	QRPA	[7]	0.00016	(a)	8.433×10^{25}		
				(b)	2.195×10^{26}		
	SRPA	[19]	4.088×10^{-3}	(a)	1.292×10^{23}		
				(b)	3.362×10^{23}		
^{150}Nd	PHFB	*	1.43×10^{-7}	(a)	1.546×10^{30}	$>8.0\times 10^{18}$	[5]
				(b)	4.024×10^{30}	$>9.1\times 10^{19}$	[23]
	SU(3)	[22]	5.38×10^{-5}	(a)	1.062×10^{25}		
				(b)	2.764×10^{25}		

†WS basis; ‡AWS basis; $^{+}$Spherical occupation wave functions; $^{++}$Deformed occupation wave functions

References:

[1] Norman (1987)
[2] Suhonen (2011)
[3] Dokania *et al.* (2017)
[4] Barabash *et al.* (1996)
[5] Arpesella *et al.* (1994)
[6] Raduta *et al.* (2007)
[7] Unlu (2013), (2014)
[8] Toivanen and Suhonen (1997)
[9] Schweiger *et al.* (1998)
[10] Stoica and Mihut (1996)
[11] Kudomi *et al.* (1992)
[12] Suhonen and Civitarese (1994)
[13] Blum *et al.* (1992)
[14] Barabash *et al.* (1993)
[15] Barabash *et al.* (1995)
[16] Hirsch *et al.* (1995)
[17] Suhonen (1998)
[18] Lehnert *et al.* (2016)
[19] Stoica (1994)
[20] Bellotti *et al.* (1987)
[21] Barabash *et al.* (2001)
[22] Hirsch *et al.* (1995*a*)
[23] Arpesella *et al.*(1999)

Chapter 4

Neutrinoless double beta decay of ^{94,96}Zr, ^{100}Mo, ^{110}Pd, ^{128,130}Te and ^{150}Nd isotopes for the $0^+ \rightarrow 0^+$ transition

The nuclear $\beta\beta$ decay in general and $0\nu\beta^-\beta^-$ decay in particular is a convenient tool to probe physics beyond the SM. The gauge theoretical models which violate the conservation of lepton number L can accommodate the mechanism of $0\nu\beta^-\beta^-$ decay. The possibilities include GUTs such as left-right symmetric SO(10), E(8) etc., extensions of the SM leading to Majoron emission, R_p-violating as well as conserving MSSM, string theories as well as the scenario of compositeness, sterile neutrinos and leptoquarks. The experimental observation of $0\nu\beta^-\beta^-$ decay is expected to be useful for judging which specific gauge theoretical model is correct. In particular for the question whether the neutrino is a

Majorana or Dirac particle, the $0\nu\beta^-\beta^-$ decay is considered to be the most sensitive way of distinguishing between these two possibilities.

Klapdor and his group in 2004 have reported that the $0\nu\beta^-\beta^-$ decay has been observed in ^{76}Ge [Klpdor *et al.* (2004)]. However, the results were controversial and the issue could not be settled down. The aim of all the present experimental activities is to observe the $0\nu\beta^-\beta^-$ decay. Hence, the models predict the half-lives assuming certain value for the neutrino mass or conversely extract various parameters from the observed limits on half-lives of the $0\nu\beta^-\beta^-$ decay. The reliability of predictions can be judged a priori only from the success of a nuclear model in explaining various observed physical properties of nuclei. The common practice is to calculate the $M_{2\nu}(0^+)$ to start with, and compare with the experimentally observed value. In Chapter 3, we have calculated the $M_{2\nu}(0^+)$ of ^{94,96}Zr, ^{100}Mo, ^{104}Ru, ^{110}Pd, ^{128,130}Te and ^{150}Nd nuclei, and it has been found that the theoretically calculated $M_{2\nu}(0^+)$ are in good agreement with the experimentally observed values. Hence, we intent to employ the same set of initial and final nuclear wave functions to study the $0\nu\beta^-\beta^-$ decay of above mentioned nuclei in the present chapter.

In Section 4.1, the theoretical formalism to calculate the decay rate of $0\nu\beta^-\beta^-$ decay has been derived in 2n mechanism for light neutrinos. The results of our calculation are presented and discussed in Section 4.2. We have calculated NTMEs in PHFB model for ^{94,96}Zr, ^{100}Mo, ^{110}Pd, ^{128,130}Te and ^{150}Nd nuclei. Further, the gauge-theoretical parameters, namely effective electron-neutrino mass $\langle m_\nu \rangle$ and effective weak coupling constants $\langle \lambda \rangle$ and $\langle \eta \rangle$ for the coupling of right-handed leptonic current with right-handed and left-handed hadronic currents, respectively, are extracted from the observed limits on half-lives $T^{0\nu}_{1/2}$ of the $0\nu\beta^-\beta^-$ decay. Finally, we present some concluding remarks in Section 4.3.

4.1 Theoretical formalism

The general form of weak interaction Hamiltonian H_W is given by

$$H_W = \frac{G}{\sqrt{2}}\left[j_{L\mu}J_L^{\mu\dagger} + \kappa j_{L\mu}J_R^{\mu\dagger} + \eta j_{R\mu}J_L^{\mu\dagger} + \lambda j_{R\mu}J_R^{\mu\dagger}\right] + h.c. \tag{4.1}$$

where $j_{L,R}$ and $J_{L,R}$ are left and right handed leptonic and hadronic currents, respectively. Further, κ, η and λ are the parameters for the admixture of $V-A$ and $V+A$ currents. The second term in the Eq. (4.1) is usually neglected as κ enters into $\beta\beta$ decay amplitude always in the combination $1 \pm \kappa$ and it is expected that $|\kappa| \ll 1$.

Using the standard approximations of Doi *et al.* (1985), with CP conservation, the rate for the $0^+ \rightarrow 0^+$ transition of $0\nu\beta^-\beta^-$ decay is given by

$$\begin{aligned}\left[T_{1/2}^{0\nu}\right]^{-1} &= \frac{\left|\langle m_\nu\rangle\right|^2}{m_e}C_{mm} + \frac{\left|\langle m_\nu\rangle\right|}{m_e}\langle\lambda\rangle C_{m\lambda} + \frac{\left|\langle m_\nu\rangle\right|}{m_e}\langle\eta\rangle C_{m\eta} \\ &\quad + \langle\lambda\rangle^2 C_{\lambda\lambda} + \langle\eta\rangle^2 C_{\eta\eta} + \langle\lambda\rangle\langle\eta\rangle C_{\lambda\eta}\end{aligned} \tag{4.2}$$

where

$$\langle m_\nu\rangle = {\sum_i}' U_{ei}^2 m_i \tag{4.3}$$

$$\langle\lambda\rangle = \lambda\left|{\sum_i}'\left(\frac{g_V'}{g_V}\right)U_{ei}V_{ei}\right| \tag{4.4}$$

$$\langle\eta\rangle = \eta\left|{\sum_i}' U_{ei}V_{ei}\right| \tag{4.5}$$

and the nuclear structure factors C_{xy} are written as

$$C_{mm} = G_{01}\left|M^{(0\nu)}\right|^2 \tag{4.6}$$

$$C_{m\lambda} = M^{(0\nu)}\left(G_{04}M_{1+} - G_{03}M_{2-}\right) \tag{4.7}$$

$$C_{m\eta} = M^{(0\nu)}(G_{03}M_{2+} - G_{04}M_{1-} - G_{05}M_P + G_{06}M_R) \quad (4.8)$$

$$C_{\lambda\lambda} = G_{02}\left|M_{2-}\right|^2 - \frac{2}{9}G_{03}(M_{1+}M_{2-}) + \frac{1}{9}G_{04}\left|M_{1+}\right|^2 \quad (4.9)$$

$$C_{\eta\eta} = G_{02}\left|M_{2+}\right|^2 - \frac{2}{9}G_{03}(M_{1-}M_{2+}) + \frac{1}{9}G_{04}\left|M_{1-}\right|^2$$
$$-G_{07}(M_PM_R) + G_{08}\left|M_P\right|^2 + G_{09}\left|M_R\right|^2 \quad (4.10)$$

$$C_{\lambda\eta} = -2G_{02}(M_{2+}M_{2-}) + \frac{2}{9}G_{03}(M_{2+}M_{1+} + M_{2-}M_{1-})$$
$$-\frac{2}{9}G_{04}(M_{1-}M_{1+}) \quad (4.11)$$

In addition, the combinations of NTMEs $M^{(0\nu)}$ and $M_{i\pm}$ $(i = 1, 2)$ are defined as

$$M^{(0\nu)} = M_{GT} - M_F + M_T \quad (4.12)$$

$$M_{1\pm} = M_{qGT} - 6M_{qT} \pm 3M_{qF} \quad (4.13)$$

$$M_{2\pm} = M_{\omega GT} \pm M_{\omega F} - \frac{1}{9}M_{1\mp} \quad (4.14)$$

Employing the generally agreed closure approximation in conjunction with the HFB wave functions, the NTMEs M_α ($\alpha = F, GT, T, \omega F, \omega GT, qF, qGT, qT, P$ and R) appearing in the expressions of nuclear structure factors C_{xy} are calculated by using the following expression [Rath *et al.* (2010)].

$$\begin{aligned} M_\alpha &= \left\langle 0_f^+ \left\| O_\alpha(\mathbf{r}, \boldsymbol{\sigma}) \right\| 0_i^+ \right\rangle \\ &= \left[n^{J_f=0}n^{Ji=0}\right]^{-1/2} \int_0^\pi d\theta sin\theta n_{(Z,N),(Z+2,N-2)}(\theta) \times \sum_{\alpha\beta\gamma\delta} \left\langle \alpha\beta \left| O_\alpha(\mathbf{r}, \boldsymbol{\sigma}) \right| \gamma\delta \right\rangle \\ &\quad \times \sum_{\varepsilon\eta} \frac{\left(f^{(\pi)*}_{Z+2,N-2}\right)_{\varepsilon\beta}}{\left[\left(1 + F^{(\pi)}_{Z,N}(\theta) f^{(\pi)*}_{Z+2,N-2}\right)\right]_{\varepsilon\alpha}} \times \frac{\left(F^{(\nu)*}_{Z,N}\right)_{\eta\delta}}{\left[\left(1 + F^{(\nu)}_{Z,N}(\theta) f^{(\nu)*}_{Z+2,N-2}\right)\right]_{\gamma\eta}} \end{aligned} \quad (4.15)$$

where

$$n^J = \int_0^\pi \left[det\left(1 + F^{(\pi)}f^{(\pi)^\dagger}\right)\right]^{1/2} \left[det\left(1 + F^{(\nu)}f^{(\nu)^\dagger}\right)\right]^{1/2} d^J_{00}(\theta)sin(\theta)d\theta \quad (4.16)$$

and

$$n_{(Z,N),(Z+2,N-2)}(\theta) = \left[det\left(1+F^{(\nu)}_{Z,N}f^{(\nu)\dagger}_{Z+2,N-2}\right)\right]^{1/2} \times \left[det\left(1+F^{(\pi)}_{Z,N}f^{(\pi)\dagger}_{Z+2,N-2}\right)\right]^{1/2} \quad (4.17)$$

The $\pi(\nu)$ represents the proton (neutron) of nuclei involved in the $\left(\beta^-\beta^-\right)_{0\nu}$ decay process. The matrices $f_{Z,N}$ and $F_{Z,N}(\theta)$ are given by

$$f_{Z,N} = \sum_i C_{ij_\alpha,m_\alpha}C_{ij_\beta,m_\beta}\left(v_{im_\alpha}/u_{im_\alpha}\right)\delta_{m_\alpha,-m_\beta} \quad (4.18)$$

$$F_{Z,N}(\theta) = \sum_{m'_\alpha m'_\beta} d^{j_\alpha}_{m_\alpha,m'_\alpha}(\theta)d^{j_\beta}_{m_\beta,m'_\beta}(\theta)f_{j_\alpha m'_\alpha,j_\beta m'_\beta} \quad (4.19)$$

The calculation of n^J, $n_{(Z,N),(Z+2,N-2)}(\theta)$, $f_{Z,N}$ and $F_{Z,N}(\theta)$ require the intrinsic wave functions $|\Phi_0\rangle$ of axially symmetric state with $K=0$ expressed by the amplitudes (u_{im}, v_{im}) and expansion coefficients $C_{ij,m}$, which are in turn obtained by minimizing the expectation value of the effective Hamiltonian given by [Rath *et al.* (2010)]

$$H = H_{sp} + V(P) + V(QQ) + V(HH) \quad (4.20)$$

in a basis constructed by using a set of deformed states. In Eq.(4.20), the H_{sp}, $V(P)$, $V(QQ)$ and $V(HH)$ denote the single particle Hamiltonian, the pairing, quadrupole-quadrupole and hexadecapole-hexadecapole parts of the effective two-body interaction, respectively. Further, the transition operators have the following general structure

$$O_\alpha\left(\mathbf{r},\boldsymbol{\sigma},\boldsymbol{\tau}\right) = S_\alpha\left(\mathbf{r},\boldsymbol{\sigma}\right)\ \tau^+_n\tau^+_m\ \frac{2R}{\pi}\int h_\alpha(qr)\ f_\alpha(q^2)\ q^2dq \quad (4.21)$$

Neglecting the induced pseudoscalar terms in the nonrelativistic reduction of right-handed $V+A$ current [Štefánik *et al.* (2015)], the explicit structure of $S_\alpha\left(\mathbf{r},\boldsymbol{\sigma}\right)$, $h_\alpha(qr)$

and $f_\alpha(q^2)$ for the rest of the NTMEs M_α is given as follows.

$$
\begin{aligned}
O_F &= \tau_n^+\tau_m^+\frac{2R}{\pi}\int \frac{f_\alpha\left(qr_{nm}\right)}{\left(q+\overline{A}\right)}\, h_F(q)qdq && (4.22)\\
O_{GT} &= \boldsymbol{\sigma}_n\cdot\boldsymbol{\sigma}_m\tau_n^+\tau_m^+\frac{2R}{\pi}\int \frac{f_\alpha\left(qr_{nm}\right)}{\left(q+\overline{A}\right)}\, h_{GT}(q)qdq && (4.23)\\
O_T &= \left[3\left(\boldsymbol{\sigma}_n\cdot\hat{\mathbf{r}}_{nm}\right)\left(\boldsymbol{\sigma}_m\cdot\hat{\mathbf{r}}_{nm}\right)-\boldsymbol{\sigma}_n\cdot\boldsymbol{\sigma}_m\right]\tau_n^+\tau_m^+ \\
&\quad\times\frac{2R}{\pi}\int \frac{f_\alpha\left(qr_{nm}\right)}{\left(q+\overline{A}\right)}\, h_T(q)qdq && (4.24)\\
O_{\omega F} &= \tau_n^+\tau_m^+\frac{2R}{\pi}\int \frac{j_0(qr)}{\left(q+\overline{A}\right)^2}\,\frac{g_V^2(q^2)}{g_A^2}\, q^2dq && (4.25)\\
O_{\omega GT} &= \boldsymbol{\sigma}_1\cdot\boldsymbol{\sigma}_2\;\tau_n^+\tau_m^+\,\frac{2R}{\pi}\int \frac{j_0(qr)}{\left(q+\overline{A}\right)^2}\,\frac{g_A^2(q^2)}{g_A^2}\, q^2dq && (4.26)\\
O_{qF} &= \tau_n^+\tau_m^+\frac{2R}{\pi}\int \frac{j_1(qr)qr}{q\left(q+\overline{A}\right)}\,\frac{g_V^2(q^2)}{g_A^2}\, q^2dq && (4.27)\\
O_{qGT} &= \boldsymbol{\sigma}_1\cdot\boldsymbol{\sigma}_2\;\tau_n^+\tau_m^+\,\frac{2R}{\pi}\int \frac{j_1(qr)qr}{q\left(q+\overline{A}\right)}\,\frac{g_A^2(q^2)}{g_A^2}\, q^2dq && (4.28)\\
O_{qT} &= \left(3(\boldsymbol{\sigma}_1\cdot\hat{\mathbf{r}}_{12})\left(\boldsymbol{\sigma}_1\cdot\hat{\mathbf{r}}_{12}\right)-\boldsymbol{\sigma}_1\cdot\boldsymbol{\sigma}_2\right)\;\tau_n^+\tau_m^+\,\frac{2R}{\pi} \\
&\quad\times\int \frac{j_1(qr)qr}{q\left(q+\overline{A}\right)}\,\frac{g_A^2(q^2)}{3g_A^2}\, q^2dq && (4.29)\\
O_P &= \left(i\frac{R}{2r^2}\left(\boldsymbol{\sigma}_1-\boldsymbol{\sigma}_2\right)\cdot\left(\frac{\mathbf{r}\times\mathbf{r}_+}{R}\right)\right)\tau_n^+\tau_m^+\frac{2R}{\pi} \\
&\quad\times\int \frac{j_1(qr)qr}{q\left(q+\overline{A}\right)}\frac{g_A(q^2)g_V(q^2)}{g_A^2}q^2dq && (4.30)\\
O_R &= \boldsymbol{\sigma}_1\cdot\boldsymbol{\sigma}_2\;\tau_n^+\tau_m^+\,\frac{2R}{\pi} \\
&\quad\times\int \frac{j_0(qr)q^2}{q\left(q+\overline{A}\right)}\,\frac{1}{3m_N}\left(1+\frac{g_M\left(q^2\right)}{g_V(q^2)}\right)\frac{g_A(q^2)g_V(q^2)}{g_A^2}\, q^2dq && (4.31)
\end{aligned}
$$

where $f_\alpha\left(qr_{nm}\right)=j_0\left(qr_{nm}\right)$ for $\alpha=F,\,GT$ and $f_T\left(qr_{nm}\right)=j_2\left(qr_{nm}\right)$. The effects due to the FNS are incorporated through the dipole form factors and the form factor related

functions $h_F(q)$, $h_{GT}(q)$ and $h_T(q)$ are written as

$$
\begin{aligned}
h_F(q) &= g_V^2\left(q^2\right) && (4.32)\\
h_{GT}(q) &= \frac{g_A^2(q^2)}{g_A^2}\left[1-\frac{2}{3}\frac{g_P(q^2)q^2}{g_A(q^2)2M_p}+\frac{1}{3}\frac{g_P^2(q^2)q^4}{g_A^2(q^2)4M_P^2}\right]+\frac{2}{3}\frac{g_M^2(q^2)q^2}{g_A^2 4M_p^2}\\
&\approx \left(\frac{\Lambda_A^2}{q^2+\Lambda_A^2}\right)^4\left[1-\frac{2}{3}\frac{q^2}{(q^2+m_\pi^2)}+\frac{1}{3}\frac{q^4}{(q^2+m_\pi^2)^2}\right]\\
&\quad+\left(\frac{g_V}{g_A}\right)^2\frac{\kappa^2q^2}{6M_p^2}\left(\frac{\Lambda_V^2}{q^2+\Lambda_V^2}\right)^4 && (4.33)\\
h_T(q) &= \frac{g_A^2(q^2)}{g_A^2}\left[\frac{2}{3}\frac{g_P(q^2)q^2}{g_A(q^2)2M_p}-\frac{1}{3}\frac{g_P^2(q^2)q^4}{g_A^2(q^2)4M_P^2}\right]+\frac{1}{3}\frac{g_M^2(q^2)q^2}{g_A^2 4M_p^2}\\
&\approx \left(\frac{\Lambda_A^2}{q^2+\Lambda_A^2}\right)^4\left[\frac{2}{3}\frac{q^2}{(q^2+m_\pi^2)}-\frac{1}{3}\frac{q^4}{(q^2+m_\pi^2)^2}\right]\\
&\quad+\left(\frac{g_V}{g_A}\right)^2\frac{\kappa^2q^2}{12M_p^2}\left(\frac{\Lambda_V^2}{q^2+\Lambda_V^2}\right)^4 && (4.34)
\end{aligned}
$$

where

$$
\begin{aligned}
g_V(q^2) &= \frac{g_V}{g_A}\left(\frac{\Lambda_V^2}{q^2+\Lambda_V^2}\right)^2\\
g_A(q^2) &= g_A\left(\frac{\Lambda_A^2}{q^2+\Lambda_A^2}\right)^2 && (4.35)\\
g_M(q^2) &= \kappa g_V\left(\frac{\Lambda_V^2}{q^2+\Lambda_V^2}\right)^2\\
g_P(q^2) &= \frac{2m_p g_A(q^2)}{(q^2+m_\pi^2)}\left(\frac{\Lambda_A^2-m_\pi^2}{\Lambda_A^2}\right) && (4.36)
\end{aligned}
$$

with $g_V = 1.0$, $g_A = 1.2701$, $\kappa = \mu_p - \mu_n = 3.70$, $\Lambda_V = 0.850$ GeV, $\Lambda_A = 1.086$ GeV and m_π is the pion mass.

In the PHFB model, the effect of short range correlations (SRC), produced by the repulsive NN potential generated through the exchange of ω and ρ mesons, can be incorporated approximately by multiplying the two nucleon wave functions by a correlation function $f(r)$ when calculating NTMEs. This is equivalent to the replacement

$$
\langle j_1^\pi\ j_2^\pi\ J\,|O_\alpha|\,j_1^\nu\ j_2^\nu J\rangle \rightarrow \langle j_1^\pi\ j_2^\pi\ J\,|f\ O_\alpha\ f|\,j_1^\nu\ j_2^\nu\ J\rangle \qquad (4.37)
$$

with

$$f(r) = 1 - ce^{-ar^2}(1 - br^2) \tag{4.38}$$

where $a = 1.1\ fm^{-2}$, $1.59\ fm^{-2}$, $1.52\ fm^{-2}$, $b = 0.68\ fm^{-2}$, $1.45\ fm^{-2}$, $1.88\ fm^{-2}$ and $c = 1.0$, 0.92, 0.46 for Miller-Spencer, Argonne V18 and CD-Bonn NN potentials, respectively.

4.1.1 Phase space factors for $0\nu\beta^-\beta^-$ decay

Doi *et al.* (1985),(1993), Tomoda (1991) and Suhonen and Civitarese (1998) have developed the formalism to calculate the phase space factors for $0\nu\beta^-\beta^-$ decay. Following the notations of Doi *et al.* (1993), we briefly outline the steps of derivation in the below.

The phase space factors for $0\nu\beta^-\beta^-$ decay G_{0k} $(k = 1, 2, ...10)$ can be obtained by evaluating the following integrals

$$G_{0k} = \frac{(Gg_A)^4 m_e^9}{64\pi^5 (m_e R)^2 \ln(2)} \int b_{0k} d\Omega_{0\nu} \tag{4.39}$$

where

$$d\Omega_{0\nu} = 2m_e^{-5} p_1 p_2 \varepsilon_1 \varepsilon_2 \delta(\varepsilon_1 + \varepsilon_2 + E_F - E_I)\, d\varepsilon_1 d\varepsilon_2 \tag{4.40}$$

Using

$$\begin{pmatrix} \alpha_+ \\ \\ \beta_+ \end{pmatrix} = \frac{1}{2}\left(\varepsilon_1\varepsilon_2 \pm m_e^2\right) C_{00}, \qquad \begin{pmatrix} \alpha_- \\ \\ \beta_- \end{pmatrix} = \frac{1}{2}\left(\varepsilon_1 \pm \varepsilon_2\right) m_e C_{00} \tag{4.41}$$

with

$$C_{00} = \frac{F_0(Z, \varepsilon_1) F_0(Z, \varepsilon_2)}{\varepsilon_1 \varepsilon_2} \tag{4.42}$$

and integrating Eq. (4.39), one obtains

$$\begin{aligned} G_{0k} &= \frac{2(Gg_A)^4 m_e^4}{64\pi^5 (m_e R)^2 \ln(2)} \int b_{0k} p_1 p_2 \varepsilon_1 \varepsilon_2 d\varepsilon_1 \\ &= \frac{g^{(0\nu)}}{(m_e R)^2} \int b_{0k}\, p_1 p_2 \varepsilon_1 \varepsilon_2 d\varepsilon_1 \end{aligned} \tag{4.43}$$

where

$$g^{(0\nu)} = \frac{(Gg_A)^4 m_e^4}{32\pi^5 \ln(2)} \tag{4.44}$$

and the nuclear radius

$$R = 1.2A^{1/3}\ fm \tag{4.45}$$

The kinematical factors b_{0k} $(k = 1, 2, ...10)$ are written as follows

$$\begin{aligned} b_{01} &= \alpha_+ + \beta_+ \\ &= F_0(Z, \varepsilon_1) F_0(Z, \varepsilon_2) \end{aligned} \tag{4.46}$$

$$\begin{aligned} b_{02} &= \left(\frac{\varepsilon_{12}}{m_e}\right)^2 \beta_+ \\ &= \frac{1}{2}\left(\frac{\varepsilon_1 - \varepsilon_2}{m_e}\right)^2 \frac{(\varepsilon_1\varepsilon_2 - m_e^2)}{\varepsilon_1\varepsilon_2} F_0(Z, \varepsilon_1) F_0(Z, \varepsilon_2) \end{aligned} \tag{4.47}$$

$$\begin{aligned} b_{03} &= 2\left(\frac{\varepsilon_{12}}{m_e}\right) \beta_- \\ &= \frac{(\varepsilon_1 - \varepsilon_2)^2}{\varepsilon_1\varepsilon_2} F_0(Z, \varepsilon_1) F_0(Z, \varepsilon_2) \end{aligned} \tag{4.48}$$

$$\begin{aligned} b_{04} &= \left(\frac{4}{9}\right) \beta_+ \\ &= \frac{2}{9}\frac{(\varepsilon_1\varepsilon_2 - m_e^2)}{\varepsilon_1\varepsilon_2} F_0(Z, \varepsilon_1) F_0(Z, \varepsilon_2) \end{aligned} \tag{4.49}$$

$$\begin{aligned} b_{05} &= \frac{4}{3}\frac{(\zeta\alpha_- - 2m_e R\alpha_+)}{(m_e R)} \\ &= \frac{2}{3}\frac{1}{\varepsilon_1\varepsilon_2}\left[\frac{\zeta(\varepsilon_1 + \varepsilon_2)m_e}{m_e R} - 2(\varepsilon_1\varepsilon_2 + m_e^2)\right] \\ &\quad \times F_0(Z, \varepsilon_1) F_0(Z, \varepsilon_2) \end{aligned} \tag{4.50}$$

$$
\begin{aligned}
b_{06} &= \left(\frac{8}{m_eR}\right)\alpha_- \\
&= \frac{4m_e(\varepsilon_1+\varepsilon_2)}{\varepsilon_1\varepsilon_2\,.\,m_eR}F_0(Z,\varepsilon_1)F_0(Z,\varepsilon_2) \qquad (4.51)\\
b_{07} &= \frac{16}{3}\frac{(\zeta\alpha_+ - 2m_eR\alpha_-)}{(m_eR)^2} \\
&= \left(\frac{8}{3m_eR}\right)\frac{1}{\varepsilon_1\varepsilon_2}\left[\frac{\zeta(\varepsilon_1\varepsilon_2+m_e^2)}{m_eR} - 2m_e(\varepsilon_1+\varepsilon_2)\right] \\
&\quad \times F_0(Z,\varepsilon_1)F_0(Z,\varepsilon_2) \qquad (4.52)\\
b_{08} &= \frac{4}{3}\frac{\left[\zeta^2\alpha_+ + 4m_e(Rm_eR\alpha_+ - \zeta\alpha_-)\right]}{(m_eR)^2} \\
&= \frac{8}{9}\frac{1}{\varepsilon_1\varepsilon_2}\left[\left\{\frac{1}{4}\left(\frac{\zeta}{m_eR}\right)^2+1\right\}(\varepsilon_1\varepsilon_2+m_e^2) - \right. \\
&\quad \left.\left(\frac{\zeta}{m_eR}\right)(\varepsilon_1+\varepsilon_2)m_e\right]F_0(Z,\varepsilon_1)F_0(Z,\varepsilon_2) \qquad (4.53)\\
b_{09} &= \left(\frac{4}{m_eR}\right)^2\alpha_+ \\
&= \frac{8}{\varepsilon_1\varepsilon_2}\frac{(\varepsilon_1\varepsilon_2+m_e^2)}{(m_eR)^2}F_0(Z,\varepsilon_1)F_0(Z,\varepsilon_2) \qquad (4.54)\\
b_{010} &= 2(\alpha_+ - \beta_+) \\
&= \frac{2m_e^2}{\varepsilon_1\varepsilon_2}F_0(Z,\varepsilon_1)F_0(Z,\varepsilon_2) \qquad (4.55)
\end{aligned}
$$

where

$$\zeta = 3\alpha Z + (T+2)\,m_eR \qquad (4.56)$$

4.2 Results and discussions

In the present work, we employ the same PHFB wave-function used in Chapter 2 and Chapter 3, i.e. wave functions generated with four different parametrizations of the effective two-body interaction, namely PQQ1, PQQHH1, PQQ2 and PQQHH2. Further, we use three different parametrizations of the SRC due to Miller-Spencer parametrization,

Argonne NN and CD-Bonn potentials and call them SRC1, SRC2 and SRC3, respectively. The required NTMEs, namely M_F, $M_{\omega F}$, M_{qF}, M_{GT}, $M_{\omega GT}$, M_{qGT}, M_T, M_{qT}, M_P and M_R are calculated for ^{94,96}Zr, ^{100}Mo, ^{104}Ru,^{110}Pd, ^{128,130}Te and ^{150}Nd nuclei for the $0^+ \rightarrow 0^+$ transition within the approximations of point nucleons (P), nucleons having finite size (FNS) and also with SRC (F+SRC). These values of NTMEs are presented in Table 4.1 for the ^{100}Mo nuclei as a representative case. The combination of NTMEs $M^{(0\nu)}$ and $M_{i\pm}$ $(i = 1, 2)$ given by Eqs.(4.12, 4.13, 4.14) are presented in Table 4.2.

In Table 4.3, the relative changes in NTMEs M_α (in %) are presented due to the different approximations. Due to FNS, the maximum change in M_F, $M_{\omega F}$, M_{qF}, M_{GT}, $M_{\omega GT}$, M_{qGT}, M_T, M_{qT}, M_P and M_R is about 16%, 18%, 38%, 11%, 11%, 24%, 57%, 18%, 57% and 34%, respectively. With the inclusion of SRC, the NTMEs $M_{F,\omega F,GT,\omega GT}$ change by about 17%, 2% and 4% due to SRC1, SRC2 and SRC3, respectively. The observed changes in $M_{qF,qGT}$ with the inclusion of SRC1, SRC2 and SRC3 are of the same order and the maximum change is about 7%. Due to the inclusion of SRC, the change in $M_{T,qT}$ is about 8% and 2%, respectively and M_P can change between 3%–33%. The maximum change in M_R due to SRC1, SRC2 and SRC3 is about 56%, 29% and 11%, respectively.

Each NTME has a set of twelve values due to four parametrizations of two-body interaction and three parametrizations of SRC. We have calculated their averages and standard deviations using Eqs. (3.44) and (3.45) of Chapter 3 and the values are presented in Table 4.4. It is observed that the uncertainty in $\overline{M}_{F,\omega F,qF}$, $\overline{M}_{GT,\omega GT,qGT}$ and $\overline{M}_P$ is about 7–15% but for ^{150}Nd, in which the standard deviation of $\overline{M}_P$ is about 28%. The NTMEs $M_{T,qT}$ are quite uncertain. The maximum uncertainty in $\overline{M}_R$ is about 30%. In present work, we use the phase space factors calculated by Štefánik *et al.* (2015)

and reevaluate them at $g_A = 1.2701$ and presented in Table 4.5. Sets of twelve nuclear structure factors C_{mm}, $C_{m\lambda}$, $C_{m\eta}$, $C_{\lambda\lambda}$, $C_{\eta\eta}$ and $C_{\lambda\eta}$ are computed for ^{96}Zr, ^{100}Mo, ^{110}Pd, ^{130}Te and ^{150}Nd isotopes and the results are reported in Table 4.6. The averages of these nuclear structure factors are given in Table 4.7.

Using the average nuclear structure factors $\overline{C}_{mm}$, $\overline{C}_{\lambda\lambda}$, $\overline{C}_{\eta\eta}$, on-axis limits on the effective mass of light neutrino $\langle m_\nu \rangle$, the effective weak coupling of right-handed leptonic current with right-handed hadronic current $< \lambda >$, and the effective weak coupling of right-handed leptonic current with left-handed hadronic current $< \eta >$ are extracted from the largest observed limits on half-lives $T^{0\nu}_{1/2}$ of $0\nu\beta^-\beta^-$decay and the results are given in Table 4.8. The extracted limits on $\langle m_\nu \rangle$, $\langle \lambda \rangle$, and $\langle \eta \rangle$ for ^{130}Te (^{100}Mo) nuclei are 0.17 eV (0.44 eV), 2.41×10^{-7} (5.62×10^{-7}) and 2.55×10^{-9} (6.09×10^{-9}), respectively. In the last two columns of the same Table 4.6, the predicted half-lives $T^{0\nu}_{1/2}$ of $0\nu\beta^-\beta^-$decay of ^{96}Zr, ^{100}Mo, ^{110}Pd, ^{130}Te and ^{150}Nd isotopes are given for two sets of parameters (i) $\langle m_\nu \rangle = 50$ meV and (ii) $\langle m_\nu \rangle = 50$ meV, $\langle \lambda \rangle = 10^{-7}$ and $\langle \eta \rangle = 10^{-9}$. It is noticed that the predicted half-lives $T^{0\nu}_{1/2}$ are smaller for the latter case than those of pure mass mechanism.

4.3 CONCLUSIONS

To summarize, sets of twelve NTMEs, namely $M_{\omega F,qF}$, $M_{\omega GT,qGT}$, M_{qT}, M_P, and M_R are calculated using PHFB wave functions generated with four different parametrization of pairing plus multipolar type of effective two-body interaction, and three different parametrizations of SRC to study the $0\nu\beta^-\beta^-$ decay of ^{94,96}Zr, ^{100}Mo, ^{110}Pd, ^{128,130}Te and ^{150}Nd

isotopes within mechanisms involving the light Majorana neutrino and right handed $V+A$ current. The maximum effect due to FNS is about 57% for $M_{T,P}$. Due to SRC1, SRC2 and SRC3, the maximum change in M_R is about 56%, 29% and 11%, respectively.

The maximum uncertainty in $\overline{M}_{F,\omega F,qF}$, $\overline{M}_{GT,\omega GT,qGT}$ and $\overline{M}_P$ is about15% but for ^{150}Nd, in which the standard deviation of $\overline{M}_P$ is about 28%. The maximum uncertainty in $\overline{M}_R$ is about 30%. The NTMEs $M_{T,qT}$ are quite uncertain. Using the average nuclear structure factors $\overline{C}_{mm}$, $\overline{C}_{\lambda\lambda}$, and $\overline{C}_{\eta\eta}$, the most stringent on-axis extracted limits on $\langle m_\nu \rangle$, $\langle \lambda \rangle$, and $\langle \eta \rangle$ from the most recent observed limits on half-lives $T^{0\nu}_{1/2}$ of ^{130}Te isotope are 0.17 eV, 2.41×10^{-7} and 2.55×10^{-9}, respectively.

Table 4.1: Calculated NTMEs M_α of ^{100}Mo for point case (P), with the inclusion of finites size of nucleons (FNS) and both the FNS and SRC (F+SRC).

Nuclei	Parametrisation		P	FNS	F+SRC		
					SRC1	SRC2	SRC3
^{100}Mo	PQQ1	M_F	1.246	1.082	0.950	1.083	1.120
		M_{GT}	-5.275	-4.798	-4.142	-4.720	-4.909
		M_T	0.102	0.077	0.078	0.080	0.079
		$M_{\omega F}$	1.074	0.918	0.797	0.917	0.951
		M_{qF}	1.419	0.994	0.957	1.036	1.044
		$M_{\omega GT}$	-5.099	-4.595	-3.884	-4.515	-4.718
		M_{qGT}	-6.949	-5.520	-5.187	-5.703	-5.781
		M_{qT}	0.170	0.163	0.164	0.164	0.164
		M_P	3.897	3.454	3.334	3.606	3.634
		M_R	-7.034	-4.735	-2.094	-3.379	-4.225
	PQQHH1	M_F	1.082	0.924	0.796	0.923	0.959
		M_{GT}	-5.072	-4.612	-3.978	-4.536	-4.719
		M_T	0.075	0.056	0.056	0.057	0.057
		$M_{\omega F}$	0.949	0.799	0.681	0.796	0.829
		M_{qF}	1.214	0.807	0.771	0.847	0.855
		$M_{\omega GT}$	-4.913	-4.426	-3.740	-4.349	-4.545
		M_{qGT}	-6.680	-5.299	-4.978	-5.476	-5.551
		M_{qT}	0.100	0.095	0.096	0.095	0.095
		M_P	3.969	3.514	3.391	3.669	3.697
		M_R	-6.794	-4.574	-2.023	-3.264	-4.081

Table 4.1 continued

Nuclei	Parametrisation		P	FNS	F+SRC		
					SRC1	SRC2	SRC3
	PQQ2	M_F	1.247	1.083	0.951	1.084	1.121
		M_{GT}	-5.257	-4.780	-4.125	-4.702	-4.891
		M_T	0.107	0.081	0.082	0.083	0.083
		$M_{\omega F}$	1.075	0.919	0.798	0.918	0.952
		M_{qF}	1.420	0.995	0.958	1.037	1.045
		$M_{\omega GT}$	-5.082	-4.579	-3.869	-4.499	-4.702
		M_{qGT}	-6.925	-5.497	-5.165	-5.680	-5.758
		M_{qT}	0.178	0.171	0.171	0.171	0.171
		M_P	3.884	3.445	3.326	3.597	3.624
		M_R	-7.024	-4.729	-2.092	-3.375	-4.220
	PQQHH2	M_F	1.065	0.909	0.781	0.908	0.944
		M_{GT}	-5.006	-4.548	-3.919	-4.473	-4.655
		M_T	0.079	0.058	0.059	0.060	0.060
		$M_{\omega F}$	0.936	0.787	0.670	0.784	0.817
		M_{qF}	1.195	0.790	0.754	0.830	0.838
		$M_{\omega GT}$	-4.853	-4.370	-3.689	-4.294	-4.488
		M_{qGT}	-6.591	-5.221	-4.901	-5.396	-5.471
		M_{qT}	0.106	0.100	0.101	0.101	0.100
		M_P	3.926	3.477	3.355	3.630	3.658
		M_R	-6.745	-4.540	-2.007	-3.240	-4.051

Table 4.2: Combination of NTMEs $M^{(0\nu)}$ and $M_{i\pm}(i = 1, 2)$.

Nuclei	Parametrization		P	FNS	F+SRC		
					SRC1	SRC2	SRC3
^{94}Zr	PQQ1	$M^{(0\nu)}$	-4.158	-3.725	-3.187	-3.662	-3.817
		M_{1+}	-2.154	-2.013	-1.867	-2.058	-2.094
		M_{1-}	-7.256	-5.451	-5.147	-5.645	-5.715
		M_{2+}	-1.939	-1.900	-1.533	-1.824	-1.932
		M_{2-}	-3.813	-3.381	-2.829	-3.311	-3.470
	PQQHH1	$M^{(0\nu)}$	-3.828	-3.423	-2.921	-3.364	-3.509
		M_{1+}	-1.976	-1.844	-1.708	-1.886	-1.920
		M_{1-}	-6.599	-4.918	-4.633	-5.097	-5.163
		M_{2+}	-1.811	-1.774	-1.432	-1.703	-1.804
		M_{2-}	-3.517	-3.114	-2.599	-3.048	-3.196
	PQQ2	$M^{(0\nu)}$	-4.467	-4.045	-3.536	-3.995	-4.142
		M_{1+}	-1.875	-1.747	-1.610	-1.798	-1.832
		M_{1-}	-6.763	-5.051	-4.764	-5.245	-5.311
		M_{2+}	-2.215	-2.177	-1.829	-2.112	-2.214
		M_{2-}	-4.012	-3.600	-3.077	-3.542	-3.692
	PQQHH2	$M^{(0\nu)}$	-3.706	-3.312	-2.822	-3.254	-3.395
		M_{1+}	-1.944	-1.816	-1.683	-1.856	-1.889
		M_{1-}	-6.471	-4.828	-4.550	-5.003	-5.067
		M_{2+}	-1.736	-1.701	-1.367	-1.631	-1.729
		M_{2-}	-3.406	-3.013	-2.510	-2.948	-3.093

Table 4.2 continued

Nuclei	Parametrization		P	FNS	F+SRC		
					SRC1	SRC2	SRC3
^{96}Zr	PQQ1	$M^{(0\nu)}$	-2.884	-2.581	-2.192	-2.534	-2.645
		M_{1+}	-1.630	-1.531	-1.424	-1.558	-1.584
		M_{1-}	-5.611	-4.295	-4.074	-4.435	-4.485
		M_{2+}	-1.174	-1.149	-.884	-1.091	-1.168
		M_{2-}	-2.617	-2.306	-1.908	-2.255	-2.369
	PQQHH1	$M^{(0\nu)}$	-2.837	-2.526	-2.128	-2.476	-2.590
		M_{1+}	-1.667	-1.563	-1.453	-1.591	-1.618
		M_{1-}	-5.277	-3.939	-3.711	-4.079	-4.131
		M_{2+}	-1.252	-1.225	-.954	-1.166	-1.245
		M_{2-}	-2.586	-2.269	-1.861	-2.215	-2.332
	PQQ2	$M^{(0\nu)}$	-2.810	-2.514	-2.134	-2.468	-2.577
		M_{1+}	-1.613	-1.516	-1.411	-1.541	-1.567
		M_{1-}	-5.503	-4.215	-3.999	-4.352	-4.402
		M_{2+}	-1.140	-1.117	-.857	-1.059	-1.135
		M_{2-}	-2.550	-2.247	-1.858	-2.197	-2.308
	PQQHH2	$M^{(0\nu)}$	-2.766	-2.463	-2.074	-2.414	-2.526
		M_{1+}	-1.647	-1.545	-1.438	-1.572	-1.598
		M_{1-}	-5.195	-3.889	-3.666	-4.025	-4.076
		M_{2+}	-1.211	-1.186	-.921	-1.127	-1.205
		M_{2-}	-2.521	-2.211	-1.813	-2.159	-2.272

Table 4.2 continued

Nuclei	Parametrization		P	FNS	F+SRC		
					SRC1	SRC2	SRC3
^{100}Mo	PQQ1	$M^{(0\nu)}$	-6.419	-5.803	-5.013	-5.723	-5.950
		M_{1+}	-3.711	-3.517	-3.299	-3.576	-3.630
		M_{1-}	-12.223	-9.479	-9.041	-9.793	-9.894
		M_{2+}	-2.666	-2.623	-2.083	-2.510	-2.668
		M_{2-}	-5.760	-5.122	-4.314	-5.034	-5.266
	PQQHH1	$M^{(0\nu)}$	-6.078	-5.480	-4.717	-5.402	-5.621
		M_{1+}	-3.639	-3.447	-3.238	-3.508	-3.559
		M_{1-}	-10.925	-8.290	-7.864	-8.589	-8.687
		M_{2+}	-2.750	-2.706	-2.186	-2.599	-2.751
		M_{2-}	-5.457	-4.842	-4.061	-4.755	-4.979
	PQQ2	$M^{(0\nu)}$	-6.397	-5.783	-4.994	-5.703	-5.930
		M_{1+}	-3.731	-3.537	-3.319	-3.596	-3.650
		M_{1-}	-12.249	-9.506	-9.068	-9.820	-9.921
		M_{2+}	-2.646	-2.603	-2.064	-2.490	-2.648
		M_{2-}	-5.743	-5.105	-4.298	-5.018	-5.249
	PQQHH2	$M^{(0\nu)}$	-5.992	-5.399	-4.641	-5.321	-5.538
		M_{1+}	-3.641	-3.450	-3.242	-3.510	-3.561
		M_{1-}	-10.809	-8.192	-7.768	-8.489	-8.586
		M_{2+}	-2.716	-2.673	-2.156	-2.566	-2.717
		M_{2-}	-5.385	-4.774	-3.998	-4.688	-4.910

Table 4.2 continued

Nuclei	Parametrization		P	FNS	F+SRC		
					SRC1	SRC2	SRC3
^{110}Pd	PQQ1	$M^{(0\nu)}$	-4.304	-3.892	-3.361	-3.844	-3.996
		M_{1+}	-2.694	-2.550	-2.406	-2.600	-2.635
		M_{1-}	-8.021	-6.169	-5.873	-6.387	-6.455
		M_{2+}	-1.884	-1.855	-1.493	-1.785	-1.890
		M_{2-}	-3.814	-3.386	-2.844	-3.332	-3.487
	PQQHH1	$M^{(0\nu)}$	-5.898	-5.335	-4.624	-5.270	-5.473
		M_{1+}	-3.330	-3.137	-2.946	-3.207	-3.254
		M_{1-}	-9.678	-7.227	-6.827	-7.512	-7.604
		M_{2+}	-2.855	-2.812	-2.328	-2.720	-2.862
		M_{2-}	-5.201	-4.629	-3.902	-4.554	-4.762
	PQQ2	$M^{(0\nu)}$	-5.627	-5.091	-4.405	-5.030	-5.227
		M_{1+}	-3.425	-3.242	-3.056	-3.306	-3.352
		M_{1-}	-10.518	-8.120	-7.739	-8.404	-8.492
		M_{2+}	-2.436	-2.399	-1.931	-2.308	-2.445
		M_{2-}	-5.000	-4.445	-3.744	-4.376	-4.576
	PQQHH2	$M^{(0\nu)}$	-5.218	-4.710	-4.067	-4.651	-4.835
		M_{1+}	-3.001	-2.822	-2.649	-2.886	-2.928
		M_{1-}	-8.418	-6.200	-5.836	-6.457	-6.540
		M_{2+}	-2.585	-2.546	-2.109	-2.464	-2.592
		M_{2-}	-4.610	-4.092	-3.435	-4.024	-4.212

Table 4.2 continued

Nuclei	Parametrization		P	FNS	F+SRC		
					SRC1	SRC2	SRC3
^{128}Te	PQQ1	$M^{(0\nu)}$	-3.231	-2.896	-2.482	-2.854	-2.973
		M_{1+}	-1.685	-1.587	-1.472	-1.623	-1.651
		M_{1-}	-6.330	-4.918	-4.683	-5.079	-5.133
		M_{2+}	-1.272	-1.245	-.965	-1.189	-1.271
		M_{2-}	-2.894	-2.561	-2.140	-2.513	-2.634
	PQQHH1	$M^{(0\nu)}$	-2.967	-2.633	-2.221	-2.590	-2.708
		M_{1+}	-1.655	-1.555	-1.440	-1.591	-1.619
		M_{1-}	-5.721	-4.324	-4.088	-4.480	-4.534
		M_{2+}	-1.245	-1.217	-.938	-1.161	-1.242
		M_{2-}	-2.693	-2.361	-1.942	-2.312	-2.432
	PQQ1	$M^{(0\nu)}$	-3.302	-2.961	-2.542	-2.920	-3.040
		M_{1+}	-1.691	-1.592	-1.475	-1.628	-1.657
		M_{1-}	-6.428	-4.994	-4.756	-5.157	-5.212
		M_{2+}	-1.304	-1.276	-.992	-1.219	-1.303
		M_{2-}	-2.957	-2.618	-2.192	-2.570	-2.693
	PQQHH2	$M^{(0\nu)}$	-2.941	-2.604	-2.190	-2.561	-2.680
		M_{1+}	-1.613	-1.511	-1.396	-1.548	-1.576
		M_{1-}	-5.585	-4.180	-3.943	-4.337	-4.392
		M_{2+}	-1.258	-1.230	-.949	-1.173	-1.255
		M_{2-}	-2.680	-2.347	-1.925	-2.297	-2.418

Table 4.2 continued

Nuclei	Parametrization		P	FNS	F+SRC		
					SRC1	SRC2	SRC3
^{130}Te	PQQ1	$M^{(0\nu)}$	-4.808	-4.343	-3.777	-4.282	-4.445
		M_{1+}	-1.998	-1.863	-1.706	-1.912	-1.950
		M_{1-}	-8.477	-6.557	-6.233	-6.770	-6.845
		M_{2+}	-1.982	-1.944	-1.561	-1.865	-1.978
		M_{2-}	-4.234	-3.779	-3.203	-3.709	-3.875
	PQQHH1	$M^{(0\nu)}$	-4.431	-3.974	-3.421	-3.911	-4.070
		M_{1+}	-1.766	-1.630	-1.476	-1.676	-1.714
		M_{1-}	-7.257	-5.400	-5.080	-5.600	-5.674
		M_{2+}	-1.979	-1.940	-1.565	-1.861	-1.971
		M_{2-}	-3.927	-3.483	-2.920	-3.411	-3.573
	PQQ2	$M^{(0\nu)}$	-4.392	-3.957	-3.427	-3.899	-4.052
		M_{1+}	-1.994	-1.867	-1.719	-1.911	-1.947
		M_{1-}	-8.017	-6.217	-5.913	-6.416	-6.486
		M_{2+}	-1.779	-1.743	-1.384	-1.668	-1.774
		M_{2-}	-3.875	-3.448	-2.908	-3.382	-3.537
	PQQHH2	$M^{(0\nu)}$	-4.822	-4.341	-3.758	-4.276	-4.444
		M_{1+}	-1.778	-1.635	-1.474	-1.686	-1.726
		M_{1-}	-7.694	-5.733	-5.397	-5.947	-6.024
		M_{2+}	-2.172	-2.131	-1.737	-2.050	-2.166
		M_{2-}	-4.266	-3.798	-3.206	-3.724	-3.894

Table 4.2 continued

Nuclei	Parametrization		P	FNS	F+SRC		
					SRC1	SRC2	SRC3
^{150}Nd	PQQ1	$M^{(0\nu)}$	-1.730	-1.565	-1.360	-1.549	-1.608
		M_{1+}	-.724	-.677	-.619	-.696	-.710
		M_{1-}	-3.430	-2.703	-2.590	-2.792	-2.819
		M_{2+}	-.633	-.622	-.483	-.595	-.636
		M_{2-}	-1.570	-1.402	-1.195	-1.383	-1.443
	PQQHH1	$M^{(0\nu)}$	-1.496	-1.344	-1.155	-1.329	-1.383
		M_{1+}	-.617	-.572	-.519	-.590	-.603
		M_{1-}	-2.854	-2.185	-2.080	-2.266	-2.291
		M_{2+}	-.587	-.577	-.449	-.552	-.590
		M_{2-}	-1.381	-1.227	-1.035	-1.208	-1.263
	PQQ2	$M^{(0\nu)}$	-1.701	-1.539	-1.337	-1.523	-1.581
		M_{1+}	-.714	-.668	-.611	-.686	-.700
		M_{1-}	-3.377	-2.661	-2.551	-2.750	-2.776
		M_{2+}	-.622	-.611	-.474	-.585	-.625
		M_{2-}	-1.543	-1.379	-1.175	-1.360	-1.418
	PQQHH2	$M^{(0\nu)}$	-1.480	-1.331	-1.146	-1.316	-1.370
		M_{1+}	-.611	-.567	-.515	-.584	-.597
		M_{1-}	-2.840	-2.183	-2.081	-2.263	-2.287
		M_{2+}	-.575	-.566	-.440	-.541	-.578
		M_{2-}	-1.363	-1.212	-1.025	-1.195	-1.249

Table 4.3: Change in the NTME M_α of $0\nu\beta^-\beta^-$decay (in %) due to the exchange of light Majorana neutrino, and admixture of $V-A$ and $V+A$ currents, with the inclusion of FNS and SRC (SRC1, SRC2, SRC3) for all four parametrizations of the effective two-body interaction.

NTME	FNS	F+SRC		
		SRC1	SRC2	SRC3
M_F	11.24–16.41	9.98–16.09	0.02–0.68	2.96–4.23
$M_{\omega F}$	12.72–17.71	11.18–17.01	0.04–0.99	3.07–4.16
M_{qF}	25.11–37.65	2.71–5.64	3.49–5.74	4.09–6.93
M_{GT}	8.36–10.56	12.45–16.19	1.34–2.20	2.21–2.77
$M_{\omega GT}$	9.11–11-17	14.05–17.60	1.42–2.31	2.57–3.05
M_{qGT}	19.10–23.95	5.34–7.33	3.13-4.04	4.39–5.76
M_T	1.18–57.05	0.03-3.21	0.20-8.04	0.19–7.48
M_{qT}	0.33–18.32	0.01–1.62	0.01–1.39	0.01–1.22
M_P	11.15–57.08	3.01–31.24	3.84–26.61	4.54–33.28
M_R	30.83–34.25	55.21–56.41	28.07–29.25	10.42–11.14

Table 4.4: Average values for NTMEs $\overline{M}_\alpha$ and uncertainty $\Delta\overline{M}_\alpha$ for the $0\nu\beta^-\beta^-$ decay of ^{94,96}Zr, ^{100}Mo, ^{110}Pd, ^{128,130}Te and ^{150}Nd isotopes.

Nuclei	^{94}Zr	^{96}Zr	^{100}Mo	^{110}Pd	^{128}Te	^{130}Te	^{150}Nd
$\overline{M}_F$	0.580	0.456	0.968	0.731	0.523	0.717	0.303
$\Delta\overline{M}_F$	0.056	0.045	0.115	0.113	0.060	0.071	0.035
$\overline{M}_{\omega F}$	0.494	0.387	0.826	0.620	0.429	0.585	0.248
$\triangle\overline{M}_{\omega F}$	0.050	0.038	0.094	0.095	0.049	0.059	0.027
$\overline{M}_{qF}$	0.544	0.432	0.914	0.679	0.516	0.704	0.307
$\triangle\overline{M}_{qF}$	0.040	0.038	0.111	0.107	0.061	0.066	0.036
$\overline{M}_{GT}$	-2.890	-1.977	-4.481	-3.872	-2.142	-3.247	-1.099
$\triangle\overline{M}_{GT}$	0.338	0.167	0.352	0.556	0.216	0.288	0.120
$\overline{M}_{\omega GT}$	-2.821	-1.912	-4.275	-3.643	-2.083	-3.054	-1.067
$\triangle\overline{M}_{\omega GT}$	0.324	0.181	0.376	0.540	0.216	0.296	0.117
$\overline{M}_{qGT}$	-3.474	-2.357	-5.420	-4.727	-2.588	-3.991	-1.345
$\triangle\overline{M}_{qGT}$	0.380	0.137	0.301	0.632	0.218	0.282	0.129
$\overline{M}_T$	0.003	0.037	0.070	0.037	0.018	-0.015	0.014
$\triangle\overline{M}_T$	0.021	0.003	0.012	0.022	0.002	0.016	0.002
$\overline{M}_{qT}$	0.001	0.078	0.133	0.041	0.086	-0.017	0.033
$\triangle\overline{M}_{qT}$	0.056	0.011	0.036	0.072	0.008	0.054	0.008
$\overline{M}_P$	2.069	1.724	3.543	3.136	1.095	1.329	0.043
$\triangle\overline{M}_P$	0.102	0.077	0.145	0.462	0.070	0.186	0.012
$\overline{M}_R$	-2.030	-1.525	-3.171	-2.771	-1.861	-2.489	-0.954
$\triangle\overline{M}_R$	0.583	0.438	0.900	0.842	0.527	0.716	0.271

Table 4.5: Phase space factor $G_{0k}(k = 1, 11)$ for ^{96}Zr,^{100}Mo, ^{110}Pd , ^{130}Te, and ^{150}Nd nuclei [Štefánik *et al.* (2015)].

	^{96}Zr	^{100}Mo	^{110}Pd	^{130}Te	^{150}Nd
G_{01}	5.366×10^{-14}	4.151×10^{-14}	1.257×10^{-14}	3.708×10^{-14}	1.644×10^{-13}
G_{02}	2.331×10^{-13}	1.506×110^{-13}	2.118×10^{-14}	9.787×10^{-14}	7.595×10^{-13}
G_{03}	3.845×10^{-14}	2.856×10^{-14}	6.953×10^{-15}	2.333×10^{-14}	1.174×10^{-13}
G_{04}	1.153×10^{-14}	8.848×10^{-15}	2.545×10^{-15}	7.861×10^{-15}	3.660×10^{-14}
G_{05}	1.072×10^{-12}	9.066×10^{-13}	3.643×10^{-13}	9.863×10^{-13}	3.870×10^{-12}
G_{06}	7.919×10^{-12}	6.448×10^{-12}	2.431×10^{-12}	5.795×10^{-12}	1.951×10^{-11}
G_{07}	6.399×10^{-10}	5.015×10^{-10}	1.559×10^{-10}	4.567×10^{-10}	2.104×10^{-9}
G_{08}	4.567×10^{-11}	3.695×10^{-11}	1.202×10^{-11}	4.031×10^{-11}	2.187×10^{-10}
G_{09}	2.243×10^{-9}	1.702×10^{-9}	5.046×10^{-10}	1.294×10^{-9}	5.062×10^{-9}
G_{10}	4.827×10^{-14}	3.536×10^{-14}	8.041×10^{-15}	2.982×10^{-14}	1.852×10^{-13}
G_{11}	1.186×10^{-14}	9.113×10^{-15}	2.628×10^{-15}	8.192×10^{-15}	3.918×10^{-14}

Table 4.6: Calculated nuclear structure factors C_{mm}, $C_{m\lambda}$, $C_{m\eta}$, $C_{\lambda\lambda}$, $C_{\eta\eta}$ and $C_{\lambda\eta}$ in (a) PQQ1, (b) PQQHH1, (c) PQQ2 and (d) PQQHH2 parametrizations. In each parametrization, the three rows correspond to SRC1, SRC2 and SRC3, respectively.

Nuclei		C_{mm}	$C_{m\lambda}$	$C_{m\eta}$	$C_{\lambda\lambda}$	$C_{\eta\eta}$	$C_{\lambda\eta}$
^{96}Zr	(a)	2.58×10^{-13}	-1.25×10^{-13}	2.09×10^{-11}	8.28×10^{-13}	3.32×10^{-9}	-7.25×10^{-13}
		3.44×10^{-13}	-1.74×10^{-13}	3.68×10^{-11}	1.16×10^{-12}	7.64×10^{-9}	-1.06×10^{-12}
		3.75×10^{-13}	-1.93×10^{-13}	4.69×10^{-11}	1.28×10^{-12}	1.14×10^{-8}	-1.20×10^{-12}
	(b)	2.43×10^{-13}	-1.17×10^{-13}	2.08×10^{-11}	7.87×10^{-13}	3.47×10^{-9}	-7.71×10^{-13}
		3.29×10^{-13}	-1.66×10^{-13}	3.68×10^{-11}	1.12×10^{-12}	8.00×10^{-9}	-1.13×10^{-12}
		3.60×10^{-13}	-1.84×10^{-13}	4.71×10^{-11}	1.24×10^{-12}	1.19×10^{-8}	-1.27×10^{-12}
	(c)	2.44×10^{-13}	-1.18×10^{-13}	1.98×10^{-11}	7.85×10^{-13}	3.16×10^{-9}	-6.83×10^{-13}
		3.27×10^{-13}	-1.65×10^{-13}	3.50×10^{-11}	1.10×10^{-12}	7.29×10^{-9}	-1.01×10^{-12}
		3.56×10^{-13}	-1.82×10^{-13}	4.47×10^{-11}	1.21×10^{-12}	1.09×10^{-8}	-1.14×10^{-12}
	(d)	2.31×10^{-13}	-1.10×10^{-13}	1.97×10^{-11}	7.47×10^{-13}	3.30×10^{-9}	-7.24×10^{-13}
		3.13×10^{-13}	-1.57×10^{-13}	3.49×10^{-11}	1.06×10^{-12}	7.60×10^{-9}	-1.06×10^{-12}
		3.42×10^{-13}	-1.74×10^{-13}	4.47×10^{-11}	1.18×10^{-12}	1.13×10^{-8}	-1.20×10^{-12}
^{100}Mo	(a)	1.04×10^{-12}	-4.71×10^{-13}	8.27×10^{-11}	2.72×10^{-12}	1.14×10-08	-2.47×10^{-12}
		1.36×10^{-12}	-6.42×10^{-13}	1.43×10^{-10}	3.72×10^{-12}	2.60×10-08	-3.51×10^{-12}
		1.47×10^{-12}	-7.04×10^{-13}	1.82×10^{-10}	4.07×10^{-12}	3.86×10-08	-3.91×10^{-12}
	(b)	9.23×10^{-13}	-4.12×10^{-13}	7.60×10^{-11}	2.41×10^{-12}	1.08×10-08	-2.48×10^{-12}
		1.21×10^{-12}	-5.66×10^{-13}	1.32×10^{-10}	3.31×10^{-12}	2.46×10-08	-3.46×10^{-12}
		1.31×10^{-12}	-6.22×10^{-13}	1.67×10^{-10}	3.63×10^{-12}	3.64×10-08	-3.85×10^{-12}
	(c)	1.04×10^{-12}	-4.66×10^{-13}	8.23×10^{-11}	2.70×10^{-12}	1.13×10-08	-2.44×10^{-12}
		1.35×10^{-12}	-6.36×10^{-13}	1.43×10^{-10}	3.69×10^{-12}	2.60×10-08	-3.46×10^{-12}
		1.46×10^{-12}	-6.97×10^{-13}	1.81×10^{-10}	4.04×10^{-12}	3.85×10-08	-3.87×10^{-12}
	(d)	8.94×10^{-13}	-3.97×10^{-13}	7.42×10^{-11}	2.34×10^{-12}	1.07×10-08	-2.40×10^{-12}
		1.18×10^{-12}	-5.47×10^{-13}	1.29×10^{-10}	3.22×10^{-12}	2.42×10-08	-3.37×10^{-12}
		1.27×10^{-12}	-6.02×10^{-13}	1.63×10^{-10}	3.53×10^{-12}	3.59×10-08	-3.75×10^{-12}

Table 4.6 continued

Nuclei		C_{mm}	$C_{m\lambda}$	$C_{m\eta}$	$C_{\lambda\lambda}$	$C_{\eta\eta}$	$C_{\lambda\eta}$
^{110}Pd	(a)	1.42×10^{-13}	-4.59×10^{-14}	1.50×10^{-11}	1.62×10^{-13}	1.72×10^{-9}	-1.57×10^{-13}
		1.86×10^{-13}	-6.36×10^{-14}	2.59×10^{-11}	2.24×10^{-13}	3.91×10^{-9}	-2.21×10^{-13}
		2.01×10^{-13}	-7.01×10^{-14}	3.27×10^{-11}	2.45×10^{-13}	5.75×10^{-9}	-2.46×10^{-13}
	(b)	2.69×10^{-13}	-9.08×10^{-14}	2.81×10^{-11}	3.07×10^{-13}	3.19×10^{-9}	-3.45×10^{-13}
		3.49×10^{-13}	-1.24×10^{-13}	4.81×10^{-11}	4.20×10^{-13}	7.17×10^{-9}	-4.72×10^{-13}
		3.76×10^{-13}	-1.36×10^{-13}	6.05×10^{-11}	4.59×10^{-13}	1.05×10^{-8}	-5.21×10^{-13}
	(c)	2.44×10^{-13}	-8.04×10^{-14}	2.53×10^{-11}	2.82×10^{-13}	2.86×10^{-9}	-2.66×10^{-13}
		3.18×10^{-13}	-1.11×10^{-13}	4.37×10^{-11}	3.86×10^{-13}	6.52×10^{-9}	-3.75×10^{-13}
		3.43×10^{-13}	-1.22×10^{-13}	5.52×10^{-11}	4.23×10^{-13}	9.60×10^{-9}	-4.17×10^{-13}
	(d)	2.08×10^{-13}	-6.97×10^{-14}	2.25×10^{-11}	2.38×10^{-13}	2.65×10^{-9}	-2.76×10^{-13}
		2.72×10^{-13}	-9.60×10^{-14}	3.86×10^{-11}	3.27×10^{-13}	5.94×10^{-9}	-3.79×10^{-13}
		2.94×10^{-13}	-1.06×10^{-13}	4.86×10^{-11}	3.59×10^{-13}	8.69×10^{-9}	-4.19×10^{-13}
^{130}Te	(a)	5.29×10^{-13}	-2.32×10^{-13}	4.01×10^{-11}	9.78×10^{-13}	4.39×10^{-9}	-8.80×10^{-13}
		6.80×10^{-13}	-3.06×10^{-13}	7.11×10^{-11}	1.31×10^{-12}	1.07×10^{-8}	-1.23×10^{-12}
		7.33×10^{-13}	-3.34×10^{-13}	9.11×10^{-11}	1.43×10^{-12}	1.63×10^{-8}	-1.37×10^{-12}
	(b)	4.34×10^{-13}	-1.93×10^{-13}	3.58×10^{-11}	8.14×10^{-13}	4.25×10^{-9}	-8.19×10^{-13}
		5.67×10^{-13}	-2.60×10^{-13}	6.37×10^{-11}	1.11×10^{-12}	1.03×10^{-8}	-1.14×10^{-12}
		6.14×10^{-13}	-2.84×10^{-13}	8.17×10^{-11}	1.22×10^{-12}	1.56×10^{-8}	-1.27×10^{-12}
	(c)	4.35×10^{-13}	-1.86×10^{-13}	3.38×10^{-11}	8.04×10^{-13}	3.78×10^{-9}	-7.04×10^{-13}
		5.64×10^{-13}	-2.49×10^{-13}	6.03×10^{-11}	1.09×10^{-12}	9.28×10^{-9}	-9.97×10^{-13}
		6.09×10^{-13}	-2.72×10^{-13}	7.74×10^{-11}	1.19×10^{-12}	1.41×10^{-8}	-1.11×10^{-12}
	(d)	5.24×10^{-13}	-2.38×10^{-13}	4.19×10^{-11}	9.83×10^{-13}	4.84×10^{-9}	-1.00×10^{-12}
		6.78×10^{-13}	-3.15×10^{-13}	7.40×10^{-11}	1.33×10^{-12}	1.16×10^{-8}	-1.38×10^{-12}
		7.32×10^{-13}	-3.44×10^{-13}	9.47×10^{-11}	1.45×10^{-12}	1.76×10^{-8}	-1.53×10^{-12}

Table 4.6 continued

Nuclei		C_{mm}	$C_{m\lambda}$	$C_{m\eta}$	$C_{\lambda\lambda}$	$C_{\eta\eta}$	$C_{\lambda\eta}$
^{150}Nd	(a)	3.04×10^{-13}	-1.60×10^{-13}	1.74×10^{-11}	1.07×10^{-12}	2.19×10^{-9}	-8.01×10^{-13}
		3.94×10^{-13}	-2.12×10^{-13}	3.19×10^{-11}	1.43×10^{-12}	5.66×10^{-9}	-1.15×10^{-12}
		4.25×10^{-13}	-2.31×10^{-13}	4.12×10^{-11}	1.56×10^{-12}	8.76×10^{-9}	-1.29×10^{-12}
	(b)	2.19×10^{-13}	-1.19×10^{-13}	1.36×10^{-11}	8.01×10^{-13}	1.86×10^{-9}	-6.52×10^{-13}
		2.90×10^{-13}	-1.60×10^{-13}	2.52×10^{-11}	1.09×10^{-12}	4.81×10^{-9}	-9.44×10^{-13}
		3.14×10^{-13}	-1.75×10^{-13}	3.27×10^{-11}	1.19×10^{-12}	7.44×10^{-9}	-1.06×10^{-12}
	(c)	2.94×10^{-13}	-1.55×10^{-13}	1.68×10^{-11}	1.03×10^{-12}	2.12×10^{-9}	-7.73×10^{-13}
		3.81×10^{-13}	-2.05×10^{-13}	3.08×10^{-11}	1.38×10^{-12}	5.48×10^{-9}	-1.11×10^{-12}
		4.11×10^{-13}	-2.23×10^{-13}	3.98×10^{-11}	1.50×10^{-12}	8.47×10^{-9}	-1.25×10^{-12}
	(d)	2.16×10^{-13}	-1.16×10^{-13}	1.33×10^{-11}	7.85×10^{-13}	1.80×10^{-9}	-6.31×10^{-13}
		2.85×10^{-13}	-1.56×10^{-13}	2.45×10^{-11}	1.07×10^{-12}	4.64×10^{-9}	-9.14×10^{-13}
		3.08×10^{-13}	-1.71×10^{-13}	3.18×10^{-11}	1.17×10^{-12}	7.18×10^{-9}	-1.02×10^{-12}

Table 4.7: Average nuclear structure factors $\overline{C}_{mm}$, $\overline{C}_{m\lambda}$, $\overline{C}_{m\eta}$, $\overline{C}_{\lambda\lambda}$, and $\overline{C}_{\eta\eta}$ for the $0\nu\beta^-\beta^-$ decay of ^{96}Zr, ^{100}Mo, ^{110}Pd, ^{130}Te and ^{150}Nd isotopes.

Nuclei	^{96}Zr	^{100}Mo	^{110}Pd	^{130}Te	^{150}Nd
$\overline{C}_{mm}$	3.102×10^{-13}	1.209×10^{-12}	2.668×10^{-13}	5.916×10^{-13}	3.202×10^{-13}
$\overline{C}_{m\lambda}$	-1.553×10^{-13}	-5.635×10^{-10}	-9.285×10^{-14}	-2.678×10^{-13}	-1.735×10^{-13}
$\overline{C}_{m\eta}$	3.400×10^{-11}	1.295×10^{-10}	3.701×10^{-11}	6.380×10^{-11}	2.660×10^{-11}
$\overline{C}_{\lambda\lambda}$	1.041×10^{-12}	3.282×10^{-12}	3.194×10^{-13}	1.143×10^{-12}	1.173×10^{-12}
$\overline{C}_{\eta\eta}$	7.446×10^{-9}	2.453×10^{-8}	5.710×10^{-9}	1.023×10^{-8}	5.034×10^{-9}
$\overline{C}_{\lambda\eta}$	-9.976×10^{-13}	-3.248×10^{-12}	-3.412×10^{-1}	-1.119×10^{-12}	-9.672×10^{-13}

Table 4.8: Experimental limits on half-lives $T^{0\nu}_{1/2}$ and the extracted on-axis limits on the effective mass of light neutrino $\langle m_\nu\rangle$, $\langle\lambda\rangle$, and $\langle\eta\rangle$ for the $0\nu\beta^-\beta^-$ decay of ^{96}Zr, ^{100}Mo, ^{110}Pd, ^{130}Te and ^{150}Nd isotopes. Predicted half-lives $T^{0\nu}_{1/2}$ of $0\nu\beta^-\beta^-$decay for two sets of parameters (i) $\langle m_\nu\rangle = 50$ meV (Case I) and (ii) $\langle m_\nu\rangle = 50$ meV, $\langle\lambda\rangle = 10^{-7}$ and $\langle\eta\rangle = 10^{-9}$ (Case II).

Nuclei	$T^{(0\nu)}_{1/2}$(Ex)	Ref.	$< m_\nu >$	$< \lambda >$	$< \eta >$	$T^{0\nu}_{1/2}$(I)	$T^{0\nu}_{1/2}$(II)
^{96}Zr	9.2×10^{21}	[1]	9.56	1.02×10^{-5}	1.21×10^{-7}	3.37×10^{26}	4.44×10^{25}
^{100}Mo	1.1×10^{24}	[2]	0.44	5.62×10^{-7}	6.09×10^{-9}	8.64×10^{25}	1.32×10^{25}
^{110}Pd	6.0×10^{17}	[3]	1.28×10^{3}	2.28×10^{-3}	1.71×10^{-5}	3.91×10^{26}	7.07×10^{25}
^{130}Te	1.5×10^{25}	[4]	0.17	2.41×10^{-7}	2.55×10^{-9}	1.76×10^{26}	3.24×10^{25}
^{150}Nd	2.0×10^{22}	[5]	6.39	6.53×10^{-6}	9.97×10^{-8}	3.26×10^{26}	4.84×10^{25}

References:

[1] Barabash *et al.* (2011) [2] Arnold *et al.* (2015) [3] Winter (1952)

[4] Alduino *et al.* (2018) [5] Arnold *et al.* (2016)

Chapter 5

Conclusions

In the present work, our aim was to study the $2\nu\beta^-\beta^-$ decay for the $0^+ \rightarrow J^+$ transition and the $0\nu\beta^-\beta^-$ decay for the $0^+ \rightarrow 0^+$ transition within mechanisms involving light Majorana neutrino mass and right handed current of some nuclei in the mass range $90 \leq A \leq 150$ in PHFB model. We used a pairing plus multipole type of effective two-body interaction and derive its four parametrizations, namely PQQ1, PQQHH1, PQQ2, PQQHH2. The single particle energies used were derived from Woods-Saxon potential. Further, we used three parametrizations of the SRC due to Miller-Spencer parametrization (SRC1), Argonne NN (SRC2) and CD-Bonn potentials (SRC3). In the absence of experimental observation of $0\nu\beta^-\beta^-$, the nuclear models predict half-lives $T^{0\nu}_{1/2}$ of $0\nu\beta^-\beta^-$ decay assuming certain value of neutrino mass or conversely, limits on various lepton number violating gauge-theoretical parameters are extracted from the observed experimental half-life limits by calculating the appropriate NTMEs. The reliability of the wave functions were checked by calculating nuclear spectroscopic properties, namely the yrast spectra, reduced $B(E2{:}0^+ \rightarrow 2^+)$ transition probabilities and β_2 parameters of the nuclei under

going $\beta^-\beta^-$ decay and comparing them with the experimental values. After getting an overall agreement between theoretically calculated and experimentally observed values, the NTMEs $M_{2\nu}(J^+)$ and half-lives $T^{2\nu}_{1/2}(2^+)$ of $2\nu\beta^-\beta^-$ decay for the $0^+ \rightarrow J^+$ transition have been calculated for ^{94,96}Zr, ^{100}Mo, ^{104}Ru, ^{110}Pd, ^{128,130}Te and ^{150}Nd nuclei. It was noticed that the validity of different nuclear models employed for nuclear structure calculations can not be uniquely established in the absence of experimental results as well as uncertainty in g_A. Further work is necessary both in the experimental as well as theoretical front to judge the relative applicability, success and failure of these nuclear models.

Subsequently, the NTMEs of $0\nu\beta^-\beta^-$ decay for the $0^+ \rightarrow 0^+$ transition were calculated within mechanisms involving the light Majorana neutrino, and right handed $V + A$ currents. The effect of finite size of nucleons and short range correlations on NTMEs has been studied. We have also esimated mean and standard deviation of claculated NTMEs. Further, the limits on effective light Majorana neutrino mass $\langle m_\nu \rangle$, effective weak coupling of right-handed leptonic current with right-handed hadronic current $\langle \lambda \rangle$ and with left-handed hadronic current $\langle \eta \rangle$ were extracted from the most recent observed half-life limits and appropriate NTMEs. The most stringent limit comes from the $0\nu\beta^-\beta^-$ decay of ^{130}Te isotope. The extracted limits on $\langle m_\nu \rangle$, $\langle \lambda \rangle$, and $\langle \eta \rangle$ are 0.17 eV, 2.41×10^{-7} and 2.55×10^{-9}, respectively.

Uncertainty in NTMEs

The main uncertainty in the calculation of decay rates or extraction of gauge theoretical parameters lies with in the NTMEs. The NTMEs are purely model dependent quantities

and one needs reliable calculation of NTMEs for better theoretical prediction. On the one hand, there is a large uncertainty in the NTMEs calculated in different nuclear models. The uncertainty in NTMEs is mainly due to different approaches used in the theoretical calculations [Engel (2015)]. In the nuclear structure calculation different nuclear models use different model spaces and different effective interactions. Further, there is no general guideline or clear cut prescription to fix the single particle energies and parameters of the two-body interactions. Simkovic *et al.* (2009) have shown that the choice of SRC and axial vector coupling constant g_A is also the source of uncertainty in the NTMEs. In table 1.2 of Chapter 1, we have compiled all the existing calculations for all the nuclei as far as possible. It can be noticed from the table that there is a large variation in NTMEs even in the same type of generic model.

Presently, we estimate the theoretical uncertainty in NTMEs $M^{(0\nu)}$ by considering all the existing calculations. To calculate the uncertainty, a statistical analysis has been done in the following manner. The mean and standard deviation are defined for a finite series of calculations as

$$\overline{M}_i = \frac{\sum_{k=1}^{N} M_i^k}{N} \tag{5.1}$$

and

$$\Delta\overline{M}_i = \frac{1}{\sqrt{N-1}} \left[\sum_{k=1}^{N} \left(\overline{M}_i - M_i^k \right)^2 \right]^{1/2} \tag{5.2}$$

The Eqs. (5.1) and (5.2) define the best estimate of the mean and standard deviation for a Gaussian distribution. The extracted values of effective light Majorana neutrino mass $\langle m_\nu \rangle$ using recent half-life limit and average of $M^{(0\nu)}$ are given in Table 5.1. For the most studied case of ^{76}Ge, the upper bound on $\langle m_\nu \rangle$ is 0.227 eV using the half-life limit

$T^{0\nu}_{1/2} > 9.0 \times 10^{25}$ [Agostini *et al.* (2019)].

Improvements in the PHFB model and further studies

In the PHFB model, it has been shown that the deformations of the intrinsic ground states play an important role in reproducing a realistic NTME in the case of $2\nu\beta^-\beta^-$ decay. The trend of results in PHFB model suggests that it is necessary to include following improvements:

(1) It is necessary to include the proton-neutron pairing in the PHFB formalism so that an isospin symmetric model Hamiltonian can be used, and the summation method will be exact.

(2) It is not possible to study the structure of odd-odd nuclei in the present version of the PHFB model. Therefore, the single beta decay rate and the distribution of Gamow-Teller strength can not be studied. However, the study of these processes has implications in the understanding of the role of the isoscalar part of the proton-neutron interaction. This is a serious draw back in the present formalism of the PHFB model. This limitation can be over come by an extended PHFB formalism based on complex Bogoliubov transformation.

(3) The fluctuations in average particle numbers is around 5%. None the less, it is necessary that number projection should be carried out for consistency.

(4) In case of 2ν $\beta^-\beta^-$ decay, it has been noticed that a reasonably large model space is more effective in reproducing the observed quenching of NTMEs. One needs appropriate effective two-body interaction for a large model space. Therefore, it will be illustrative to study $\beta\beta$ decay in the PHFB model using a large model space along with appropriate two-body effective interaction.

Alternatively, the deformed Hartree-Fock (DHF) model [Ripka (1968), Brink (1966), Guney and Warke (1967), Praharaj (1988)] is one of the another convenient choices to incorporate pairing and deformation degrees of freedom on equal footing. In DHF, the pairing interaction is taken into account by mixing particle-hole excitations (2p-2h, 4p-4h etc.) of $K = 0$ type across the Fermi surface over the Hartree-Fock ground state. Further, the deformation effects are included in a natural way through band mixing. Ahlpara *et al.* (1985) have shown that it is possible to get the shell-model results in DHF by mixing a few intrinsic states. Hence, it is advantageous to work with such a basis instead of a large shell model basis needed to study even the low lying spectra of nuclei [Pandya *et al.* (1985)]. It is difficult to perform a shell-model calculation without truncating the model space severely in the medium-heavy and heavy nuclei, and it has been shown that the DHF is one of the best alternatives for the latter. In the light of above discussions, it is clear that a band mixing in an extended PHFB model using complex Bogoliubov transformation will also be the best alternative.

The possible occurrence of $0\nu\beta^-\beta^-$ decay in grand unified theories (GUT) requires the existence of Majorana neutrino with non-vanishing mass and/or right handed lepton current. However, the $0\nu\beta^-\beta^-$ decay is also possible in other gauge theoretical models like Majoron models, R_p-violating minimal supersymmetric standard model (MSSM), lepto-quark exchange mechanism and compositeness scenario. The study of other decay processes like positron emission, electron capture and double electron capture of $\beta\beta$ decay will be interesting both from experimental as well as theoretical point of view.Last but not the least, a study of $0\nu\beta\beta$ decay can draw inferences regarding exotic phenomena such as dark energy, dark matter and violation of weak equivalence principle.

Table 5.1 : Calculated limits on effective light Majorana neutrino mass $\langle m_\nu \rangle$ (in eV) along with average NTMEs $\overline{M}^{(0\nu)}$, uncrtainties $\Delta\overline{M}^{(0\nu)}$ and the present half-life limits $T^{0\nu}_{1/2}$ (in yr) for the $0\nu\beta^-\beta^-$ decay.

Nuclie	$\overline{M}^{(0\nu)}$	$\Delta\overline{M}^{(0\nu)}$	$T^{0\nu}_{1/2}$	Reference	$\langle m_\nu \rangle$
^{48}Ca	1.470	1.032	$>1.3 \times 10^{22}$	[Barabash *et al.*(2011)]	19.344
^{76}Ge	4.877	1.507	$>9.0\times10^{25}$	[Agostini *et al.* (2019)]	0.227
^{82}Se	4.261	1.478	$>2.4\times10^{24}$	[Azzolini *et al.* (2018)]	0.767
^{96}Zr	2.593	2.211	$>9.2\times10^{21}$	[Barabash *et al.* (2011)]	14.609
^{100}Mo	4.538	3.184	$>1.1\times10^{24}$	[Arnold *et al.* (2015)]	0.850
^{116}Cd	3.405	2.144	$>7.0\times10^{22}$	[Danevich *et al.* (2000)]	4.385
^{130}Te	3.815	2.523	$>1.5\times10^{25}$	[Alduino *et al.* (2018)]	0.290
^{136}Xe	2.654	1.971	$>2.1\times10^{23}$	[Kaixiang *et al.* (2019)]	3.474
^{150}Nd	3.094	1.229	$>2.0\times10^{22}$	[Arnold *et al.* (2016)]	4.647

Bibliography

[1] C. E. Aalseth *et al.,* Phys. Rev. Lett. 120, 132502 (2018).

[2] J. N. Abdurashitov *et al.,* (SAGE Collaboration) Phys. Lett. B 328, 234 (1994)

[3] Y. Abe *et al.,* Phys. Rev. Lett. 108, 131801 (2012).

[4] K. Abe *et al.,* Phys. Rev. Lett. 112, 061802 (2014).

[5] K. Abe *et al.,* (XMASS) Phys. Lett. B 759, 64 (2016).

[6] K. Abe *et al.,* (XMASS) PTEP 053, D 03 (2018).

[7] N. Abgrall *et al.,* (LEGEND) AIP Conf. Proc. 1894 020027 (2017).

[8] C. V. Achar *et al.,* Phys. Lett. 18, 196 (1965).

[9] P. Adamson *et al.,* Phys. Rev. Lett. 112, 191801 (2014).

[10] M. Agostini *et al.,* J. Phys. G 42, 115201 (2015).

[11] M. Agostini *et al.,* Eur. Phys. J. C 78, 388 (2018)a.

[12] M Agostini *et al.,* (GERDA) Phys. Rev Lett. 120, 132503 (2018)b.

[13] D. P. Ahalpara, K. H. Bhatt and R. Sahu, J. Phys. G Nucl. Phys. 11 735 (1985).

[14] Q. R. Ahmad *et al.,* (SNO Collaboration) Phys. Rev. Lett. 87, 071301 (2001).

[15] J. K. Ahn, *et al.,* (RENO Collaboration) arXiv:1003.1391 [hep-ex](2010).

[16] J. K. Ahn *et al.,* Phys. Rev. Lett. 108, 191802 (2012).

[17] M. H. Ahn *et al.,* Phys. Rev. D 74, 072003 (2006).

[18] J. B. Albert *et al.,* (EXO-200) Phys. Rev. Lett. 120, 072701 (2018).

[19] C. Alduino *et al.,* (CUORE) Phys. Rev. Lett. 120, 132501 (2018).

[20] C. Alduino *et al.,* Eur. Phys. Jour. C 77, 13 (2017).

[21] V. Alenkov *et al.,* Eur. Phys. Jour. C 79, 791 (2019).

[22] E. Aliu *et al.,* (The K2K Collaboration) Phys. Rev. Lett. 94, 081802 (2005).

[23] V. Alvarez *et al.,* (NEXT collaboration) Nucl. Instrum. Meth. A 708, 101 (2013).

[24] S.I. Alvis *et al.,* arXiv:1902.02299(2019).

[25] F. P. An *et al.,* Phys. Rev. Lett. 108, 171803 (2012)

[26] V. D'Andrea arXiv:1905.06572v1(2019)

[27] S. Andringa *et al.,* (SNO+) Adv. High Energy Phys. 61, 94250 (2016).

[28] P. Anselmann *et al.,* (GALLEX Collaboration) Phys. Lett. B 285, 376 (1992).

[29] M. Apollonio *et al.,* Phys. Lett. B 420, 397 (1998).

[30] M. Apollonio *et al.,* Phys. Lett. B 466, 415(1999).

[31] T. Araki *et al.,* Nature 436, 499 (2005).

[32] J. Argyriades *et al.,* Nucl. Phys. A 847, (2010).

[33] C. Arnaboldi *et al.,* Phys. Rev. Lett. 95 142501(2005).

[34] R. Arnold *et al.,* (NEMO3) Phys. Rev. D 92, 072011(2015).

[35] R. Arnold *et al.,* (NEMO3) Phys. Rev .D 94, 072003(2016).

[36] C. Arpesella, A.S. Barabash, E. Bellotti, C. Brofferio, E. Fiorini, P.P. Sverzellati, and V.I. Umatov, Europhys. Lett. 27, 29 (1994).

[37] C. Arpesella, E. Bellotti, N. Ferrari, and L. Zanotti, Nucl. Phys. B (Proc. Suppl.) 70, 249 (1999).

[38] G.M.Asatrian and A.N.Ioannisian, Phys. Atom. Nucl. 59 1768 (1996).

[39] F. T. Avignone III, G.S. King III and Yu. G Zdesenko, New Journal of Physics 7, 6 (2005)

[40] O. Azzolini *et al.,* (CUPID-0) Phys. Rev. Lett.120, 232502 (2018).

[41] J. N. Bahcall, Phys. Rev. Lett. 12, 300 (1964).

[42] A. Bakalyarov *et al.,* Pisma Zh. Eksp. Teor. Fiz. 76, 643 (2002).

[43] A. S. Barabash, F. T. Avignoue III, C. K. Guerard, R. L. Brodzinski, H. S. Miley, J. H. Reeves, and V. I. Umatov, Proc. 3-rd Int. Syrup. on Weak and Electromagn. Interactions in Nuclei WEIN-92. Dubna, Russia, June 16-22, 1992 (World Sci. Publ. Co., 1993).

[44] A. S. Barabash *et al.,* Phys. Lett. B 345, 408 (1995).

[45] A. S. Barabash, R. Gurriaran, F. Hubert, Ph. Hubert, J. L. Reyss, J. Suhonen and V. I. Umatov, J. Phys. G 22, 487 (1996).

[46] A. S. Barabash, F. Hubert, Ph. Hubert and V.I. Umatov, Eur. Phys. J. A 11, 143 (2001).

[47] A. S. Barabash *et al.,* Phys. Rev. C 79, 045501 (2009).

[48] A. S. Barabash, Phys. Rev. C 81, 035501 (2010).

[49] A. S. Barabash, V. B. Brudanin, Phys. At. Nucl. 74, 312 (2011).

[50] A. S. Barabash, AIP Conference Proceedings 1572, 11 (2013).

[51] A. S. Barabash, Nuclear Physics, A 935, 52 (2015).

[52] A. S. Barabash, Nucl Instrum Methods A 868 (2017).

[53] A. S. Barabash, Int. Jour. of Mod. Phys. A 33, 09 1843001 (2018)

[54] M. Baranger, Phys. Rev. 120, 957 (1960); Cargese lectures in theoretical physics, 1962 (W.A. Benjamin,New York, 1963).

[55] M. Baranger and K. Kumar, Nucl. Phys. A 110, 490 (1968).

[56] J. Barea and F. Iachello, Phys. Rev C 79, 044301 (2009).

[57] J. Barea, J. Kotila and F. Iachello, Phys. Rev. Lett. 109, 042501 (2012).

[58] J. Barea, J. Kotila and F. Iachello, Phys. Rev. C 87, 014315 (2013).

[59] J. Barea, J. Kotila and F. Iachello, Phys. Rev. C 91, 034304 (2015).

[60] M. Beck *et al.,* Z. Phys. A 343, 397 (1992)

[61] M. Beck *et al.,* Phys. Rev. Lett. 70, 2853 (1993).

[62] J. W. Beeman *et al.,* Eur. Phys. J. C75, 591 (2015).

[63] E. Bellotti, *et al.,* Lett. Nuovo Cimento 33, 273 (1982).

[64] E. Bellotti, C. Cattadori, O. Cremonesi, E. Fiorini, C. Liguori, A. Pullia, P. P. Sverzellati and L. Zanotti, Euro. Phys. Lett. 3, 889 (1987).

[65] E. Bellotti, *et al.,* J. Phys. G 17, S 231 (1991).

[66] Z. G. Berezhiani and R. N. Mohapatra, Phys. Rev. D 52 6607-6611(1995) Preprinthep-ph/950538 5(1995).

[67] J. Beringer *et al.*, Particle Data Group, Phys. Rev. D 86, 01001 (2012).

[68] J. Bernabeu, B. Desplanques and J. Navarro, Z. Phys. C 46, 323 (1990).

[69] H. A. Bethe Rev. Mod. Phys. 62, 801(1990).

[70] R. M. Bionta *et al.,* Phys. Rev. Lett. 58, 1494 (1987).

[71] C. Bloch and A. Messiah, Nucl. Phys. 39, 95 (1962).

[72] J. Blomqvist and S. Wahlborn, Ark. Fys. 16/46, 545 (1960).

[73] D. Blum *et al.*, Phys. Lett. B 275, 506 (1992).

[74] A. Bobyk and W. A. Kaminski, Phys. Rev. C 63, 051301(R) (2001).

[75] F. Boehm *et al.,* (Cal Tech-SIN-TUM Collaboration) Phys.Lett. 97B 310-314 (1980).

[76] F. Boehm, *et al.,* Phys. Rev. Lett. 84, 3764 (2000).

[77] A. Bohr and B. R. Mottelson, Nuclear Structure Vol. II p. 356 (New York, Benjamin, 1975).

[78] D. M. Brink, Int. School of Phys. "Enrico Fermi" course 36 , editor C. Bloch (Academic Press, NY) (1966).

[79] V. B. Brudanin *et al.,* Phys. Lett. B 495 63 (2000)a.

[80] V. B. Brudanin *et al.,* Phys. Atom. Nucl. 63 1218 (2000)b.

[81] D. Bryman and C. Picciotto, Rev. Mod. Phys. 50, 11 (1978).

[82] A. Caminata *et al.,* Universe 5, 10 (2019).

[83] L. Cardani on behalf of the LUCIFER collaboration Journal of Physics: Conference Series: 375, 042016 (2012).

[84] O. Castanos, J. G. Hirsch, O. Civitarese and P. O. Hess, Nucl. Phys. A 571, 276 (1994).

[85] M. Cascella, (SuperNEMO) Nucl Instrum Methods A 824 (2016).

[86] E. Caurier, A. Poves, A. P. Zuker, Phys. Lett. B 252, 13 (1990).

[87] E. Caurier, F. Nowacki, A. Poves and J. Retamosa, Phys. Rev. Lett. 77, 1954 (1996).

[88] E. Caurier, F. Nowacki, A. Poves and J. Retamosa, Nucl. Phys. A 654, 973 (1999).

[89] E. Caurier, J. Menendez, F. Nowacki and A. Poves, Phys. Rev. Lett. 100, 052503 (2008).

[90] E. Caurier, F. Nowacki and A. Poves, Eur. Phys. J. A 36, 195 (2008).

[91] J. F. Cavaignac *et al.,* Phys.Lett. 148 B 387 (1984).

[92] V. E. Ceron, J. G. Hirsch Phys. Lett. B 471, 1(1999).

[93] K. Chaturvedi, R. Chandra, P. K. Rath, P. K. Raina and J. G. Hirsh, Phys. Rev. C 78, 054302 (2008).

[94] M. K. Cheoun, A. Bobyk, A. Faessler, F. Simkovic and G. Teneva, Nucl. Phys. A 561, 74 (1993); Nucl. Phys. A 564, 329 (1993).

[95] M. K. Cheoun, A. Faessler, F. Simkovic, G. Teneva and A. Bobyk, Nucl. Phys. A 587, 301 (1995).

[96] C. Ching, T. Ho and X. Wu, Phys. Rev. C 40, 304 (1989).

[97] O. Civitarese *et al.*, Phys. Lett. B 25, 333 (1990).

[98] O. Civitarese, A. Faessler, J. Suhonen and X. R. Wu, Nucl. Phys. Lett. A 524, 404 (1991); J. Phys. G 17, 943 (1991).

[99] O. Civitarese and J. Suhonen, Phys. Rev. C 47, 2410 (1993).

[100] O. Civitarese and J. Suhonen, Nucl. Phys. A 575, 251 (1994).

[101] O. Civitarese, J. Suhonen and A. Faessler, Nucl. Phys. A591, 195 (1995).

[102] O. Civitarese and J. Suhonen, Phys. Rev. C 58, 1535 (1998).

[103] O. Civitarese and J. Suhonen, Nucl. Phys. A 653, 321 (1999).

[104] O. Civitarese and J. Suhonen, Phys. Lett. B 482, 368 (2000).

[105] O. Civitarese and J. Suhonen, Nucl. Phys. A 729, 867 (2003).

[106] O. Civitarese, J. Phys.: Conference Series 173, 012012 (2009).

[107] C. L. Cowan, F. Reines, F. B. Harrison, H. W. Kruse and A. D. McGuire, Science 124 103 (1956).

[108] F. A. Danevich, V. V. Kobychev, O. A. Ponkratenko, V. I. Tretyak and Yu. G. Zdesenko, Nucl. Phys. A 694, 375 (2001).

[109] R. Davis Jr., Phys.Rev.9 7 766 (1955)

[110] R. Davis, Jr. Phys. Rev. Lett. 12, 303 (1964).

[111] S. Dell'oro *et al.,* 2015 Review. Adv. High Eng. Phys. 2016: 2162659 (2016).

[112] A. V. Derbin, A. I. Egorov, V. N. Muratova, and S. V. Bakhlanov, Phys. At. Nucl.59, 2037 (1996).

[113] R. Derrhisek and S. Raby, Phys. Rev. D 6 2 015007 (2000).

[114] B. M. Dixit, P. K. Rath and P. K. Raina, Phys. Rev. C 65, 034311 (2002); ibid 67, 059901 (E) (2003).

[115] B. M. Dixit Ph.D. Thesis, University of Lucknow (2002).

[116] M. Doi, T. Kotani, H. Nishiura, K. Okuda and E. Takasugi, Phys. Lett. 103 B 219 (1981); Prog. Theor. Phys. 66 1739 (1981).

[117] M. Doi, T. Kotoni and E. Takasugi, Prog. Theor. Phys. Suppl. 83, 1 (1985).

[118] M. Doi and T. Kotani, Prog. Theor. Phys. 87, 1207 (1992).

[119] N. Dokania *et al.,* Eur. Phys. J. A 53, 74 (2017).

[120] H. Ejiri *et al.,* Nucl. Phys. A 611, 85 (1996).

[121] H. Ejiri *et al.,* Phys. Rev. Lett. 85, 245 (2000).

[122] S. R. Elliott, A. A. Hann and M. K. Moe, Phys. Rev. Lett. 59, 2020 (1987); ibid 59, 1649 (1987).

[123] S. R. Elliott, A. A. Hann and M. K. Moe, Nucl. Instrum. Methods A 273, 54 (1988).

[124] S. R. Elliott, M. K. Moe, M. A. Nelson and M. A. Vient, J. Phys. G 17, S145 (1991).

[125] S. R. Elliott *et al.,* Phys. Rev. C46, 1535 (1992).

[126] S. R. Elliott, M. K. Moe, M. A. Nelson and M. A. Vient, Nucl. Phys. B (Proc. Suppl.) 31, 68 (1993).

[127] S. R. Elliott and P. Vogel, Annu. Rev. Nucl. Part. Sci. 52 (2002).

[128] S. R. Elliott and J. Engel, J. Phys. G 30, R183 (2004).

[129] J. Engel, W. C. Haxton and P. Vogel, Phys. Rev. C 46, 2153 (1992).

[130] J. Engel, J. Phys. G: Nucl. Part. Phys. 42 034017 (2015).

[131] J. Engel, and J. Menéndez, Reports on Progress in Physics 80, 046301 (2017).

[132] A. Faessler and F. Simkovic, J. Phys. G 24, 2139 (1998).

[133] A. Faessler and F. Simkovic, Prog. Part. Nucl. Phys. 46, 233 (2001).

[134] A. Faessler, V. Rodin, F. Šimkovic, Phys. Rev. C 82, 051301(R) (2010)

[135] A. Faessler, V. Rodin and F. Simkovic, Jour. of Phyis. G: Nucl. Part. Phys. 39, 124006 (2012).

[136] D L. Fang, A. Faessler, V. Rodin and F. Šimkovic, Phys. Rev. C 83, 034320 (2011).

[137] D. Fang, A. Faessler and F. Simkovic, Phys. Rev. C 97 045503 (2018).

[138] E. Fermi, Z. Phys.8 8 161 (1934).

[139] E. L. Fireman, Phys. Rev.7 4 1238 (1948).

[140] E. L. Fireman, Phys. Rev.7 5 323 (1949).

[141] E. L. Fireman and D.Schwarzer, Phys. Rev.86 451 (1952).

[142] V. Fischer, (SNO+) arXiv:1809.05986.

[143] R. Foot and R. R.Volkas, Phys. Rev. D 52, 6595 (1995) Preprinthep-ph/950535 9 (1995).

[144] S. J. Freeman *et al.,* Phys. Rev. C 96, 054325 (2017).

[145] H. Fritzsch and P. Minkowski, Annals Phys.93 193 (1975).

[146] Y. Fukuda *et al.,* (Super-Kamiokande Collaboration) Phys. Rev. Lett. 81, 1562 (1998).

[147] W. H. Furry, Phys. Rev. 5, 6 1184 (1939).

[148] K. Fushimi *et al.,* Phys.Lett. B 531, 194 (2002).

[149] A. Gando *et al.,* Phys Rev. C. 85, 045504 (2012).

[150] A. Gando *et al.,* Phys Rev. C. 86, 021601(R) (2012).

[151] A. Gando *et al.,* (KamLAND-Zen) Phys Rev Lett. 117, 082503 (2016).

[152] A. Sh. Georgadze, F. A. Danevich, Yu. G. Zdesenko, V. V. Kobychev, B. N. Kropivyanskki, V. N. Kuts, V. V. Nikolaiko and V. I. Tretyak, Phys. At. nucl. 58, 1093 (1995).

[153] H. Georgi and S. L. Glashow Phys. Lett. 32, 8 438(1974).

[154] M. Goeppert-Mayer, Phys.Rev 4, 8 512 (1935).

[155] M.Goldhaber, L.Grodzins and A.W.Sunyar, Phys.Rev. 109, 1015 (1958).

[156] A. L. Goodman, "Advances in Nuclear Physics", Ed. J. W. Negele and E. Voget (Plenum, New York, 1979).

[157] K. Greisen,Ann. Rev. Nucl. Sci. 10, 63 (1960).

[158] V. N. Gribov and B. Pontecorvo, Phys. Lett. B 28 493 (1969).E.W.Hennecke, O.K.Manuel and D.D.Sabu, Phys.Rev C 11, 1378 (1975).

[159] A. Griffiths and P. Vogel, Phys. Rev. C 46, 181 (1992).

[160] M. R. Gunye and C. S. Warke, Phys. Rev. 155, 108 (1967).

[161] W. C. Haxton and G. J. Stephenson Jr., Prog. Part. Nucl. Phys. 12, 409 (1984).

[162] K. Hirata, *et al.,* Phys. Rev. Lett. 58, 1490 (1987).

[163] K. S. Hirata *et al.,* (Kamiokande-II Collaboration) Phys.Lett. B 205, 416 (1988).

[164] K. S. Hirata *et al.,* Phys. Rev. Lett. 63, 16 (1989)..

[165] J. G. Hirsch, O. Castanos, P. O. Hess and O. Civitarese, Phys. Rev. C 51, 2252 (1995).

[166] J. G. Hirsch, O. Castanos, P. O. Hess and O. Civitarese, Nucl. Phys. A 589, 445 (1995a).

[167] J. G. Hirsch, P. O. Hess and O. Civitarese, Phys. Rev. C 54, 1976 (1996).

[168] J. G. Hirsch, P. O. Hess and O. Civitarese, Phys. Lett. B 390, 36 (1997); Phys. Rev. C 56, 199 (1997).

[169] J. G. Hirsch, O. Castanos, P. O. Hess and O. Civitarese, Phys. Lett. B 534, 57 (2002).

[170] M. Hirsch, X. Wu, H. V. Klapdor, C. Ching, T. Ho, Z. Phys. A 345, 163 (1993).

[171] M. Hirsch *et al.*, Z. Phys. A 347,51 (1994).

[172] M. Hirsch, X. R. Wu, H. V. Klapdor-Kleingrothaus, Ching Cheng-rui and Ho Tso-hsiu, Phys. Rep. 242, 403 (1994).

[173] M. Horoi and S. Stoica, Phys. Rev. C 81, 024321 (2010).

[174] G. S. Hurst, M. G. Payne, S. Kramer and C. H. Chen, Phys. Today, 33, no. 9, 24 and private communication (1980).

[175] J. Hyvarinen and J. Suhonen, Phys. Rev. C 91, 024613 (2015).

[176] F. Iachello and J. Barea, Nucl. Phys. B (Proc. Suppl.) 217 5 (2011)

[177] M. G. Inghram and J. H. Reynolds, Phys. Rev. 76, 1265 (1949).

[178] M. G. Inghram and J .H. Reynolds, Phys. Rev. 78, 822 (1950).

[179] N. Ishihara, *et al.,* Nucl.Instrum.Meth. A 443, 101 (2000).

[180] C. F. Jiao, M. Horoi and A. Neacsu, Phys. Rev. C 98, 064324 (2018).

[181] B. P. Kay *et al.,* Phys. Rev. C57, 011302 (R)(2013).

[182] H. V. Klapdor-Kleingrothaus arXiv:hep-ph/0307330 (2003)

[183] H. V. Klapdor-Kleingrothaus and I. V. Krivosheina, Modern Phys. Lett. A 21, 1547 (2006)

[184] G. B. Kim *et al.,* (AMoRE) Adv. High Energy Phys. 2015 817530 (2015).

[185] T. Kirsten,W.Gentner and O.A.Schaeffer, Z. Phys.202 273-292(1967)

[186] T. Kirsten, O.A.Schaeffer, E.Norton and R.W.Stoenner, Phys. Rev. Lett. 2 01300 (1968).

[187] T. Kishimoto *et al.*, AIP Conf. Proc. 1388, 142 (2011).

[188] S. E. Koonin, D. J. Dean and K. Langanke, Phys. Rep. 278, 1 (1997).

[189] M. Kortelainena, O.Civitarese, J. Suhonen and J. Toivanen, Phys. Lett. B 647 128 (2007).

[190] L. Krauss, S. L. Glashow, and D.N. Schramm, Nature 310, 191 (1984).

[191] F. Krmpotic, A. Mariano, T. T. S. Kuo and K. Nakayama, Phys. Lett. B 319, 393 (1993).

[192] F. Krmpotic, T. T. S. Kuo, A. Mariano, E. J. V. de Passos, A. F. R. de Toledo Piza, Nucl. Phys. A 612, 223 (1997).

[193] N. Kudomi, H. Ejiri, K. Nagata, K. Okada, T. Shibata, T. Shima, and J. Tanaka, Phys. Rev. C 461, 2132 (1992).

[194] T. D. Lee and C. N. Yang, Phys. Rev. 104, 254 (1956).

[195] B. Lehnert *et al.,* J. Phys G: Nucl. Part. Phys. 43, 115201 (2016).

[196] G.K.Leontaris and S.Lola, Preprinthep-ph/950935 1(1995), Preprint HD-THEP-95-S1A (1995) and 5^{th} Hellenic School and Workshops on Elementary Particle Physics, Corfu, Greece (1995)

[197] E. Majorana, Nuovo Cimento 14, 171 (1937).

[198] Z. Maki, M. Nakagawa and S. Sakata, Progress of Theoretical Physics 28, 870 (1962).

[199] O. K.Manuel, J. Phys.G 17, S 221 (1991).

[200] M.A. Markov, Proc. 10^{th} Int. Conf. on High-Energy Physics, Rochester(1960).

[201] J. Martin-Albo *et al.,* (NEXT collaboration) Jour. of High Energy. Physics 1605, 159 (2016), arXiv:1511.09246

[202] J. Menéndez, A.Poves, E. Caurier and F. Nowacki, Nucl. Phys. A 818 139 (2009).

[203] J. Meng, L. S. Song and J. M. Yao, Int. Jou. of Mod. Phys. E Vol. 26 1740020 (2017).

[204] M. Moe and P. Vogel, Ann. Rev. Nucl. Part. Sci. 44, 247 (1994).

[205] M. T. Mustonen and J. Engel, Phys. Rev. C. 87, 064302 (2013).

[206] K. Muto, E. Bender, H.V. Klapdor, Z. Phys. A 334, 177, 187 (1989).

[207] K. Muto, Phys. Rev. C 48, 402 (1993).

[208] A. Neacsu and M. Horoi, Jour. of Phys. G: Nucl. Part. Phys. 41, 015201 (2014).

[209] A. Neacsu and S. Stoica, Phys. Rev. C 91, 024309 (2015).

[210] E. B. Norman, D. M. Meekhof, Phys. Lett. B 195, 126 (1987).P. Raghavan, Atomic Data and Nuclear Data Table 42, 189 (1989).

[211] I. Ogawa *et al.,* Nucl. Phys. A 730, 215 (2004).

[212] N. Onishi and S. Yoshida, Nucl. Phys. A 260, 226 (1966), Nucl. Phys. 80, 367 (1966).

[213] T. E. Pahomi, A. Neacsu, M. Mirea, S. Stoica, Romanian Reports in Phys. 66, 370 (2014).

[214] S. P. Pandya, R. Sahu and A. K. Rath, Ind. J. Phys. 70 A, 69 (1996).

[215] J. Paton, arXiv:1904.01418 (2019).

[216] W. Pauli Zurich,1930 (1930).

[217] A. Piepke *et al.,* Nucl. Phys. A 577, 493 (1994).

[218] B. Pontecorvo, Sov. Phys. JETP 6 429 (1957); Zh. Eksp. Teor. Fiz. 33, 549 (1957).

[219] B. Pontecorvo, Sov. Phys. JETP 26 984 (1968); Zh. Eksp. Teor. Fiz. 53, 1717 (1967).

[220] C. R. Praharaj, J. Phys. G14, 843 (1988).

[221] G. Racah, Nuovo Cimento 14, 322 (1937).

[222] P. B. Radha, D. J. Dean, S. E. Koonin, T. T. S. Kuo, K. Langanke, A. Poves, J. Retamosa and P. Vogel, Phys. Rev. Lett. 76, 2642 (1996).

[223] P. B. Radha, D. J. Dean, S. E. Koonin, K. Langanke and P. Vogel, Phys. Rev. C 56, 3079 (1997).

[224] A. A. Raduta, A. Faessler and S. Stoica, Nucl. Phys. A 534, 149 (1991).

[225] A. A. Raduta, D. S. Delion and A. Faessler, Phys. Rev. C 51, 3008 (1995).

[226] A. A. Raduta, C. M. Raduta, Phys. Lett. B 647, 265 (2007).

[227] P. Raghavan, Atomic Data and Nuclear Data Table, 42, 189 (1989).

[228] S. Raman, C. W. Nestor Jr., S. Kahane and K. H. Bhatt, Atomic Data and Nuclear Data Table, 42, 1 (1987).

[229] S. Raman, C. W. Nestor Jr. and P. Tikkanen, Atomic Data and Nuclear Data Table, 78, 1 (2001).

[230] P. K. Rath and S. K. Sharma, Phys. Rev. C 38, 2928 (1988).

[231] P. K. Rath, R. Chandra, K. Chaturvedi, P. K. Raina and J. G. Hirsh, Phys. Rev. C 82, 064310 (2010).

[232] R. A. Senekov and Horoi, Phys. Rev. C 90, 051301(R)(2014).

[233] F. Reines and C. L. Cowan, Phys.Rev. 113, 273 (1959).

[234] F . Reines, H.W Sobel and E. Pasierb, Phys. Rev . Lett. 45, 1307 (1980).

[235] J. Retamosa, E. Caurier and F. Nowacki, Phys. Rev. C 51, 371 (1995);Review of Particle Physics, Phys. Lett. B, 592 (2004).

[236] G. Ripka, In Advances in Nuclear Physics, Ed. M. Baranger and E. Vogt, (Plenum, New York) Vol. I, p183 (1968).

[237] V. Rodin, A. Faessler, F. Simkovic and P. Vogel, Phys. Rev. C 68 044302 (2003).

[238] T. R. Rodríguez and G. M. Pinedo, Phys. Rev. Lett. 105, 252503 (2010).

[239] T. R. Rodríguez and G. M. Pinedo, Eur. Phys. J web of conf. 66, 08006 (2014).

[240] N I Rukhadze *et al.,* J. Phys. Conf. Ser. 375, 042020 (2012).

[241] O. A. Rumyantsev and M. H. Urin, JETP Lett. 61, 361 (1995).

[242] M. Sakai, Atomic Data and Nucl. Data Tables 31, 400 (1984).

[243] M. Sambataro and J. Suhonen, Phys. Rev. C 56, 782 (1997).

[244] J. Schechter and J .W. F. Valle, Phys.Rev. D 22 2227 (1980).

[245] J. Schechter and J. W. F. Valle, Phys. Rev. D 24 1883 (1981).

[246] J. Schechter and J. W. F. Valle, Phys. Rev. D 25 2951 (1982).

[247] J. Schwieger, F. Simkovic and A. Faessler, Nucl. Phys. A 600, 179 (1996).

[248] J. Schweiger, F. Simkovic, A. Faessler and W.A. Kominski, Phys. Rev. C 57, 1738 (1998).

[249] J. Shirai, (KamLAND-Zen) Proceedings of XVII International Workshop on Neutrino Telescopes. Venezia p. 027(2018).

[250] F. Simkovic, G. Teneva, A. Bobyk, M. K. Cheoun, A. Faessler and S. B. Khadkikar, Prog. Part. Nucl. Phys. 32, 329 (1994).

[251] F. Simkovic, G. Pantis and A. Faessler, Phys. Atom. Nucl. 61 1218-1228(1998).

[252] F. Simkovic, J. Schwieger, G. Pantis and A. Faessler, Found.Phys. 27 1275 (1997)

[253] F. Simkovic and G. Pantis, Czech. J. Phys. B 48, 235 (1998).

[254] F. Simkovic and Veselesky, Proc. Int. Workshop MEDEX97, Praha, June 1997, Czech. J. Phys. B48, 245 (1998).

[255] F. Simkovic, G. Pantis, J. D. Vergados and A. Faessler, Phys. Rev. C 60, 055502 (1999).

[256] F. Simkovic, P. Domin and S.V. Semenov, Found.Phys. 27 1275 (1997)

[257] F. Simkovic, M. Nowak, W. A. Kaminski, A. A. Raduta and A. Faessler, Phys. Rev. C 64, 035501 (2001).

[258] F. Šimkovic, A. Faessler, V. Rodin, P. Vogel, and J. Engel, Phys. Rev. C 77, 045503 (2008).

[259] F. Šimkovic, A. Faessler, H. Müther, V. Rodin, and M. Stauf, Phys. Rev. C 79, 055501 (2009).

[260] F. Šimkovic, V. Rodin, A. Faessler, and P. Vogel, Phys. Rev. C 87, 045501 (2013).

[261] L. D. Skouras and J. D. Vergados, Phys. Rev. C 28, 2122 (1983).

[262] L. S. Song, J. M. Yao, P. Ring and J. Meng, Phys. Rev. C 95, 024305 (2017).

[263] A. Staudt, K. Muto and H.V. Klapdor-Kleingrothaus, Eur.Phys. Lett. 13, 31 (1990).

[264] D. Štefánik, R. Dvornický and F. Šimkovic and P. Vogel, Phys. Rev. C 92, 055502 (2015).

[265] S. Stoica and W. A. Kaminski, Phys. Rev. C 47, 867 (1993).

[266] S. Stoica, Phys. Rev. C 49, 2240 (1994).

[267] S. Stoica, Phys. Lett. B 350, 152 (1995).

[268] S. Stoica and I. Mihut, Nucl. Phys. A 602, 197 (1996); S. Stoica, Phys. Lett. B 350, 152 (1995).

[269] S. Stoica and H. V. Klapdor-Kleingrothaus, Eur. Phys. J. A 9, 345 (2000).

[270] S. Stoica and H. V. Klapdor-Kleingrothaus, Phys. Rev. C 63, 064304 (2001); Nucl. Phys. A654, 269 (2001).

[271] S. Stoica, and M. Mirea, Phys. Rev. C 88, 037303 (2013).

[272] J. Suhonen and O. Civitarese, Phys. Lett. B 280, 191 (1992).

[273] J. Suhonen, Nucl. Phys. A 563, 205 (1993).

[274] J. Suhonen and O. Civitarese, Phys. Lett. B 308, 212 (1993); ibid 312, 367 (1993).

[275] J. Suhonen and O. Civitarese, Phys. Rev. C 49, 3055 (1994).

[276] J. Suhonen, P. C. Divari, L. D. Skouras and I. P. Johnstone, Phys. Rev.C 55, 714 (1997).

[277] J. Suhonen and O. Civitarese, Phys. Rep. 300, 123 (1998).

[278] J. Suhonen, Nucl. Phys. A 864, 63 (2011).

[279] N. Takaoka and K. Ogata, Z. Naturforsch A 21, 84 (1966).

[280] G. Teneva, F.Simkovic, A. Bobyk, M. K. Cheoun, A. Faessler and S. B. Khadkikar, Nucl. Phys. A 249, 586 (1995).

[281] J. Terasaki, Phys. Rev. C 91, 034318 (2015).

[282] J. Toivanen and J. Suhonen, Phys. Rev. Lett. 75, 410 (1995).

[283] J. Toivanen and J. Suhonen, Phys. Rev. C 55, 2314 (1997).

[284] T. Tomoda, Rep. Prog. Phys. 54, 53 (1991).

[285] V. I. Tretyak and Y. G. Zdesenko, Atomic data and Nuclear data Tables, 61, 43 (1995), ibid 80, 83 (2002).

[286] S. Unlu , Chin. Phy. Lett. 31, 4, 042101 (2014); Phys. Scr. 87, 045202 (2013).

[287] N. L. Vaquero, T. R. Rodrı´guez and J. L. Egido, Phys. Rev. Lett. 111, 142501 (2013).

[288] D. M. Vladimirov and Yu. V. Gaponov, Sov. J. Nucl. Phys. 55, 1010 (1992).

[289] S.K.Vempati ,Pramana 5, 4 133 (2000).

[290] J. D. Vergados, Phys. Rev. C 13, 865 (1976).

[291] F. Villars, Proceedings of International School of Physics, "Enrico Fermi" Course 36 edited by C. Bloch (Academic, New York) (1966).

[292] P. Vogel and M. R. Zirnbauer, Phys. Rev. Lett. 57, 3148 (1986).

[293] P. Vogel, $arXiv : nucl - th/0005020$.

[294] J. L. Vuilleumier *et al.,* (Cal Tech-SIN-TUM Collaboration) Phys. Lett. B 114 298 (1982).

[295] R. G. Winter, Phys. Rev. 83, 1070 (1951).

[296] L. Wolfenstein, Nucl. Phys. B 18, 5 147(1981).

[297] C. S.Wu, E.Ambler, R. W.Hayward, D. D.Hoppes and R. P.Hudson, Phys. Rev. 105, 1413 (1957).

[298] J. M. Yao, L. S. Song, K. Hagino, P. Ring and J. Meng, Phys. Rev. C 91, 024316 (2015).

[299] N. Yosida and F. Iachello, arXiv:1301.7172v1 [nucl-th].

[300] L. Zhao, B. A. Brown and W.A. Richter, Phys. Rev. C 42, 1120 (1990).

[301] L. Zhao and B.A. Brown, Phys. Rev. C 47, 2641 (1993).

I. List of Publications

1. "Nuclear transition matrix elements for neutrinoless double β decay of ^{76}Ge isotope within PHFB approach", P. K. Rath, A. Kumar, R. Chandra, R. Gautam, P. K. Raina and B. M. Dixit, International Journal of Modern Physics E Vol. 28 10 1950096 (2019).

2. "Study of spectroscopic properties of some Ni, Cu and Zn isotopes in nuclear shell model", Priti Pandey, Vivekanand, K. Chaturvedi, R. Gautam, R. Chandra, Proceedings of the the DAE-BRNS Symposium on Nuclear Physics 64, 178 (2019).

3. "Occupancies of proton and neutron orbits of nuclei in the mass range A=90-150 participating in $0\nu\beta\beta$ decay", R. Gautam, Brijesh Shukla, P. Chaturvedi, R. Chandra, K. Chaturvedi, P.K. Rath, P.K. Raina, Proceedings of the the DAE-BRNS International Symposium on Nuclear Physics 63, 250 (2018).

4. "Correlations in the nuclear transition matrix elements of $0\nu\beta\beta$ decay within PHFB model" , R. Gautam,V. K. Nautiyal, R. Chandra, P. K. Rath, P. K. Raina, Proceedings of the DAE-BRNS Symposium on Nuclear Physics 62, 324 (2017).

5. "Neutrinoless double beta decay and Physics beyond the Standard Model", Y. K. Singh, P. Lohani, V. K. Nautiyal, R. Gautam, R. Chandra, K. Chaturvedi, P. K. Rath, P. K. Raina, Proceedings of the the DAE-BRNS Symposium on Nuclear Physics 61, 286 (2016).

6. "Study of squark-neutrino mechanism of neutrinoless double beta decay in R-parity violating supersymmetric models", R. Chandra,V. K. Nautiyal, R. Gautam, K. Chaturvedi, P. K. Rath, P. K. Raina, Proceedings of the DAE-BRNS Symposium on Nuclear Physics 60, 300 (2015).

II. Participation in Conference /Workshop/Schools/Symposium

1. Participated and presented a poster in 64^{th} DAE-BRNS Symposium on Nuclear Physics held at University of Lucknow from December 23^{rd}-27^{th} 2019.

2. Participated and presented a poster in 63^{nd} DAE-BRNS International Symposium on Nuclear Physics held at Bhaba Atomic Research Centre, Mumbai from Dec 10^{th}-14^{th} 2018.

3. Attended "School cum First Collaboration Meeting on Computation Nuclear Structure and Reaction" held at Saha Institute of Nuclear Physics and V. E. C. C., Kolkata from Jan 2^{th}-Jan 22^{nd} 2018.

4. Participated and presented a poster in 62^{nd} DAE-BRNS Symposium on Nuclear Physics on held at Thappar Institute of Engineering and Technology, Patiala from Dec 20^{th}-24^{th} 2017.

5. Participated and gave an Oral Presentation at XXXII Annual IAPT Convention 2017 and National Symposium on Recent Trends in Physics at Different Scales organized by Gurukul Kangri Viswavidyalay, Haridwar from October 29^{th}-31^{st} 2017.

6. Attended SERC School on “Nuclear Physics from New Perspectives” held at Bharthiyar University, Coimbatore, from Feb 8^{th}-28^{th} 2017.

7. Participated and presented a poster in 61^{th} DAE-BRNS Symposium on Nuclear Physics at Saha Institute of Nuclear Physics, Kolkata, from December 7^{th}-11^{th}, 2016.

8. Participated in the Workshop on "Neutrinoless Double Beta Decay (NDBD-2016)" held at IIT Ropar, Rupnagar(Punjab) from October 17^{th}-21^{st}, 2016.

9. Attended the Winter School on "Beyond the Standard Model Physics"(under the UGC networking Programme) held at Banaras Hindu University, Varanasi, from Jan 24^{th}- Feb 14^{th}, 2016.

10. Participated and presented a poster in 60^{th} DAE-BRNS Symposium on Nuclear Physics with an orientation course on December 6, 2015 at Sri Sathya Sai Institute of Higher Learning, Prasanthi Nilayam, from December 7^{th}-11^{th}, 2015.

11. Participated and presented a poster at the 3^{rd} Lucknow Science Congress and National conference on "Science for Society:An Interdisciplinary Approach" organized by B.B.A.U. Lucknow from October 31^{st}-November 2^{nd}, 2015.

12. Participated in the Workshop on "Recent Development on Quantum Theories" held at Banaras Hindu University on Feb-2015.

13. Attended Winter School on "Astro-particle Physics at Tata Institute of Fundamental Research", Ooty in Dec 2014.

International Journal of Modern Physics E
Vol. 28, No. 10 (2019) 1950096 (12 pages)

DOI: 10.1142/S0218301319500964

World Scientific
www.worldscientific.com

Nuclear transition matrix elements for neutrinoless double-β decay of ^{76}Ge isotope within PHFB approach

P. K. Rath and A. Kumar

Department of Physics, University of Lucknow, Lucknow, Uttar Pradesh 226007, India

R. Chandra* and R. Gautam

Department of Physics, Babasaheb Bhimrao Ambedkar University, Lucknow, Uttar Pradesh 226025, India
**ramesh.luphy@gmail.com*

P. K. Raina

Department of Physics, Indian Institute of Technology, Ropar, Rupnagar, Punjab 140001, India

B. M. Dixit

Faculty of Physical Sciences, SRM University, Barabanki 225013, India

Received 15 October 2019
Revised 19 November 2019
Accepted 9 December 2019
Published

Employing projected–Hartree–Fock–Bogoliubov (PHFB) model, nuclear transition matrix elements (NTMEs) $M^{(K)}$ for the neutrinoless double-β^- decay of ^{76}Ge isotope are calculated within mechanisms involving light as well as heavy Majorana neutrinos, and classical Majorons. By considering the spin-tensor decomposition of realistic KUO and empirical JUN45 effective two-body interactions, it is noticed that the effect due to SRC on NTMEs $M^{(0\nu)}$ and $M^{(0N)}$ involving the exchange of light and heavy Majorana neutrinos, respectively, is maximally incorporated by the central part of the effective two-body interaction, which varies by a small amount with the inclusion of spin-orbit and tensor components. Presently, the model-dependent uncertainties in the average NTMEs $\overline{M}^{(0\nu)}$ and $\overline{M}^{(0N)}$ turn out to be about 10% and 37%, respectively.

Keywords: PHFB model; neutrinoless double beta decay; nuclear transition matrix elements.

PACS Number(s): 21.60.Jz, 23.20.−g, 23.40.Hc

*Corresponding author.

1. Introduction

In any gauge theoretical model, the possible occurrence of neutrinoless double beta ($0\nu\beta\beta$) decay is intimately associated with the violation of lepton number L conservation. Out of several possible mechanisms involving left-right symmetry, R_p-violating suspersymmetry, Majorons, sterile neutrinos, leptoquarks, compositeness and extra-dimensional scenarios,[1,2] the Majorana neutrino mass mechanism is considered as the standard one to ascertain the Majorana nature of neutrinos. The half-life $T^{0\nu}_{1/2}$ of $0\nu\beta\beta$ decay is a product of phase space factors, nuclear transition matrix elements (NTMEs) and corresponding gauge theoretical parameters. As the phase space factors have been calculated to good accuracy in the recent past,[3–5] the accuracy of the extracted limits on the parameters of a particular gauge theoretical model depends on the reliability of model-dependent NTMEs. Specifically, the effective mass of light and heavy Majorana neutrinos is extracted in the standard mass mechanism. Over the past years, the theoretical studies devoted to the calculation of NTMEs have been excellently reviewed in Ref. 6 and references there in.

In the evaluation of NTMEs, different theoretical approaches, namely interacting shell-model (ISM) calculations based on direct diagonalization,[7–10] QRPA[11,12] and its extensions,[13,14] QRPA with isospin restoration,[15] deformed QRPA[16,17] with isospin restoration,[18] projected–Hartree–Fock–Bogoliubov (PHFB),[19–22] interacting boson model (IBM)[23,24] with isospin restoration,[25] the generator coordinate method (GCM),[26] and beyond mean field covariant density functional theory (BMFCDFT)[27] have been employed. In spite of the fact that several alternatives are available for the choice of model space, effective two-body residual interactions, model-dependent form factors to include the finite size of nucleons (FNS), short range correlations (SRC) with Miller–Spencer parametrization,[28] unitary correlation operator method (UCOM)[29] parametrization based on coupled cluster method (CCM),[30] and the value of axial vector current coupling constant g_A,[25,31–33] the calculated NTMEs $M^{(0\nu)}$ interestingly differ by factor of 2–3.

In addition to these exciting developments in the theoretical front, the remarkable experimental studies of the $\beta\beta$ decay[34] have resulted in measuring half-lives $T^{0\nu}_{1/2}$ of $0\nu\beta^-\beta^-$ decay of ^{76}Ge, ^{100}Mo, ^{130}Te and ^{136}Xe isotopes to be $>8.0\times10^{25}$ yr by GERDA[35] ($>1.9\times10^{25}$ yr by MAJORANA[36]), $>1.1\times10^{24}$ yr by NEMO-3,[37] $>4.0\times10^{24}$ yr by CUORE[38] and $>1.1\times10^{26}$ yr by KamLAND-Zen[39] ($>1.6\times10^{25}$ yr by EXO[40]), respectively. Our present concern is to calculate NTMEs for the $0\nu\beta^-\beta^-$ decay of ^{76}Ge isotope, which in turn requires reliable wave functions of ^{76}Ge and ^{76}Se nuclei. As the wave functions are model-dependent, the employed model should be versatile enough to reproduce as many observed properties of nuclei as possible.

An important observed characteristic feature of nuclei in Ge region is the shape transitions at $N = 40$. The onset of deformation at $N = 40$ necessitates to adopt a calculational framework treating the interplay of pairing and deformation degrees of freedom simultaneously, and on equal footing.[41] Calculations have already been

performed by using ISM in a valance space spanned by the $1p_{1/2}$, $1p_{3/2}$, $0f_{5/2}$ and $0g_{9/2}$ orbits treating the doubly even ^{56}Ni as an inert core. The present calculation is performed employing the PHFB approach in the above-mentioned valance space with a realistic and an empirical two-body effective interaction, namely KUO[42] and JUN45,[43] respectively. The purpose of such a calculation is to demonstrate the difference between the two approaches and infer about the role of neglected configurations and quasiparticle interactions.

2. Theoretical Formalism

The detailed theoretical formalism required for the study of $0\nu\beta^-\beta^-$ decay within the Majorana neutrino mass mechanism has been given in Refs. 44 and 45. Within the PHFB model, the calculation of NTMEs due to the exchange of light[20] and heavy Majorana[21] neutrinos has already been reported. In the following, we present a brief outline of the required formalism for the clarity in notations used in this paper.

Within Majorana neutrino mass mechanism, the half-life $T^{(0\nu)}_{1/2}$ for the $0^+ \to 0^+$ transition of $0\nu\beta^-\beta^-$ decay is given by

$$[T^{(0\nu)}_{1/2}(0^+ \to 0^+)]^{-1} = G_{01} \left| \frac{\langle m_\nu \rangle}{m_e} M^{(0\nu)} + \frac{m_p}{\langle M_N \rangle} M^{(0N)} \right|^2 , \tag{1}$$

where

$$\langle m_\nu \rangle = \sum_i{}' U^2_{ei} m_i, \quad m_i < 10\,\text{eV}, \tag{2}$$

$$\langle M_N \rangle^{-1} = \sum_i{}'' U^2_{ei} m_i^{-1}, \quad m_i > 10\,\text{GeV}, \tag{3}$$

$$M^{(K)} = -\frac{M^{(K)}_F}{g^2_A} + M^{(K)}_{\text{GT}} + M^{(K)}_T, \tag{4}$$

and $K = 0\nu(0N)$ denotes mass mechanism due to the exchange of light (heavy) Majorana neutrinos. It is noteworthy that within the seesaw model, the $0\nu\beta^-\beta^-$ decay has been studied by Blenow *et al.*[46] and Šimkovic *et al.*[47] and the conclusions need due attention. The phase space factors

$$G_{01} = \left[\frac{2(G_F g_A)^4 m^9_e}{64\pi^5 (m_e R)^2 \ln(2)} \right] \int_1^{T+1} f^{(0)}_{11} p_1\ p_2\ \varepsilon_1 \varepsilon_2 d\varepsilon_1 \tag{5}$$

have been recently calculated with good accuracy incorporating the screening correction[3–5] and the calculation of the NTMEs $M^{(K)}$ of the $0\nu\beta^-\beta^-$ decay within the PHFB model has already been discussed in Refs. 19–21.

Employing the HFB wave functions, one obtains the following expression for the NTME $M_\alpha^{(K)}$ of $0\nu\beta^-\beta^-$ decay corresponding to an operator $O_\alpha^{(K)}$.[19]

$$\begin{aligned} M_\alpha^{(K)} &= \langle 0_f^+ \| O_\alpha^{(K)} \| 0_i^+ \rangle \\ &= [n^{J_i=0} n^{J_f=0}]^{-1/2} \int_0^\pi n_{(Z,N),(Z+2,N-2)}(\theta) \sum_{\alpha\beta\gamma\delta} \langle \alpha\beta | O_\alpha^{(K)} | \gamma\delta \rangle \\ &\quad \times \sum_{\varepsilon\eta} \frac{(f^{(\pi)*}_{Z+2,N-2})_{\varepsilon\beta}}{[(1 + F^{(\pi)}_{Z,N}(\theta) f^{(\pi)*}_{Z+2,N-2})]_{\varepsilon\alpha}} \\ &\quad \times \frac{(F^{(\nu)*}_{Z,N})_{\eta\delta}}{[(1 + F^{(\nu)}_{Z,N}(\theta) f^{(\nu)*}_{Z+2,N-2})]_{\gamma\eta}} \sin\theta d\theta, \end{aligned} \tag{6}$$

where

$$n^J = \int_0^\pi [\det(1 + F^{(\pi)} f^{(\pi)^\dagger})]^{1/2} [\det(1 + F^{(\nu)} f^{(\nu)^\dagger})]^{1/2} d^J_{00}(\theta) \sin(\theta) d\theta. \tag{7}$$

The required amplitudes (u_{im}, v_{im}) and expansion coefficients $C_{ij,m}$ of axially symmetric HFB intrinsic state $|\Phi_0\rangle$ with $K = 0$ for evaluating the expressions n^J, $n_{(Z,N),(Z+2,N-2)}(\theta)$, $f_{Z,N}$ and $F_{Z,N}(\theta)$[19] are obtained by minimizing the expectation value of the effective Hamiltonian in a basis constructed by using a set of deformed states.

3. Results and Discussions

Two different sets of wave functions are generated using two distinct effective interactions, namely KUO[42] and JUN45 due to Honma *et al.*[43] The former is a realistic interaction while the latter is an empirical one. The wave functions obtained by using KUO and JUN45 effective two-body interactions are referred to as HFB1 and HFB2, respectively. The single-particle energies (SPE) used in HFB1 (HFB2) calculation are $\varepsilon_{p_{3/2}} = 0.0$ (-9.828) MeV, $\varepsilon_{f_{5/2}} = 0.78$ (-9.048) MeV, $\varepsilon_{p_{1/2}} = 1.08$ (-8.7480) MeV and $\varepsilon_{g_{9/2}} = 4.0$ (-6.828) MeV. Usually, a mass-dependent term of the type $(58/\mathrm{A})^{1/3}$ is introduced[48] in the effective two-body interaction to compensate for the noticed over attractiveness of the interaction in nuclei with high neutron number occurring towards the end of the shell.[49]

In addition, the two-body effective interaction is further decomposed into central (C), spin-orbit (S) and tensor (T) components[50] and the effect of these components on NTMEs $M^{(K)}$ involved in $0\nu\beta^-\beta^-$ decay is studied. In spin-tensor decomposition, the most general two-body interaction is written as

$$V(1,2) = \sum_{k=0,1,2} [X^{(k)} \times S^{(k)}]^{(0)} = \sum_{k=0,1,2} V^{(k)}, \tag{8}$$

where the two-particle spin operators are written as $S_1^{(0)} = 1$, $S_2^{(0)} = [\sigma_1 \times \sigma_2]^{(0)}$, $S_3^{(1)} = [\sigma_1 + \sigma_2]^{(1)}$, $S_4^{(1)} = [\sigma_1 - \sigma_2]^{(1)}$, $S_5^{(1)} = [\sigma_1 \times \sigma_2]^{(1)}$ and $S_6^{(2)} = [\sigma_1 \times \sigma_2]^{(2)}$.

The central and tensor parts of effective two-boy interaction are represented by $V^{(0)}$ and $V^{(2)}$, respectively. The $V^{(1)}$ term contains the symmetric $S_3^{(1)}$ as well as antisymmetric $S_4^{(1)}$ and $S_5^{(1)}$ spin-orbit operators. Employing the spin-tensor decomposition, the central (C), central plus spin-orbit (CS) and central plus spin-orbit plus tensor (CST) parts of the above-mentioned effective two-body interactions, namely KUO and JUN45 are adjusted to reproduce the excitation energies E_{2^+} of yrast 2^+ states.

To ascertain the reliability of generated wave functions HFB1 and HFB2, the calculated and experimentally observed excitation energies E_{2^+} of the yrast 2^+ states,[51] deformation parameters β_2[52] and g-factors $g(2^+)$[53] are presented in Table 1. The deformation parameters β_2 are calculated with effective charges $e_p = 1 + e_{\text{eff}}$ and $e_n = e_{\text{eff}}$, where $e_{\text{eff}} = 0.78$. The g-factors $g(2^+)$ are calculated with two different prescriptions. In the first prescription, the $g(2^+)$ values are calculated with $g_l^\pi = 1.0$, $g_l^\nu = 0.0$, $g_{s,\text{eff}}^{\pi/\nu} = 0.6(g_s^{\pi/\nu})_{\text{bare}}$. In the second prescription, effective operators calculated with a set of first- and second-order diagrams are $(g_l, g_s, g_p)^\pi = (0.89, 3.18, 0.73)$ and $(g_l, g_s, g_p)^\nu = (0.07, -1.52, -0.89)$.[54] In Table 2, the calculated occupation numbers are given along with the experimentally observed data.[55,56] It is noticed that the overall agreement between the calculated spectroscopic properties of ^{76}Ge and ^{76}Se isotopes and the experimentally observed data is reasonably good. Although the closure approximation is not valid for the $2\nu\beta^-\beta^-$ decay, an estimate of $M_{2\nu}$ with closure for ^{76}Ge provides 0.157 (0.132) with HFB1 (HFB2), respectively. This implies $g_{A,\text{eff}} = 0.667$ and 0.729 for ^{76}Ge with HFB1 and HFB2, respectively. Further, the NTMEs $M_{2\nu}$ for C and CS parts of effective two-body interaction turn out to be 0.024, 0.124 (0.017, 0.090) with HFB1 (HFB2), respectively. This implies that in the evolution of NTMEs, the spin-orbit part of two-body interaction plays a dominant role and the contribution of the tensor part is about half of the spin-orbit part.

Employing these reliable wave functions, various NTMEs, namely Fermi $M_F^{(K)}$, Gamow–Teller (GT) $M_{\text{GT}}^{(K)}$ consisting of $M_{\text{GT-AA}}^{(K)}$, $M_{\text{GT-AP}}^{(K)}$, $M_{\text{GT-PP}}^{(K)}$, $M_{\text{GT-MM}}^{(K)}$ and tensor $M_T^{(K)}$ consisting of $M_{T-\text{AP}}^{(0\nu)}$, $M_{T-\text{PP}}^{(0\nu)}$, $M_{T-\text{MM}}^{(0\nu)}$ are calculated with

Table 1. Comparison of calculated and observed excited energies E_{2^+} (MeV) of yrast 2^+ states,[51] deformation parameters β_2[52] and g-factors $g(2^+)$[53] of ^{76}Ge and ^{76}Se isotopes.

		Theory		
Nuclei	Properties	HFB1	HFB2	Exp.
^{76}Ge	E_{2+}	0.563	0.535	0.563
	β_2	0.2610	0.2483	0.2623 ± 0.0039
	$g(2^+)$	0.353 (0.353)	0.299 (0.306)	0.334 ± 0.038
^{76}Se	E_{2+}	0.559	0.507	0.559
	β_2	0.2991	0.3004	0.3090 ± 0.0037
	$g(2^+)$	0.394 (0.394)	0.305 (0.322)	0.40 ± 0.11

Table 2. Calculated (Theo.) and observed (Expt.) occupation numbers for neutrons[55] and protons[56] in ^{76}Ge and ^{76}Se isotopes with (a) HFB1 and (b) HFB2.

		^{76}Ge		^{76}Se	
Orbits		Theo.	Expt.	Theo.	Expt.
Protons					
$1p_{1/2} + 1p_{3/2}$	(a)	1.60	1.75 ± 0.15	2.54	2.09 ± 0.15
	(b)	0.96		1.88	
$0f_{5/2}$	(a)	2.30	2.04 ± 0.25	3.20	3.17 ± 0.25
	(b)	2.77		3.42	
$0g_{9/2}$	(a)	0.10	0.23 ± 0.25	0.26	0.86 ± 0.25
	(b)	0.26		0.70	
Neutrons					
$1p_{1/2} + 1p_{3/2}$	(a)	4.95	4.87 ± 0.20	4.09	4.41 ± 0.20
	(b)	4.48		3.75	
$0f_{5/2}$	(a)	4.24	4.56 ± 0.40	3.73	3.83 ± 0.20
	(b)	4.73		3.96	
$0g_{9/2}$	(a)	6.81	6.48 ± 0.30	6.18	5.80 ± 0.30
	(b)	6.79		6.29	

$g_V = 1.0$, $g_A = 1.2701$,[57] $\kappa = \mu_p - \mu_n = 3.70$, $\Lambda_V = 0.850\,\text{GeV}$ and $\Lambda_A = 1.086\,\text{GeV}$. Three sets of NTMEs are calculated by considering a Jastrow type of SRC simulating the effects of Argonne V18 and CD-Bonn potentials in the self-consistent CCM,[30] given by

$$f(r) = 1 - ce^{-ar^2}(1 - br^2), \tag{9}$$

where $a = 1.1,\ 1.59,\ 1.52\,\text{fm}^{-2}$, $b = 0.68,\ 1.45,\ 1.88\,\text{fm}^{-2}$ and $c = 1.0, 0.92, 0.46$ for Miller–Spencer parametrization, Argonne NN, CD-Bonn Potentials, and are denoted by SRC1, SRC2 and SRC3, respectively.

As already mentioned, three sets of wave functions are generated with C, CS and CST parts of the effective two-body interaction, and are subsequently employed to calculate the required NTMEs $M^{(K)}$. In Table 3, the NTMEs $M^{(0\nu)}$ and $M^{(0N)}$ due to the exchange of light and heavy Majorana neutrinos, respectively, are displayed. In the case of light neutrino exchange, the contributions of C and CS parts of the two-body interaction to the total NTMEs $M^{(0\nu)}$ of ^{76}Ge calculated within HFB1 and HFB2 are about 24–29% and 67–72%, respectively. The contributions of C and CS parts of the two-body interaction to the total NTMEs $M^{(0N)}$ of ^{76}Ge due to the heavy neutrino exchange, are about 34–42% and 64–67%, within HFB1 and HFB2, respectively. Thus, it turns out that the C, spin-orbit and tensor parts of the effective two-body interactions contribute more or less equally.

Relative changes (in %) in NTMEs $M^{(0\nu)}$ and $M^{(0N)}$ with the inclusion of SRC1, SRC2 and SRC3, and average energy denominator $A/2$ are given in Table 4. The maximum relative change in NTMEs $M^{(0\nu)}$, when the energy denominator is taken as $\overline{A}/2$ instead of $\overline{A}$ is of the order of 10%, which confirms that the dependence

Table 3. NTMEs for $0\nu\beta^-\beta^-$ decay of ^{76}Ge isotope due to the light and heavy Majorana neutrino exchange with three sets of wave functions having C, CS and CST for both (a) HFB1 and (b) HFB2.

		HFB1			HFB2		
TME	Case	C	CS	CST	C	CS	CST
$M^{(0\nu)}$	FNS	1.574	3.982	5.628	1.321	3.560	5.346
	SRC1	1.277	3.490	4.858	1.060	3.024	4.507
	SRC2	1.560	3.945	5.564	1.311	3.515	5.270
	SRC3	1.646	4.087	5.785	1.386	3.669	5.511
$M^{(0N)}$	FNS	121.44	194.58	298.33	109.50	204.92	320.41
	SRC1	45.40	69.89	104.34	42.35	70.36	110.10
	SRC2	75.62	118.68	179.84	69.26	122.77	191.67
	SRC3	100.85	160.12	244.35	91.52	167.51	261.63

Table 4. Relative changes (in %) of the NTMEs $M^{(0\nu)}$ and $M^{(0N)}$ with the inclusion of SRC (SRC1, SRC2 and SRC3), and average energy denominator $\overline{A}/2$.

		HFB1			HFB2		
NTME	Cases	C	CS	CST	C	CS	CST
$M^{(0\nu)}$	SRC1	18.9	12.4	13.7	19.8	15.0	15.7
	SRC2	0.9	0.9	1.1	0.8	1.3	1.4
	SRC3	4.5	2.6	2.8	4.9	3.0	3.1
	SRC1($\overline{A}/2$)	6.2	9.7	9.4	5.6	8.7	8.7
	SRC2($\overline{A}/2$)	6.0	9.1	8.8	5.4	8.2	8.2
	SRC3($\overline{A}/2$)	5.9	8.9	8.6	5.3	8.0	8.0
$M^{(0N)}$	SRC1	62.6	64.1	65.0	61.3	65.7	65.6
	SRC2	37.7	39.0	39.7	36.8	40.1	40.2
	SRC3	17.0	17.7	18.1	16.4	18.3	18.3

of NTMEs on the average excitation energy $\overline{A}$ is small and thus, the validity of the closure approximation for the $0\nu\beta^-\beta^-$ decay is supported. In comparison to the case FNS, the NTMEs $M^{(0\nu)}$ are approximately reduced by 14–16%, 1–1.4% and 2.8–3.0% with the addition of SRC1, SRC2 and SRC3, respectively. With the addition of SRC1, SRC2 and SRC3, the NTMEs $M^{(0N)}$ are approximately reduced by 64–66%, 40% and 15–18%, respectively in comparison to the case FNS. It is worth mentioning that the effects due to SRC on NTMEs $M^{(0\nu)}$ and $M^{(0N)}$ is maximally incorporated by the C part of the effective two-body interaction, which varies by a small amount with the inclusion of spin-orbit and tensor parts.

In Tables 5 and 6, all the available NTMEs $M^{(0\nu)}$ and $M^{(0N)}$ calculated in different nuclear models along with this work have been compiled. In comparison to the recent SM values, presently calculated NTMEs $M^{(0\nu)}$ using HFB1 (HFB2) wave functions differ by a factor of about 1.6–1.8 (1.5–1.7), respectively. However, the difference between the calculated values of $M^{(0N)}$ turns out to be a factor of

Table 5. Available NTMEs due to light neutrino exchange $M^{(0\nu)}$ in different nuclear models.

			$M^{(0\nu)}$			
Model	Refs.	g_A	Jastrow	UCOM	AV18	CD Bonn
PHFB	HFB1	1.2701	4.858		5.564	5.785
	HFB2	1.2701	4.507		5.270	5.511
SM	58	1.25	2.72		3.37	3.57
ISM	7	1.25	2.35			
ISM	8	1.25	2.30	2.81		
ShM	59	1.25	2.378		2.979	3.177
QRPA	16	1.254	4.92	5.98	6.34	6.89
pnQRPA	60	1.25	4.029	5.355		
pnQRPA	61	1.26				5.26
QRPA(I)	15	1.27			5.157	5.571
RQRPA	16	1.254	4.28	5.17	5.42	5.93
DQRPA	62	1.25				4.69
DQRPA(I)	18	1.27			3.12	3.40
EDF	26	1.25		4.60		
EDF	63	1.25		5.551		
IBM-2	23	1.269	5.42		5.98	6.16
IBM-2(I)	25	1.269			4.68	
CDFT	27, 64	1.254	6.36	6.13	7.48	7.84

Table 6. Available NTMEs due to heavy neutrino exchange $M^{(0N)}$ in different nuclear models.

			$M^{(0N)}$		
Model	Refs.	g_A	Jastrow	AV18	CD Bonn
PHFB	HFB1	1.2701	104.34	179.84	244.35
	HFB2	1.2701	110.10	191.67	261.63
SM	58	1.25		126	202
pnQRPA	61	1.26			401.3
RQRPA	67	1.25			363
DQRPA(I)	18	1.27		187.3	293.7
IBM-2	23	1.269	48.1	107	163
IBM-2(I)	25	1.269		104	
CDFT	27, 64	1.254	135.7	267.0	378.1

about 1.2–1.4 (1.3–1.5) for HFB1 (HFB2), respectively. In general, NTMEs calculated in SM and other models differ by a factor 2–3. This implies that the role of configuration mixing may be quite crucial in the calculation of reliable NTMEs. In the present context, it is worth mentioning that the consideration of ground states with prolate and oblate shapes suppresses the NTMEs $M_{2\nu}$.[65]

Limits on the effective neutrino mass $\langle m_\nu \rangle$ and $\langle M_N \rangle$ are extracted from the available limits on experimental half-lives $T^{0\nu}_{1/2}$ using NTMEs $M^{(0\nu)}$ and $M^{(0N)}$ calculated within the PHFB model (Table 7). In the case of ^{76}Ge isotope using the HFB1 (HFB2) wave functions, one obtains the best limit on the effective neutrino

Table 7. Extracted limits on the effective mass of neutrino $\langle m_\nu \rangle$, $\langle M_N \rangle$ using experimental half-life limit 8.0×10^{25} yr,[35] predicted half-lives $T^{(0\nu)}_{1/2}$ (yrs) for $\langle m_\nu \rangle = 0.01$ eV and Majoron-neutrino coupling constant $\langle g_M \rangle$ from the observed limits on $T^{(0\nu\phi)}_{1/2}$ with two sets of wave functions HFB1 and HFB2 and (a) SRC1, (b) SRC2 and (c) SRC3. In the last column, the extracted parameters are given using average NTMEs.

Parameters	SRC	HFB1	HFB2	Avg.
$\langle m_\nu \rangle$ (eV)	(a)	0.15	0.16	0.14
	(b)	0.13	0.14	
	(c)	0.13	0.13	
$T^{(0\nu)}_{1/2}$ (yr)	(a)	1.80×10^{28}	2.09×10^{28}	1.54×10^{28}
	(b)	1.37×10^{28}	1.53×10^{28}	
	(c)	1.27×10^{28}	1.40×10^{28}	
$\langle M_N \rangle$ (GeV)	(a)	6.87×10^{7}	7.26×10^{7}	1.20×10^{8}
	(b)	1.18×10^{8}	1.26×10^{8}	
	(c)	1.61×10^{8}	1.72×10^{8}	
$\langle g_M \rangle$	(a)	7.59×10^{-5}	8.18×10^{-5}	7.02×10^{-5}
	(b)	6.62×10^{-5}	6.99×10^{-5}	
	(c)	6.37×10^{-5}	6.69×10^{-5}	

mass $\langle m_\nu \rangle < 0.15$ eV, 0.13 eV, 0.13 eV (0.16 eV, 0.14 eV, 0.13 eV) and $\langle M_N \rangle > 6.87 \times 10^7 - 1.61 \times 10^8$ GeV ($7.26 \times 10^7 - 1.72 \times 10^8$ GeV) due to SRC1, SRC2 and SRC3, respectively. In the classical Majoron model, the inverse half-life $T^{(0\nu\phi)}_{1/2}$ for the $0^+ \rightarrow 0^+$ transition of Majoron emitting $0\nu\beta^-\beta^-\phi$ decay is given by[66]

$$[T^{(0\nu\phi)}_{1/2}(0^+ \rightarrow 0^+)]^{-1} = |\langle g_M \rangle|^2 G_{\beta\beta\phi} |M^{(0\nu\phi)}|^2, \tag{10}$$

where $\langle g_M \rangle$ is the effective Majoron-neutrino coupling constant, and the NTME $M^{(0\nu\phi)}$ is same as the $M^{(0\nu)}$ for the exchange of light Majorana neutrinos. The phase space factors $G_{\beta\beta\phi}$ for the $0^+ \rightarrow 0^+$ transition of $0\nu\beta^-\beta^-\phi$ decay mode have been given by Kotila and Iachello.[68] The extracted limits on the effective Majoron-neutrino coupling parameter $\langle g_M \rangle$ form the largest limits on the half-lives $T^{(0\nu\phi)}_{1/2} = 6.4 \times 10^{22}$,[69] are given in Table 7. The most stringent extracted limit on $\langle g_M \rangle$ is $(6.37 - 8.18) \times 10^{-5}$.

In spite of the fact that there are only a set of six NTMEs $M^{(0\nu)}$ and $M^{(0N)}$ for a statistical analysis to estimate uncertainties therein, the calculated average NTMEs $\overline{M}^{(K)}$ with standard deviation $\Delta\overline{M}^{(K)}$ are $\overline{M}^{(0\nu)} = 5.249 \pm 0.481$ and $\overline{M}^{(0N)} = 181.99 \pm 65.61$. Hence, the model-dependent uncertainties in average NTMEs $\overline{M}^{(0\nu)}$ and $\overline{M}^{(0N)}$ turn out to be about 10% and 37%, respectively. Using the estimated average NTMEs $\overline{M}^{(0\nu)}$ and $\overline{M}^{(0N)}$ calculated in the PHFB model, the most stringent extracted limits on the effective neutrino mass $\langle m_\nu \rangle$ and $\langle M_N \rangle$ from the available limit on experimental half-live $T^{0\nu}_{1/2}$ of ^{76}Ge are 0.14 eV and 1.20×10^8 GeV, respectively. Further, the extracted limit on the effective Majoron-neutrino coupling parameter $\langle g_M \rangle$ is 7.02×10^{-5}.

4. Conclusions

In the Majorana neutrino mass mechanism, the required NTMEs $M^{(0K)}$ to study the $0\nu\beta^-\beta^-$ decay of ^{76} Ge isotope are calculated within the PHFB approach, using two sets of HFB intrinsic wave functions, generated with KUO and JUN45 effective two-body interactions. The reliability of wave functions has been tested by calculating the yrast spectra, deformation parameters β_2 and g-factors $g(2^+)$ as well as $M_{2\nu}$ of nuclei participating in the $2\nu\beta^-\beta^-$ decay and comparing them with the available experimental data. An overall agreement between the calculated and observed spectroscopic properties as well as $M_{2\nu}$ suggests that the PHFB wave functions generated by reproducing the E_{2^+} are quite reliable. Further, the contributions of the C, spin-orbit and tensor components of the effective two-body interaction to the total $M^{(0K)}$ have been obtained by performing a spin-tensor decomposition of KUO and JUN45 two-body matrix elements.

The NTMEs $M^{(0\nu)}$ have a weak dependence on the average excitation energy $\overline{A}$ of intermediate nucleus and as expected, the closure approximation is quite valid. In comparison to the case FNS, the NTMEs $M^{(0\nu)}$ ($M^{(0N)}$) are approximately reduced by 15% (65%), 1% (40%) and 3% (16%) with the addition of SRC1, SRC2 and SRC3, respectively. Specifically, the strong dependence of $M^{(0N)}$ in the case of heavy neutrino exchange on the SRC is a major source of uncertainty in the calculation of NTMEs. It has been noticed that the C part of the effective two-body interaction picks up maximally the effects due to SRC on NTMEs $M^{(0\nu)}$ and $M^{(0N)}$, which varies by a small amount with the inclusion of spin-orbit and tensor parts.

Limits on the effective light neutrino mass $\langle m_\nu \rangle$, effective heavy neutrino mass $\langle M_N \rangle$ and neutrino-Majoron coupling constant $\langle g_M \rangle$ of the classical Majoron model have been extracted from the available limits on experimental half-lives $T^{(0\nu)}_{1/2}$ and $T^{(0\nu\phi)}_{1/2}$, respectively. The most stringent extracted limits on $\langle m_\nu \rangle$, $\langle M_N \rangle$ and $\langle g_M \rangle$ from the available experimental limit on $T^{(0\nu)}_{1/2}$ of ^{76}Ge are 0.14 eV and 1.20×10^8 GeV and 7.02×10^{-5}, respectively.

Acknowledgments

This work is partially supported by DST-SERB, India vide Grant No. SB/S2/HEP-007/2013 and Council of Scientific and Industrial Research (CSIR), India vide sanction No. 03(1216)/12/EMR-II.

References

1. J. D. Vergados, H. Ejiri and F. Šimkovic, *Int. J. Mod. Phys. E* **25** (2016) 1630007; *Rep. Prog. Phys.* **75** (2012) 106301.
2. S. Dell'Oro, S. Marcocci, M. Viel and F. Vissani, *Adv. High Energy Phys.* **2016** (2016) 2162659.
3. J. Kotila and F. Iachello, *Phys. Rev. C* **85** (2012) 034316.
4. S. Stoica and M. Mirea, *Phys. Rev. C* **88** (2013) 037303.

5. D. Stefanik, R. Dvornicky, F. Simkovic and P. Vogel, *Phys. Rev. C* **92** (2015) 055502.
6. J. Engel and J. J. Menéndez, *Rep. Prog. Phys.* **80** (2017) 046301.
7. E. Caurier, F. Nowacki and A. Poves, *Eur. Phys. J. A* **36** (2008) 195; E. Caurier, J. Menéndez, F. Nowacki and A. Poves, *Phys. Rev. Lett.* **100** (2008) 052503; E. Caurier, F. Nowacki, A. Poves and J. Retamosa, *Nucl. Phys. A* **654** (1999) 973c; *Phys. Rev. Lett.* **77** (1996) 1954; E. Caurier, A. Poves and A. P. Zuker, *Phys. Lett. B* **252** (1990) 13.
8. J. Menéndez, A. Poves, E. Caurier and F. Nowacki, *Nucl. Phys. A* **818** (2009) 139.
9. B. A. Brown, M. Horoi and R. A. Sen'kov, *Phys. Rev. Lett.* **113** (2014) 262501; M. Horoi and B. A. Brown, *Phys. Rev. Lett.* **110** (2013) 222502; M. Horoi and S. Stoica, *Phys. Rev. C* **81** (2010) 024321.
10. R. A. Sen'kov and M. Horoi, *Phys. Rev. C* **93** (2016) 044334; B. A. Brown, D. L. Fang and M. Horoi, *Phys. Rev. C* **92** (2015) 041301(R); A. Neacsu and M. Horoi, *Phys. Rev. C* **91** (2015) 024309; R. A. Sen'kov and M. Horoi, *Phys. Rev. C* **90** (2014) 051301(R); R. A. Sen'kov, M. Horoi and B. A. Brown, *Phys. Rev. C* **89** (2014) 054304.
11. P. Vogel and M. R. Zirnbauer, *Phys. Rev. Lett.* **57** (1986) 3148.
12. O. Civitarese, A. Faessler and T. Tomoda, *Phys. Lett. B* **194** (1987) 11.
13. J. Suhonen and O. Civitarese, *Phys. Rep.* **300** (1998) 123.
14. A. Faessler and F. Šimkovic, *J. Phys. G* **24** (1998) 2139.
15. F. Šimkovic, V. Rodin, A. Faessler and P. Vogel, *Phys. Rev. C* **87** (2013) 045501.
16. A. Faessler, V. Rodin and F. Šimkovic, *J. Phys. G*, *Nucl. Part. Phys.* **39** (2012) 124006; D. L. Fang, A. Faessler, V. Rodin and F. Šimkovic, *Phys. Rev. C* **83** (2011) 034320; *Phys. Rev. C* **82** (2010) 051301(R).
17. M. T. Mustonen and J. Engel, *Phys. Rev. C* **87** (2013) 064302.
18. D. L. Fang, A. Faessler and F. Šimkovic, *Phys. Rev. C* **97** (2018) 045503.
19. P. K. Rath, R. Chandra, K. Chaturvedi, P. K. Raina and J. G. Hirsch, *Phys. Rev. C* **82** (2010) 064310.
20. P. K. Rath, R. Chandra, K. Chaturvedi, P. Lohani, P. K. Raina and J. G. Hirsch, *Phys. Rev. C* **88** (2013) 064322.
21. P. K. Rath, R. Chandra, P. K. Raina, K. Chaturvedi and J. G. Hirsch, *Phys. Rev. C* **85** (2012) 014308.
22. P. K. Rath, R. Chandra, K. Chaturvedi, P. Lohani and P. K. Raina, *Phys. Rev. C* **93** (2016) 024314.
23. J. Barea, J. Kotila and F. Iachello, *Phys. Rev. C* **87** (2013) 014315; F. Iachello, J. Barea and J. Kotila, *AIP Conf. Proc.* **1417** (2011) 62; F. Iachello and J. Barea, *Nucl. Phys. B Proc. Suppl.* **217** (2011) 5; J. Barea and F. Iachello, *Phys. Rev. C* **79** (2009) 044301.
24. N. Yosida and F. Iachello, *Prog. Theor. Exp. Phys.* **2013** (2013) 043D01.
25. J. Barea, J. Kotila and F. Iachello, *Phys. Rev. C* **91** (2015) 034304.
26. T. R. Rodríguez and G. Martínez-Pinedo, *Phys. Rev. Lett.* **105** (2010) 252503.
27. J. M. Yao, L. S. Song, K. Hagino, P. Ring and J. Meng, *Phys. Rev. C* **91** (2015) 024316.
28. G. A. Miller and J. E. Spencer, *Ann. Phys.* (*NY*) **100** (1976) 562.
29. M. Kortelainen and J. Suhonen, *Phys. Rev. C* **76** (2007) 024315; M. Kortelainen, O. Civitarese, J. Suhonen and J. Toivanen, *Phys. Lett. B* **647** (2007) 128.
30. F. Šimkovic, A. Faessler, H. Muther, V. Rodin and M. Stauf, *Phys. Rev. C* **79** (2009) 055501.
31. J. Menéndez, D. Gazit and A. Schwenk, *Phys. Rev. Lett.* **107** (2011) 062501.
32. J. Suhonen and O. Civitarese, *Phys. Lett. B* **725** (2013) 153.
33. J. Engel, F. Šimkovic and P. Vogel, *Phys. Rev. C* **89** (2014) 064308.

34. R. Saakyan, *Annu. Rev. Nucl. Part. Sci.* **63** (2013) 503.
35. M. Agostini *et al.*, *Phys. Rev. Lett.* **120** (2018) 132503.
36. C. E. Aalseth *et al.*, *Phys. Rev. Lett.* **120** (2018) 132502.
37. A. S. Barabash and V. B. Brudanin, *Phys. At. Nucl.,* **74** (2011) 312; R. Arnold *et al.*, *Phys. Rev. D* **92** (2015) 072011.
38. K. Alfonso *et al.*, *Phys. Rev. Lett.* **115** (2015) 102502; C. Alduino *et al.*, *Phys. Rev. C* **93** (2016) 045503.
39. A. Gando *et al.*, *Phys. Rev. Lett.* **117** (2016) 082503.
40. M. Auger *et al.*, *Phys. Rev. Lett.* **109** (2012) 32505.
41. A. L. Goodman, Hartree-Fock-Bogoliubov Theory with Applications to Nuclei in *Advances in Nuclear Physics*, eds. J. W. Negele and E. Vogt, Vol. 11 (Plenum, New York, 1979) 263.
42. T. T. S. Kuo, Private Communication.
43. M. Honma, T. Otsuka, T. Mizusaki and M. Hjorth-Jensen, *Phys. Rev. C* **80** (2009) 064323.
44. F. Šimkovic, G. Pantis, J. D. Vergados and A. Faessler, *Phys. Rev. C* **60** (1999) 055502.
45. J. D. Vergados, *Phys. Rep.* **361** (2002) 1.
46. M. Blenow, E. F. Martinez, J. L. Pavon and J. Menéndez, *J. High Energy Phys.* **7** (2010) 96.
47. F. Šimkovic, D. Štefánik and R. Dvornický, *Front. Phys.* **5** (2017) 57.
48. B. H. Wildental, *Prog. Part. Nucl. Phys.* **11** (1984) 5.
49. P. N. Tripathi, S. K. Sharma and S. K. Khosa, *Phys. Rev. C* **29** (1984) 1951.
50. M. W. Kirson, *Phys. Lett. B* **47** (1973) 110; J. P. Schiffer and W. W. True, *Rev. Mod. Phys.* **48** (1976) 191; K. Klingenbeck, W. Knufer, M. G. Huber and P. W. M. Glaudemans, *Phys. Rev. C* **15** (1977) 1483; B. A. Brown, W. A. Richter and B. H. Wildental, *J. Phys. G* **11** (1985) 1191.
51. M. Sakai, *At. Data Nucl. Data Tables* **31** (1984) 399.
52. S. Raman, C. W. Nestor Jr. and P. Tikkanen, *At. Data Nucl. Data Tables* **78** (2001) 1; S. Raman, C. H. Malarkey, W. T. Milner, C. W. Nestor Jr. and P. H. Stelson, *At. Data Nucl. Data Tables* **36** (1987) 1.
53. P. Raghavan, *At. Data Nucl. Data Tables* **42** (1989) 189.
54. P. K. Rath and S. K. Sharma, *Phys. Rev. C* **38** (1988) 2928.
55. J. P. Schiffer *et al.*, *Phys. Rev. Lett.* **100** (2008) 112501.
56. B. P. Kay *et.al.*, *Phys. Rev. C* **79** (2009) 021301(R).
57. Particle Data Group (J. Beringer *et al.*), *Phys. Rev. D* **86** (2012) 010001.
58. R. A. Sen'kov and M. Horoi, *Phys. Rev. C* **90** (2014) 051301(R).
59. A. Neacsu and S. Stoica, *J. Phys. G*, *Nucl. Part. Phys.* **41** (2014) 015201.
60. O. Civitarese and J. Suhonen, *J. Phys. Conf. Ser.* **173** (2009) 012012.
61. J. Hyvarinen and J. Suhonen, *Phys. Rev. C* **91** (2015) 024613.
62. D.-L. Fang, A. Faessler and V. Rodin, *Phys. Rev. C* **83** (2011) 034320.
63. N. L. Vaquero, T. R. Rodríguez and J. L. Egido, *Phys. Rev. Lett.* **111** (2013) 142501.
64. L. S. Song, J. M. Yao, P. Ring and J. Meng, *Phys. Rev. C* **95** (2017) 024305.
65. F. Šimkovic, L. Pacearescu and A. Faessler, *Nucl. Phys. A* **733** (2004) 321.
66. M. Doi, T. Kotani and E. Takasugi, *Prog. Theor. Phys. Suppl.* **83** (1985) 1.
67. F. Šimkovic, J. Vergados and A. Faessler, *Phys. Rev. D* **82** (2010) 113015.
68. J. Kotila, J. Barea and F. Iachello,*Phys. Rev. C* **91** (2015) 064310.
69. H. V. Klapdor-Kleingrothaus *et al.*, *Eur. Phys. J. A* **12** (2001) 147.

Occupancies of proton and neutron orbits of nuclei in the mass range A=90–150 participating in $0\nu\beta^-\beta^-$ decay

R. Gautam[1], Brijesh Shukla[2], P. Chaturvedi[3], R. Chandra[1],* K. Chaturvedi[3], P. K. Rath[2] and P. K. Raina[4]

[1] *Department of Physics, Babasaheb Bhimrao Ambedkar University, Lucknow - 226025, INDIA*
[2]*Department of Physics, University of Lucknow, Lucknow, 226007, INDIA*
[3]*Department of Physics, Bundelkhand University, Jhansi – 284128, INDIA*
[4]*Department of Physics, IIT Ropar, Nangal Road, Rupnagar, Punjab – 140001, INDIA*
** email: ramesh.luphy@gmail.com*

Introduction

The sixteen rare modes of nuclear double beta ($\beta\beta$) decay, namely double-electron emission ($\beta^-\beta^-$), double-positron emission ($\beta^+\beta^+$), electron-positron conversion ($\varepsilon\beta^+$) and double-electron capture ($\varepsilon\varepsilon$) with the emission of two neutrinos, no neutrinos, single Majoron and double Majorons provide fundamental information on mass and nature of neutrinos as well as nuclear structure aspects. Among all these modes, the $0\nu\beta\beta$ decay, which violates the conservation of lepton number by two units, is of paramount importance as its observation will immediately imply the Majorana nature of neutrinos with finite mass. The $0\nu\beta\beta$ decay has not been observed yet and major projects are under the way to detect this peculiar decay mode [1,2].

In any gauge theory allowing the violation of lepton number conservation, the inverse half-life of $0\nu\beta\beta$ decay is a product of gauge theoretical parameter of the underlying theory, appropriate phase space factors and nuclear transition matrix elements (NTMEs) $M^{0\nu}$. The phase space factors are accurately calculable [3–5]. However, the calculation of NTMEs is highly dependent on the nuclear models employed and the extraction of various lepton number violating gauge parameters depends on the reliability of NTMEs calculated. On the other hand there exist noticeable uncertainties in the value of $M^{0\nu}$ calculated in different models [6].

Prior to the calculation of $M^{0\nu}$, the reliability of the wave functions can be checked by reproducing the experimentally observed values, namely yrast energies, reduced transition probabilities, quadrupole moments, deformation parameters and NTMEs $M_{2\nu}$ of $2\nu\beta^-\beta^-$ decay. Recently, the occupation of valence orbits by nucleons have been studied experimentally [7-10]. These experimental values can provide a further check on the reliability of wave functions by comparing them with calculated values. In the present work we have calculated the occupation numbers of various orbits for protons and neutrons within the projected Hartree-Fock Bogoliubov (PHFB) model.

Theoretical framework

The sub-shell occupation numbers η_J in a yrast state J is given by

$$\eta_J = \frac{\langle \Phi_0 | \left(\sum_m C^+_{jm} C_{jm} \right) P^J_{00} | \Phi_0 \rangle}{\langle \Phi_0 | P^J_{00} | \Phi_0 \rangle} = \frac{\int_0^\pi p(\theta) d^J_{00}(\theta) \sin\theta \, d\theta}{\int_0^\pi n(\theta) d^J_{00}(\theta) \sin\theta \, d\theta} \quad (1)$$

where

$$p(\theta) = n(\theta) \left[\sum_m \left(\frac{M}{1+M} \right)_{jm,jm} \right] \quad (2)$$

An approximate estimate of the subshell occupation numbers can be easily obtained in terms of the expectation value of the operator η_J with respect to the intrinsic state $|\Phi_0\rangle$

$$\eta_J^{\text{intrinsic}} = \langle \Phi_0 | \hat{\eta}_J | \Phi_0 \rangle = \sum_{i,m} |c^m_{Ji}|^2 \left(V_i^m \right)^2 \quad (3)$$

Results and discussions

In the present work we use four parametrizations of pairing plus multipolar effective two-body interaction, namely *PQQ*1, *PQQHH*1, *PQQ*2 and *PQQHH*2. The model

space and details about these parametrizations and method to fix them have been provided in our earlier work [11]. We have calculated the values of occupation numbers of orbits for protons (p) and neutrons (n) in the ground states of ^{94,96}Zr, ^{94,96,100}Mo, ^{100}Ru, ^{110}Pd, ^{110}Cd, ^{128,130}Te, ^{128,130}Xe, ^{150}Nd and ^{150}Sm nuclei for all the four parametrizations of effective two-body interaction. In Table 1 and 2, we present the results for ^{100}Mo, ^{100}Ru, ^{130}Te and ^{130}Xe nuclei for *PQQ*1 and *PQQHH*1 parametrizations.

Table 1: The calculated values of the occupation numbers of orbits for protons and neutrons in the ground states of ^{100}Mo and ^{100}Ru nuclei for (a) *PQQ*1 and (b) *PQQHH*1 parametrizations.

Orbits		^{100}Mo		^{100}Ru	
		p	n	p	n
$2s_{1/2}$	a	0.042	0.705	0.044	0.635
	b	0.042	0.691	0.044	0.628
$1p_{1/2}$	a	0.114	1.994	1.035	1.998
	b	1.144	1.994	1.042	1.199
$1d_{3/2}$	a	0.020	1.298	0.028	1.190
	b	0.020	1.262	0.029	1.172
$1d_{5/2}$	a	0.485	3.233	0.456	3.036
	b	0.461	3.258	0.454	3.031
$0g_{7/2}$	a	0.021	1.419	0.037	0.994
	b	0.021	1.373	0.037	1.005
$0g_{9/2}$	a	3.278	9.843	4.329	9.879
	b	3.255	9.854	4.316	9.880
$0h_{11/2}$	a	0.037	1.505	0.689	0.267
	b	0.055	1.565	0.075	0.284

Table 2: The calculated values of the occupation numbers of orbits for protons and neutrons in the ground states of ^{130}Te and ^{130}Xe nuclei for (a) *PQQ*1 and (b) *PQQHH*1 parametrizations.

Orbits		^{130}Te		^{130}Xe	
		p	n	p	n
$2s_{1/2}$	a	0.477	1.970	0.552	1.916
	b	0.546	1.923	0.546	1.923
$1d_{3/2}$	a	0.236	3.917	0.973	3.726
	b	0.933	3.750	0.933	3.750
$1d_{5/2}$	a	1.258	5.948	1.891	5.907
	b	1.996	5.910	1.996	5.910
$1f_{7/2}$	a	0.000	0.422	0.004	0.823
	b	0.004	0.758	0.004	0.758
$0g_{7/2}$	a	0.028	7.597	0.515	6.582
	b	0.456	6.683	0.456	6.683
$0g_{9/2}$	a	0.000	0.186	0.003	0.242
	b	0.003	0.226	0.003	0.226
$0h_{11/2}$	a	0.000	7.956	0.059	6.800
	b	0.060	6.746	0.060	6.746

Conclusions

To summarize, we have calculated the occupation numbers of orbits for protons and neutrons for ^{94,96}Zr, ^{94,96,100}Mo, ^{100}Ru, ^{110}Pd, ^{110}Cd, ^{128,130}Te, ^{128,130}Xe, ^{150}Nd and ^{150}Sm nuclei employing four sets of wave functions generated through PHFB model. Complete results will be presented in the symposium.

References

[1] I. Ostrovskiy, Modern Physics Letters A, **31**, 1630017 (2016).

[2] Reyco Henning, Reviews in Physics 1, **29**, (2016).

[3] M. Doi, T. Kotoni and E. Takasugi, Prog. Theor. Phys. Suppl. **83**, 1 (1985).

[4] J. Kotila and F. Iachello, Phys. Rev. C **85**, 034316 (2012).

[5] D. Štefánik, R. Dvornický, F. Šimkovic, and P. Vogel, Phys. Rev. C **92**, 055502 (2015).

[6] J. Engel, J. Phys. G: Nucl. Part. Phys. **42**, 034017 (2015).

[7] J. P. Schiffer et al. Phys. Rev. Lett. 100, 112501 (2008).

[8] B. P. Kay *et al*. Phys. Rev. C. **79**, 021301(R) (2009).

[9] B. P. Kay *et al*. Phys. Rev. C. **87**, 011302(R) (2013).

[10] D. K. Sharp, AIP Conference proceedings **1686**, 020021 (2015).

[11] P. K. Rath, R. Chandra, K. Chaturvedi, P. K. Raina and J. G. Hirsch, Phys. Rev. C. **82**, 064310 (2010).

Acknowledgment

One of the authors RC thanks DST-SERB, India for financial support vides Dy. No. SR/FTP/PS-085/2011.

Correlations in the nuclear transition matrix elements of $(\beta\beta)_{0\nu}$ decay within PHFB model

R. Gautam[1], V. K. Nautiyal[1], R. Chandra[1],* P. K. Rath[2] and P. K. Raina[3]
[1] *Department of Applied Physics, Babasaheb Bhimrao Ambedkar University, Lucknow - 226025, INDIA*
[2]*Department of Physics, University of Lucknow, Lucknow, 226007, INDIA*
[3]*Department of Physics, IIT Ropar, Nangal Road, Rupnagar, Punjab – 140001, INDIA*
* *email: ramesh.luphy@gmail.com*

Introduction

The neturinoless double beta $(\beta\beta)_{0\nu}$ decay is one of the potential keys to open the window for physics beyond standard model of electroweak unification (SM) as it violates the lepton number conservation. In order to get the absolute mass and unfold the nature of neutrinos i.e. Dirac or Majorana, the $(\beta\beta)_{0\nu}$ decay is the natural choice theoretically as well as experimentally [1,2]. The $(\beta\beta)_{0\nu}$ has not been observed experimentally and only limits on half-lives are available. The neutrino mass and other gauge theoretical parameters can be extracted from the available half-life limits using appropriate nuclear transition matrix elements (NTMEs) and accurately calculable phase space factors of $(\beta\beta)_{0\nu}$ decay. The accuracy of these extracted gauge theoretical parameters highly depends on the reliability of NTMEs of $(\beta\beta)_{0\nu}$ decay. The NTME $M^{0\nu}$ is a model dependent quantity and in the absence of experimental data the calculation of the $M^{0\nu}$ of $(\beta\beta)_{0\nu}$ decay is a formidable task. The two-neutrino double beta $(\beta\beta)_{2\nu}$ decay has been observed experimentally for twelve nuclei [3] and experimental NTMEs $M_{2\nu}$ for this mode are available. In practice, the reliability of $M^{0\nu}$ for $(\beta\beta)_{0\nu}$ decay is tested by reproducing the experimentally extracted $M_{2\nu}$ of $(\beta\beta)_{2\nu}$ decay as both the modes involve same set of wave functions.

The NTMEs $M^{0\nu}$ are mainly calculated in three types of models namely, shell-model, quasiparticle random phase approximation (QRPA) and alternative models along with their several variants and extensions [4,5]. It is found that there is a large uncertainty in the values of $M^{0\nu}$ calculated in these models. Even the NTMEs calculated in the same type of generic model have noticeable uncertainty. There are several reasons for the observed uncertainty in NTMEs. There is no specific prescription in practice to fix the two basic ingredients of any nuclear model i.e. the model space and appropriate effective two-body interaction. Generally, different model space and different effective interactions are used in models. Further, even for the same model space the basic approach to fix the parameters of effective two-body interactions is different. Moreover, the choice of axial vector coupling constant g_A and short range correlations also contribute to uncertainty in the NTMEs. Faessler et al. [6] has shown the importance of correlated nuclear matrix elements uncertainties within QRPA model in comparing the decay rates of $(\beta\beta)_{0\nu}$ decay for different nuclei.

The projected Hartree-Fock Bogoliubov (PHFB) model has been successfully employed to study the $(\beta\beta)_{0\nu}$ decay (see [7] and references therein). In the present work we establish correlations between NTMEs $M^{0\nu}$ of ^{96}Zr, ^{100}Mo, ^{110}Pd, ^{128,130}Te and ^{150}Nd calculated within PHFB model.

Theoretical framework

In the approximation of light Majorona neutrinos, the inverse half-life of $(\beta\beta)_{0\nu}$ decay for $0^+ \rightarrow 0^+$ transition is given by [8],

$$\left[T_{1/2}^{0\nu}\right]^{-1} = \left(\frac{\langle m_\nu \rangle}{m_e}\right)^2 G_{01} \left|\left(M_{GT}^{0\nu} - M_F^{0\nu}\right)\right|^2 \quad (1)$$

where G_{01} is the phase space factor which can be calculated exactly and the NTMEs are given by

$$M_k = \Sigma \left\langle 0_F^+ \left\| O_{k,nm} \tau_n^+ \tau_m^+ \right\| 0_I^+ \right\rangle \quad (2)$$

with

$$O_F = \left(\frac{g_V}{g_A}\right)^2 H(r_{12}), \qquad O_{GT} = \sigma_1.\sigma_2 H(r_{12}) \quad (3)$$

Results and discussions

The model space, single particle energies (SPE's), parameters of the pairing plus multipole (PQQHH) type of effective two-body interaction have been already given in Ref. [9]. The effective Hamiltonian used in the present work is given as

$$H = H_{s.p.} + V(P) + V(QQ) + V(HH) \quad (4)$$

where $H_{s.p.}$, $V(P)$, $V(QQ)$ and $V(HH)$ denote the single particle Hamiltonian, pairing, quadrupole-quadrupole and hexadecapole-hexadecapole parts of the effective two-body interaction. We use four parametrizations of effective two-body interaction namely, PQQ1, PQQHH1, PQQ2 and PQQHH2. The details about these parametrizations and method to fix them have been provided in our earlier work [10]. Further, the NTMEs have been calculated by considering the finite size of nucleon and Jastrow type of short range correlations with Miller-Spencer, Argonne V18 and CD-Bonn NN potentials. Hence, with four parametrizations and three short range correlations we have a set of twelve NTMEs for each nucleus.

Following Faessler et al. [6], the associated covariance matrx is given as

$$\mathrm{cov}(n_i,n_j) = \rho_{ij}\sigma_i\sigma_j$$

where diagonal elements coincide with the variances σ_i^2, n_i is matrix element, σ_I is the error and ρ_{ij} is the correlation. Here, we analyze the correlation between NTMEs of ^{96}Zr, ^{100}Mo, ^{110}Pd, ^{128,130}Te and ^{150}Nd nuclei calculated within PHFB model. The results are given in Table 1.

Table 1: Correlation matrix ρ_{ij} between NTMEs $M^{0\nu}$ of $(\beta\beta)_{0\nu}$ decay of ^{96}Zr, ^{100}Mo, ^{110}Pd, ^{128,130}Te and ^{150}Nd nuclei calculated within PHFB model.

	Correlation matrix ρ_{ij}					
	^{96}Zr	**^{100}Mo**	**^{110}Pd**	**^{128}Te**	**^{130}Te**	**^{150}Nd**
^{96}Zr	1.00					
^{100}Mo	0.86	1.00				
^{110}Pd	0.74	0.82	1.00			
^{128}Te	0.52	0.44	0.40	1.00		
^{130}Te	0.70	0.90	0.96	0.34	1.00	
^{150}Nd	0.53	0.80	0.92	0.20	0.97	1.00

It is observed from Table 1 that there is a positive correlation between NTMEs of $(\beta\beta)_{0\nu}$ decay of two or more nuclei within PHFB model. The detailed results will be presented in the symposium.

References

[1] J. Engel and J. Menéndez, Rep. Prog. Phys. **80**, 046301 (2017).

[2] I. Ostrovskiy, Modern Physics Letters A, **31**, 1630017 (2016).

[3] R. Saakyan, Annu. Rev. Nucl. Part. Sci. **63**, 503 (2013).

[4] J. Suhonen, O. Civitarese, Phys. Rep. **300**, 123 (1998).

[5] A. Faessler and F. Simkovic, J. Phys. G **24**, 2139 (1998).

[6] A. Faessler, G. L. Fogli, E. Lisi, V. Rodin, A. M. Rotunno and F. Simkovic, Phys. Rev. D **79**, 053001 (2009).

[7] P. K. Rath, R. Chandra, K. Chaturvedi, P. Lohani, P. K. Raina, and J. G. Hirsch, Phys. Rev. C **88**, 064322 (2013**)**.

[8] W. C. Haxton and G. J. Stephenson Jr., Prog. Part. Nucl. Phys. **12**, 409 (1984).

[9] R. Chandra, K. Chaturvedi, P. K. Rath, P. K. Raina and J. G. Hirsch, Europhys. Lett. **86**, 32001 (2009).

[10] P. K. Rath, R. Chandra, K. Chaturvedi, P. K. Raina and J. G. Hirsch, Phys. Rev. C. **82**, 064310 (2010).

Acknowledgment

One of the authors RC thanks DST-SERB, India for financial support vides Dy. No. SERB/F/6190/2015-16.

Neutrinoless double beta decay and Physics beyond the Standard Model

Yash Kaur Singh[1], Pooja Lohani[2], V. K. Nautiyal[1], R. Gautam[1], R. Chandra[1],* K. Chaturvedi[3], P. K. Rath[2] and P. K. Raina[4]

[1] *Department of Applied Physics, Babasaheb Bhimrao Ambedkar University, Lucknow - 226025, INDIA*
[2]*Department of Physics, University of Lucknow, Lucknow, 226007, INDIA*
[3] *Department of Physics, Bundelkhand University, Jhansi – 284128, INDIA*
[4]*Department of Physics, IIT Ropar, Nangal Road, Rupnagar, Punjab – 140001, INDIA*
* *email: ramesh.luphy@gmail.com*

Introduction

The nuclear ββ decay, in which the charge *Z* of an even *Z*-even *N* nucleus is changed by two units while the mass number *A* remains the same, is a rare and spontaneous process of weak interaction in nature. The ββ decay can be categorized in mainly two modes, namely two neutrino double beta $(\beta\beta)_{2\nu}$ decay and neutrinoless double beta $(\beta\beta)_{0\nu}$ decay. The $(\beta\beta)_{2\nu}$ decay establishes the validity of different nuclear models employed for nuclear structure calculations by calculating the nuclear transition matrix elements (NTMEs) $M_{2\nu}$. The $(\beta\beta)_{0\nu}$ decay violates the lepton number conservation by two units and can be studied in any theory in which lepton number conservation is not exact. Hence $(\beta\beta)_{0\nu}$ decay is an excellent process to probe the new physics beyond the standard model (SM) of electroweak unification. Apart from the well studied left-right symmetric model, the $(\beta\beta)_{0\nu}$ decay can also be studied in Majoron models, R-parity violating as well as conserving supersymmetric (SUSY) models. Further, the $(\beta\beta)_{0\nu}$ decay can verify issues like compositeness, leptoquarks, sterile neutrinos and violation of weak equivalence principle. The detailed progress of experimental as well as theoretical studies on ββ decay in general and $(\beta\beta)_{0\nu}$ decay in particular can be found in references [1,2] and references there in.

The PHFB model in conjunction with pairing plus multipole type of two-body effective interaction has been successfully applied to study the $(\beta\beta)_{0\nu}$ decay [3-7]. In present work the same PHFB model has been applied to study the $(\beta\beta)_{0\nu}$ decay in various theories beyond the SM.

Theoretical framework

The details about the model space, single particle energies, *PQQ* type of effective two-body interaction and the procedure to fix its parameters have been given in Refs. [3,4]. The Hamiltonian of the effective two-body interaction used in the present work is given as

$$H = H_{s.p.} + V(P) + V(QQ) + V(HH) \quad (1)$$

where $H_{s.p.}$, $V(P)$, $V(QQ)$ and $V(HH)$ denote the single particle Hamiltonian, pairing, quadrupole-quadrupole and hexadecapole-hexadecapole parts of the effective two-body interaction. We use four different parametrizations of the interaction Hamiltonian, namely *PQQ*1, *PQQ*2, *PQQHH*1 and *PQQHH*2 [5]. Further, we use the Jastrow type of short range correlations with Miller-Spencer, Argonne V18 and CD-Bonn NN potentials [5,8]. The detailed theoretical formalism to study the $(\beta\beta)_{0\nu}$ decay in Majoron and SUSY models are given in refs. [9,10,11]. Further, the theory of compositeness and leptoquark in connection with $(\beta\beta)_{0\nu}$ decay is given in refs. [12,13].

Results and discussions

The NTMEs involved in $(\beta\beta)_{0\nu}$ decay in various theories stated above are calculated within PHFB model using pairing plus multipole type of two-body interaction. The NTMEs have been calculated by considering the finite size of nucleon (F) and Jastrow type of short range correlations (SRC) with Miller-Spencer, Argonne V18 and CD-Bonn NN potentials for $(\beta\beta)_{0\nu}$ decay of ^{94,96}Zr, ^{100}Mo, ^{128,130}Te and ^{150}Nd isotopes for the $0^+ \rightarrow 0^+$ transition. At present, some results are presented for the case of ^{100}Mo

with *PQQ1* parametrization. The detailed results will be presented in the symposium.

Table 1: NTMEs for the Majoron accompanied $(\beta\beta)_{0\nu}$ decay of ^{100}Mo for the *PQQ1* parametrization.

NTME	F	F+S		
		SRC1	SRC2	SRC3
$M^{(\chi)}_{Fm_\nu}$	2.15	1.89	2.15	2.22
$M^{(\chi)}_{GTm_\nu}$	-5.52	-4.72	-5.43	-5.66
$M^{(\chi)}_{Tm_\nu}$	0.05	0.05	0.05	0.05
$M^{(\chi)}_{CR}$	-0.26	-0.23	-0.26	-0.27
$M^{(\chi)}_{F\omega^2}$ $\times 10^3$	1.18	1.14	1.19	1.20
$M^{(\chi)}_{GT\omega^2}$ $\times 10^3$	-5.79	-5.60	-5.86	-5.91

Table 2: NTMEs of $(\beta\beta)_{0\nu}$ decay in SUSY models via exchange of gluinos for ^{100}Mo with in PHFB model using *PQQ1* interaction.

NTME	F	F+S		
		SRC1	SRC2	SRC3
M^N_F	0.716	0.037	0.056	0.067
M^P_F	0.007	0.003	-0.002	0.002
M^N_{GT}	-0.210	-0.108	-0.164	-0.196
M^P_{GT}	-0.023	0.009	0.004	-0.007
$M^{1\pi}_{GT}$	5.422	2.169	3.80	4.831
$M^{2\pi}_{GT}$	2.613	1.856	2.45	2.661
M^P_T	0.001	0.001	0.001	0.001
$M^{1\pi}_T$	0.285	0.285	0.302	0.302
$M^{2\pi}_T$	0.130	0.132	0.134	0.134

Table 3: NTMEs of $(\beta\beta)_{0\nu}$ decay in SUSY models via exchange of squark for ^{100}Mo with in PHFB model using *PQQ1* interaction.

NTME	F	F+S		
		SRC1	SRC2	SRC3
M_F	-258.7	-131.7	-201.4	-241.1
$M_{GT\text{-}MT}$	412.4	207.4	318.8	382.1
$M_{GT\text{-}AP}$	-25.77	-20.00	-24.92	-26.57
$M_{GT\text{-}\pi}$	506.4	441.8	511.2	528.9
$M_{T\text{-}MT}$	-10.33	-10.36	-10.85	-10.83
$M_{T\text{-}AP}$	-1.13	-1.14	-1.15	-1.15
$M_{T\text{-}\pi}$	17.90	18.06	18.09	18.07

In Table 1, 2 and 3, SRC1, SRC2 and SRC3 denote the Jastrow type of short range correlations (SRC) with Miller-Spencer, Argonne V18 and CD-Bonn NN potentials, respectively.

References

[1] F. T. Avignone III, S. R. Elliott, and J. Engel, Rev. Mod. Phys.**80**, 481 (2008).

[2] J. D. Vergados, H. Ejiri, and F. Simkovic, Rep. Prog. Phys. **75**,106301 (2012).

[3] R. Chandra, J. Singh, P. K. Rath, P. K. Raina, and J. G. Hirsch, Eur. Phys. J. A **23**, 223 (2005).

[4] S. Singh, R. Chandra, P. K. Rath, P. K. Raina, and J. G. Hirsch, Eur. Phys. J. A **33**, 375 (2007).

[5] P. K. Rath, R. Chandra, K. Chaturvedi, P. K. Raina, and J. G. Hirsch, Phys. Rev. C. **82**, 064310 (2010).

[6] P. K. Rath, R. Chandra, K. Chaturvedi, P. Lohani, P. K. Raina, and J. G. Hirsch, Phys. Rev. C **88**, 064322 (2013).

[7] P. K. Rath, R. Chandra, K. Chaturvedi, P. Lohani, and P. K. Raina, Phys. Rev. C **93**, 024314 (2016).

[8] F. Simkovic, A. Faessler, H. Muther, V. Rodin, and M. Stauf, Phys. Rev. C **79**, 055501 (2009).

[9] M. Hirsch, H. V. Klapdor-Kleingrothaus, S. G. Kovalenko and H. Pas, Phys. Lett. B **372**, 8 (1996).

[10] M. Hirsch, H. V. Klapdor-Kleingrothaus and S. G. Kovalenko, Phys. Lett. B **372**, 181 (1996).

[11] A. Faessler, T. Gutsche, S. Kovalenko and F. Simkovic, Phys. Rev. D **77**, 113012 (2008).

[12] O. Panella, C. Carimalo, Y.N. Srivastava and A. Widom, Phys. Rev. D **56**, 5766 (1997).

[13] M. Hirsch, H.V. Klapdor-Kleingrothaus and S.G. Kovalenko, Phys. Rev. D **54**, R4207 (1996).

Acknowledgment

One of the authors RC thanks DST-SERB, India for financial support vide Dy. No. SERB/F/6190/2015-16.

Study of squark-neutrino mechanism of neutrinoless double beta decay in R-parity violating supersymmetric models

R. Chandra[1],* V. K. Nautiyal[1], R. Gautam[1], K. Chaturvedi[2], P. K. Rath[3] and P. K. Raina[4]

[1] *Department of Applied Physics, Babasaheb Bhimrao Ambedkar University, Lucknow - 226025, INDIA*
[2]*Department of Physics, Bundelkhand University, Jhansi – 284128, INDIA*
[3]*Department of Physics, University of Lucknow, Lucknow, 226007, INDIA*
[4]*Department of Physics, IIT Ropar, Nangal Road, Rupnagar, Punjab – 140001, INDIA*
* *email: ramesh.luphy@gmail.com*

Introduction

The non-observation of $(\beta^-\beta^-)_{0\nu}$ decay is usually interpreted in terms of an upper limit on the Majorana mass of the neutrino. However, in principle in any kind of extension of the standard model (SM) of electroweak unification, which allows lepton number violation at some level, one can expect contributions to $(\beta^-\beta^-)_{0\nu}$ decay, not necessarily related to the mass of the neutrino. Supersymmetric (SUSY) theories with R-parity violation are the most prominent examples of this class of models. In SUSY models, the new SUSY partner differ from the SM field content in a discrete multiplicative quantum number R-parity (R_p) defined as $R_p=(-1)^{3B+L+2S}$ where B, L and S denote the baryon number, lepton number and spin of a particle leading to $R_p=+1$ for the SM particles and $R_p=-1$ for superpartners.

The quark-level lepton number violating interactions and nuclear structure aspects relevant for the R_p-violating SUSY mechanism have been widely studied in the literature [1]. The two types of R_p-violating SUSY mechanism at quark level are (i) the short range mechanism with the exchange of heavy superpartners [2] and (ii) the long range mechanism involving the exchange of heavy squark and the light neutrino [3] known as squark-neutrino mechanism [4].

Faessler et al. [4] has shown that R_p-violating SUSY contributes to the $(\beta^-\beta^-)_{0\nu}$ decay dominantly via exchange of charged pion between the decaying nucleons by employing QRPA model for the calculation of relevant nuclear transition matrix elements (NTMEs).

In reference [5] and references there in, the PHFB model has been successfully applied to study the $(\beta\beta)_{0\nu}$ decay in left-right symmetric models and majoron models. This motivates us to calculate the relevant NTMEs of $(\beta^-\beta^-)_{0\nu}$ decay of nuclei in the mass range 94–150 within R_p-violating SUSY models involving squark-neutrino mechanism using PHFB model in conjunction with pairing plus multi pole type of two body interaction. Finally the constraints on the lepton number violating SUSY parameters are extracted from the available half-life limits of $(\beta^-\beta^-)_{0\nu}$ decay.

Theoretical framework

The inverse half life of $(\beta^-\beta^-)_{0\nu}$ decay in Rp-violating SUSY model is given by [4]

$$T_{1/2}^{-1} = G_{01}\left|M_h^{\bar{q}}\right|^2\left|\eta^{11}_{(q)LR}\right|^2 \tag{1}$$

where G_{01} is phase space factor. The nuclear matrix elements $M_h^{\bar{q}}$ are denoted as $M_{2N}^{\bar{q}}$ and $M_\pi^{\bar{q}}$ for the 2N and pion mode, respectively and expressed as

$$M_{2N}^{\bar{q}} = M_{AP}^{\bar{q}} + M_{MT}^{\bar{q}} + M_{VT}^{\bar{q}} \tag{2}$$

with

$$M_{AP}^{\bar{q}} = \left\langle H_{AP-GT}^{\bar{q}}(r_{12})\sigma_{12} + H_{AP-T}^{\bar{q}}(r_{12})S_{12}\right\rangle \tag{3}$$

$$M_{MT}^{\bar{q}} = \left\langle H_{MT-GT}^{\bar{q}}(r_{12})\sigma_{12} + H_{MT-T}^{\bar{q}}(r_{12})S_{12}\right\rangle \tag{4}$$

$$M_{VT}^{\bar{q}} = \left\langle H_{VT-F}^{\bar{q}}(r_{12})\right\rangle \tag{5}$$

and

$$M_\pi^{\bar{q}} = \left\langle H_{\pi NN-GT}^{\bar{q}}(r_{12})\sigma_{12} + H_{\pi NN-T}^{\bar{q}}(r_{12})S_{12}\right\rangle \tag{6}$$

In PHFB model using closure approximation the NTMEs M_α are calculated as

$$M_\alpha = \sum_{n,m}\left\langle 0_F^+\left\|O_{\alpha,nm}\tau_n^+\tau_m^+\right\|0_I^+\right\rangle \tag{7}$$

Results and discussions

The NTMEs involved in $(\beta^-\beta^-)_{0\nu}$ decay in Rp-violating SUSY model calculated within PHFB model using pairing plus quadrupole-quadrupole (PQQ) interaction are presented in Table 1. Further, the NTMEs have been calculated by considering the finite size of nucleon (F) and Jastrow type of short range correlations (SRC) with Miller-Spencer, Argonne V18 and CD-Bonn NN potentials for the SUSY accompanied $(\beta^-\beta^-)_{0\nu}$ decay of ^{94,96}Zr, ^{98,100}Mo, ^{104}Ru, ^{110}Pd, ^{128,130}Te and ^{150}Nd isotopes for the $0^+ \rightarrow 0^+$ transition. At present, the results are presented for the case of ^{100}Mo and ^{150}Nd.

Table 1: The NTMEs M_α of squark-neutrino R_p-violating SUSY mechanism of $(\beta^-\beta^-)_{0\nu}$ decay of ^{100}Mo and ^{150}Nd in the PHFB model using PQQ interaction.

Nuclei	M_α	F+SRC		
		SRC1	SRC2	SRC3
^{100}Mo	$M_{2N}^{\bar{q}}$	44.16	80.48	103.35
	$M_{\pi}^{\bar{q}}$	459.81	529.26	547.01
^{150}Nd	$M_{2N}^{\bar{q}}$	21.02	37.55	47.67
	$M_{\pi}^{\bar{q}}$	219.22	249.90	257.56

In Table 1, SRC1, SRC2 and SRC3 denote the Jastrow type of short range correlations (SRC) with Miller-Spencer, Argonne V18 and CD-Bonn NN potentials, respectively. The calculation of NTMEs for rest of the nuclei stated above along with the extracted limits on SUSY parameters will be presented in the symposium.

Conclusions

To summarize, we study the $(\beta^-\beta^-)_{0\nu}$ decay of ^{94,96}Zr, ^{98,100}Mo, ^{104}Ru, ^{110}Pd, ^{128,130}Te and ^{150}Nd isotopes for the $0^+ \rightarrow 0^+$ transition within R_p-violating SUSY models involving squark-neutrino mechanism using PHFB model. The lepton number violating parameters of R_p-violating SUSY model using calculated NTMEs and experimental data will be extracted and presented in the symposium.

References

[1] J.D. Vergados, Phys. Rep. **361**, 1 (2002).
[2] R.N. Mohapatra, Phys. Rev. D **34**, 909 (1986); ibid **34**, 3457 (1986).
[3] M. Hirsch, H.V. Klapdor-Kleingrothaus and S.G. Kovalenko, Phys. Lett. B **372**, 181 (1996).
[4] A. Faessler, T. Gutsche, S. Kovalenko and F. Simkovic, Phys. Rev. D **77**, 113012 (2008).
[5] P. K. Rath, R. Chandra, K. Chaturvedi, P. Lohani, P. K. Raina and J. G. Hirsch, Phys. Rev. C **88**, 064322 (2013).

Acknowledgment

One of the authors RC thanks DST-SERB, India for financial support vide Dy. No. SERB/F/5139/2013-14.